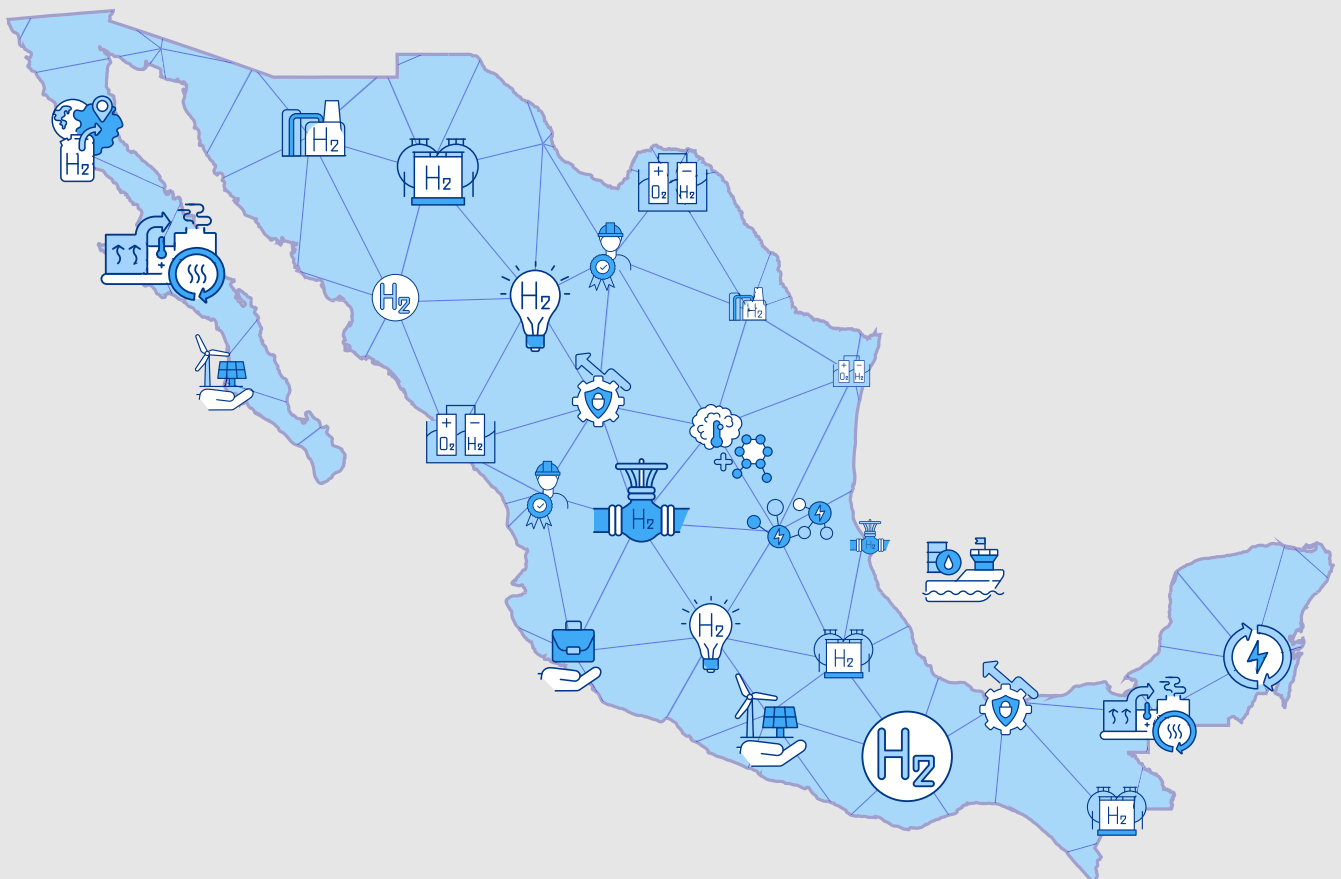


# Green Hydrogen in Mexico: towards a decarbonization of the economy

*Volume II: Green Hydrogen integration into the grid*



---

# Imprint

---

## Commissioned and published by

Deutsche Gesellschaft für Internationale Zusammenarbeit  
(GIZ) GmbH  
Registered offices Bonn and Eschborn

## Programs

Bilateral Energy Partnerships in Developing and Emerging  
Countries & Energy Transition Support Program in Mexico  
(TrEM)

[www.energypartnership.mx](http://www.energypartnership.mx)  
[www.giz.de/en/worldwide/76471.html](http://www.giz.de/en/worldwide/76471.html)

## Edition and supervision

William Jensen Díaz  
[william.jensen@giz.de](mailto:william.jensen@giz.de)

Lorena Espinosa Flores  
[lorena.espinosa@giz.de](mailto:lorena.espinosa@giz.de)

Javier Arturo Salas Gordillo  
[javier.salasgordillo@giz.de](mailto:javier.salasgordillo@giz.de)

Natalia Escobosa Pineda

## Authors

HINICIO

## As at

October 2021

## Digital Version

## Design

Sk3 Estudio Creativo  
[www.sk3.mx](http://www.sk3.mx)

## Photo credits

© Shutterstock | 35070573 page 12  
© Shutterstock | 18944601 page 28  
© Shutterstock | 93272194 page 48  
© Shutterstock | 18825059 page 70  
© Shutterstock | 1747003955 page 74

All rights reserved. Any use is subject to consent by the Secretariat of the German–Mexican Energy Partnership (EP) and the Energy Transition Support Program in Mexico (TrEM).

All content has been prepared with the greatest possible care and is provided in good faith, considering official sources and public information. The assumptions, views and opinions expressed in this publication do not necessarily reflect the official policy or position of the EP, the TrEM, the Federal Ministry for Economic Affairs and Energy of Germany (BMWi), the German Ministry of Economic Cooperation (BMZ), nor the Deutsche Gesellschaft für Internationale Zusammenarbeit (GIZ) GmbH.

Information is provided in summary form and is therefore intended for general guidance only. This publication is not intended to be a substitute for detailed research or the exercise of professional judgment. The Secretariat of the EP and the TrEM program provide no guarantee regarding the currency, accuracy and completeness of the information provided. They accept no liability for damages of a tangible or intangible nature caused directly or indirectly by the use of or failure to use the information provided.

---

## Acknowledgments

---

**The German-Mexican Energy Partnership and the Energy Transition Support Program in Mexico (TrEM) appreciates the participation and enthusiasm of all the experts consulted for the preparation of this study.**

### **Special acknowledgements**

Patrick Maio (HINICIO)

Ana Ángel (HINICIO)

Luis Miguel Diazgranados (HINICIO)

Jorge Luis Hinojosa (HINICIO)

Juan Antonio Gutiérrez (HINICIO)

---

# Contents

---

Imprint	
Acknowledgments	1
Contents	2
Abbreviations	4
List of Tables	5
List of Figures	6
Executive summary	8
Introduction	11
2. Renewable energy and green hydrogen potential	13
2.1. Methodology	13
2.1.1. Assessment definition	14
2.1.2. Geospatial Analysis	14
2.1.3. Renewable potential assessment	15
2.1.4. Hydrogen production simulation	17
2.2. Results	18
2.2.1. Onshore wind energy potential	19
2.2.2. Solar PV energy potential	20
2.2.3. Hybrid solar PV-wind energy potential	22
2.2.4. Green hydrogen potential	23
2.3. Comparison of results with official estimates	26
2.4. Conclusions	27
3. Energy Storage Technologies	29
3.1. Introduction	29
3.2. Methodology	31
3.3. Technologies description	30
3.3.1. Pumped Hydro Storage (PHS)	33
3.3.2. Compressed Air Energy Storage (CAES)	34
3.3.3. Flywheel Energy Storage (FES)	35
3.3.4. Molten Salt Energy Storage (MSES)	35
3.3.5. Hydrogen (H <sub>2</sub> )	36
3.3.5.1 Electrolyzers	37
3.3.5.2 Hydrogen storage	38

<b>3.3.5.3</b> Large-scale storage (more than 100 ton H <sub>2</sub> )	39
<b>3.3.5.4</b> Small-scale storage (less than 1 ton H <sub>2</sub> )	40
<b>3.3.5.5</b> Fuel Cells	40
<b>3.3.6.</b> Lithium-ion Batteries (BESS)	40
<b>3.3.7.</b> Lead-acid Batteries	42
<b>3.3.8.</b> Flow Batteries (FB)	43
<b>3.4.</b> Summary and results	44
<b>3.5.</b> Conclusions	46
<b>4.</b> Hydrogen integration potential in the National and Mulegé energy systems	49
<b>4.1.</b> Introduction	49
<b>4.2.</b> Methodology	49
<b>4.2.1.</b> Scenarios definition	50
<b>4.2.1.1</b> National power system	50
<b>4.2.1.2</b> Mulegé energy system	51
<b>4.2.2.</b> Energy data collection	51
<b>4.2.3.</b> Energy system model	53
<b>4.3.</b> Results	54
<b>4.3.1.</b> National power system	54
<b>4.3.1.1</b> Control scenario - BaU2020	54
<b>4.3.1.2</b> Hydrogen integration by 2030 - BaU2030 and H <sub>2</sub> MX2030 scenarios	55
<b>4.3.1.3</b> Hydrogen integration by 2050 - BaU2050 and H <sub>2</sub> MX2050 scenarios	58
<b>4.3.1.4.</b> Hydrogen in the H <sub>2</sub> MX2050 scenario	60
<b>4.3.2.</b> Mulegé zero-emission system	64
<b>4.3.3.</b> Summary table	66
<b>4.4.</b> Conclusions	67
<b>5.</b> Conclusions and recommendations	71
<b>Bibliography</b>	73

## Abbreviations

AA-CAES	Advanced Adiabatic Compressed Air Energy Storage
ALK	Alkaline Electrolyser
AZEL	Clean Energy Atlas (Mexico)
BaU	Business as Usual Scenario
BESS	Battery Energy Storage System
CAES	Compressed Air Energy Storage
CAPEX	Capital Expenditure
CCGT	Combined-Cycle Gas Turbine
CSP	Concentrated Solar Power
EPS	Electric Power Systems
ESS	Energy Storage Systems
EZ	Electrolyzer
FES	Flywheel Energy Storage
H <sub>2</sub>	Hydrogen
H <sub>2</sub> MX	Hydrogen Mexico Scenario
KTON	Kiloton, thousand metric tons
KTPA	Kiloton Per Annum
LFP	Lithium Iron Phosphate
LCOE	Levelized Cost of Electricity
LCOH	Levelized Cost of Hydrogen
LCOS	Levelized Cost of Storage
LTO	Lithium Titanate
MSES	Molten Salt Energy Storage
MTCO <sub>2</sub>	Megaton (million tons) of carbon dioxide
MTON	Megaton, million metric tons
NG	Natural Gas
NMC	Lithium Nickel Manganese Cobalt Oxide
OCGT	Open-Cycle Gas Turbine
OPEX	Operational Expenditure
PEMEL	Proton Exchange Membrane Electrolyzer
PHS	Pumped Hydro Storage
PRODESEN	Development Program of the National Electricity System
PV	Photovoltaic
RES	Renewable Energy Source (non variable)
SOEC	Solid Oxide Electrolyzer Cell
TAC	Total Annual Cost
VRES	Variable Renewable Energy Source
VRFB	Valve-regulated Lead Acid
VRLA	Vanadium Redox Flow Battery
ZBFB	Zinc Bromine Flow Battery

---

## List of Tables

---

Table 1.	Competitive analysis of energy storage technologies. Ratings shown on a scale of 1 (worst) to 5 (best), and rankings from 1 (most) to (11) least competitive.	9
Table 2-1.	Land exclusion criteria for PV parks deployment.	15
Table 2-2.	Land exclusion criteria for onshore wind turbines deployment.	15
Table 2-3.	Main techno-economical parameters by 2050 for solar PV and onshore wind turbines according to estimations by HINICIO.	17
Table 2-4.	Proton exchange membrane electrolyzer (PEMEL) techno-economical parameters used according to technology development expected by HINICIO by 2050.	18
Table 2-5.	Green hydrogen production parameters by state.	24
Table 3-1.	Techno-economic characteristics of ALK and PEM electrolyzers (2020,2030).	38
Table 3-2.	Comparison of lithium-Ion chemistry properties, advantages, and disadvantages.	41
Table 3-3.	Commercial characteristics of energy storage systems.	44
Table 3-4.	Technical characteristics of energy storage systems.	44
Table 3-5.	Look-up table for competitive scores.	45
Table 3-6.	Competitive scores for storage.	45
Table 3-7.	Parameter weightings for the selected.	45
Table 3-8.	Suitability matrix for the selected applications.	45
Table 3-9.	Final weighted scores, their average, and ranking.	46
Table 3-10.	Ranking of the technologies for each application.	46
Table 4-1.	Energy data inputs.	52
Table 4-2.	Comparison of the scenarios modeled.	54
Table 4-3.	Summary table of integration potential.	66
Table 4-4.	Water consumption comparison.	66

## List of Figures

Figure 1.	Levelized cost of hydrogen from hybrid wind-solar PV production for 2050.	8
Figure 2.	Installed capacity for Mexican power system by 2030 for the evaluated scenarios.	9
Figure 3.	Installed capacity in the Mexican power system by 2050 under two scenarios.	10
Figure 4.	Installed capacity for 100% renewable Mulegé power system by 2050.	10
Figure 2-1.	Methodology block diagram.	13
Figure 2-2.	Geospatial analysis block diagram	14
Figure 2-3.	Capacity assignment block diagram.	16
Figure 2-4.	Potential simulation block diagram.	16
Figure 2-5.	Hydrogen production simulation block diagram.	17
Figure 2-6.	Potential maps derivation from the potential assessment results.	18
Figure 2-7.	Onshore wind LCOE potential map.	19
Figure 2-8.	Onshore wind capacity potential by LCOE.	20
Figure 2-9.	Solar PV LCOE potential map.	21
Figure 2-10.	Solar PV capacity potential by LCOE [USD/MWh].	21
Figure 2-11.	Hybrid wind-solar PV levelized cost of electricity potential map.	22
Figure 2-12.	Levelized cost of hydrogen from hybrid wind-solar PV production.	23
Figure 2-13.	Water use of green H <sub>2</sub> production as a share of the total water consumption in 2017.	24
Figure 2-14.	Green hydrogen potential by LCOH.	25
Figure 2-15.	PEMEL capacity factor potential map.	26
Figure 3-1.	Scientific categorization of energy storage technologies.	29
Figure 3-2.	Worldwide installed capacity of ESS by technology, Nov-2020.	30
Figure 3-3.	Global operational energy storage power capacity by technology excluding PHS, Nov-2020.	30
Figure 3-4.	Comparison of nominal power, energy capacity, and time of response.	31
Figure 3-5.	Diagram of the operation of a typical pump hydro station.	33
Figure 3-6.	Diagram of a Diabatic (left) and an Adiabatic (right) Compressed Air Energy Storage Systems.	34
Figure 3-7.	Diagram of a Flywheel Energy System.	35
Figure 3-8.	Diagram of a Molten Salt Energy Storage System.	36
Figure 3-9.	Topology of hydrogen storage and fuel cell system.	37
Figure 3-10.	Topology of ALK and PEM electrolyzers.	37
Figure 3-11.	Hydrogen storage options available and their working capacity.	39
Figure 3-12.	Charge and discharge cycle of a lithium-Ion battery energy storage system.	41
Figure 3-13.	Working principle of a lead-acid battery [18].	43
Figure 3-14.	Working principle of a flow battery.	43
Figure 4-1.	Energy system modeling block methodology.	49
Figure 4-2.	Scenarios modeled for the national power system evaluation.	50
Figure 4-3.	Scenarios modeled for the Mulegé renewable system.	51
Figure 4-4.	PRODESEN 2019 and BaU2020 capacity mix comparison.	55
Figure 4-5.	Capacity installed in the Mexican power system by 2030 under two scenarios.	55
Figure 4-6.	Electricity generation by source in the Mexican power system by 2030 under two scenarios.	56

Figure 4-7. Renewable production in the Mexican power system by 2030 under two scenarios.	56
Figure 4-8. Storage capacity needs in the Mexican power system by 2030 under two scenarios.	56
Figure 4-9. Total annual costs of the Mexican power system by 2030 under two scenarios.	56
Figure 4-10. Capacity installed in the Mexican power system by 2030 under two scenarios compared to the 2020 status (CHANGE to PRODESEN 2019).	57
Figure 4-11. Installed capacity in the Mexican power system by 2050 under two scenarios.	58
Figure 4-12. Renewable production in the Mexican power system by 2050 under two scenarios.	58
Figure 4-13. Changes in electricity production in the Mexican power system by 2050 under the two scenarios.	59
Figure 4-14. Storage needs for a Mexican power system by 2050 under two scenarios.	60
Figure 4-15. Total annual cost (TAC) of a Mexican power system by 2050 under two scenarios.	60
Figure 4-16. Share of electricity from hydrogen re-electrification in the total electricity consumed in the H <sub>2</sub> MX2050 scenario.	61
Figure 4-17. Hydrogen production by region of transmission in the H <sub>2</sub> MX2050 scenario.	61
Figure 4-18. Proton exchange membrane electrolyzer installed capacity per region in the H <sub>2</sub> MX2050 scenario.	62
Figure 4-19. Combined-cycle gas turbine (hydrogen) installed capacity per region in the H <sub>2</sub> MX2050 scenario.	63
Figure 4-20. Investment in hydrogen infrastructure by region under the H <sub>2</sub> MX2050 scenario.	63
Figure 4-21. Capacity installed in a zero-emissions Mulegé power system by 2050 under two scenarios.	64
Figure 4-22. Electricity production by source in a zero-emissions Mulegé power system by 2050.	64
Figure 4-23. Changes in electricity generation capacity and operation in a zero-emissions Mulegé power system by 2050 under two scenarios.	65
Figure 4-24. Storage needs for a zero-emissions Mulegé power system by 2050 under two scenarios.	65
Figure 4-25. Total annual costs (TAC) comparison for a renewable Mulegé system by 2050 under two scenarios.	65

## Executive summary

One of the most promising enablers for the decarbonization of the power sector is the use of hydrogen produced by electrolysis using renewable energy.

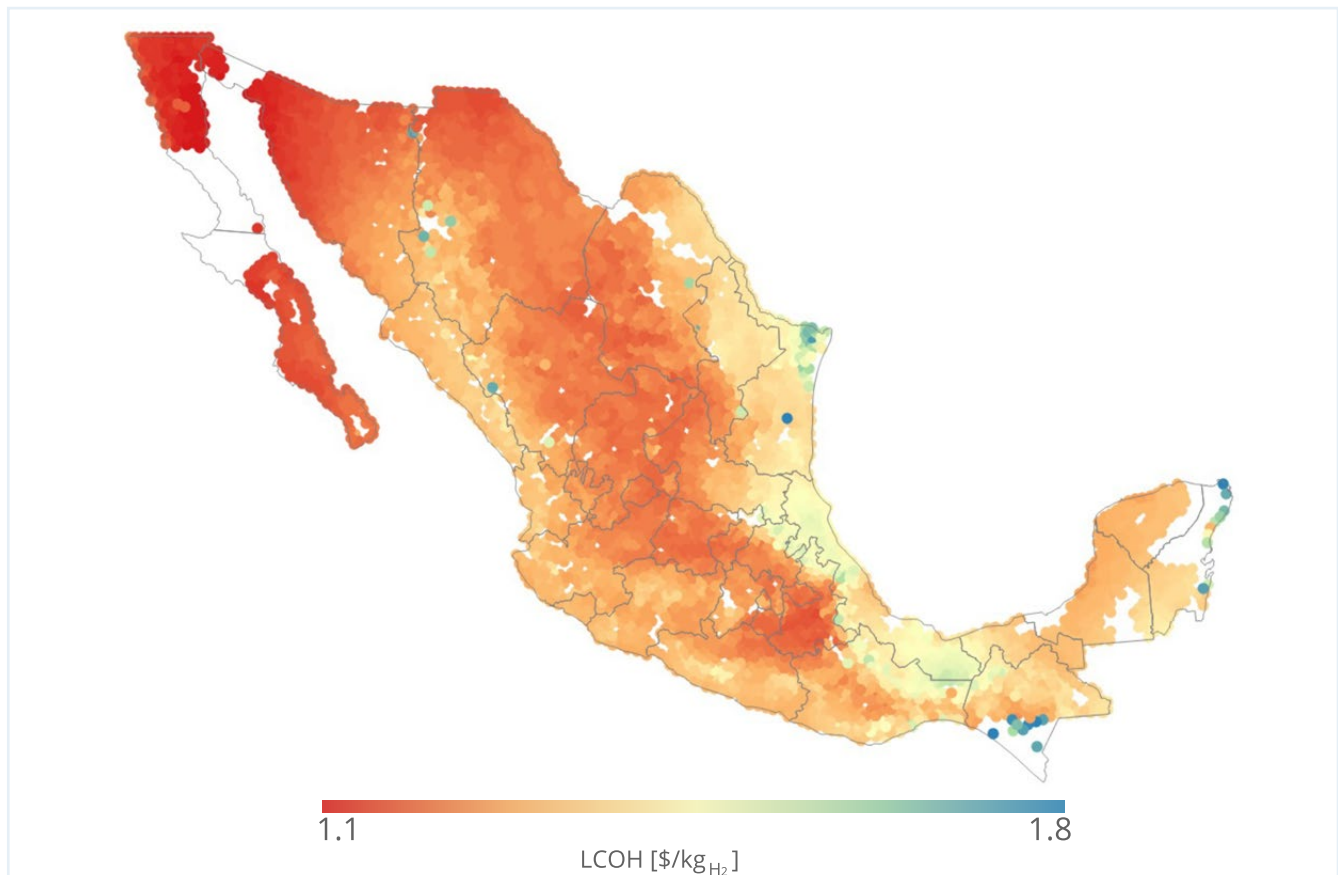
Using variable renewable energy sources such as wind, generates both a challenge for the massive production of hydrogen, providing limited and discontinuous working hours for the electrolyzers, as well as an opportunity to use hydrogen to store the energy coming from these intermittent sources. This study analyzes how suitable renewable energy sources are for producing green hydrogen in Mexico and what is the role such hydrogen would play in the decarbonization of the power system towards 2050.

A glimpse of what could be achieved in Mexico with the use of wind and solar PV by 2050 is found in a first assessment, which starts from the total Mexican territory and integrates historical meteorological data, land restrictions related to

its different uses, and current trends in the technology's performance and price. For on-shore wind generation, up to 2.7 TW of installed capacity that generates around 6.3 PWh of yearly energy with an LCOE equal or lower than 60 USD/MWh could be installed using 22% of the Mexican territory. For solar PV, up to 33.5 TW of installed capacity that generates 69 PWh yearly with an LCOE lower or equal than 25 USD/MWh could be installed using around one third of the national territory.

An analysis of green hydrogen production potential shows that, in theory, up to 22 TW of electrolysis capacity could be installed across the country to produce 1,400 MtonH<sub>2</sub> per year in 2050 with an average cost of 1.4 USD/kg H<sub>2</sub>, driven mainly by low-cost PV generation. The yearly water demand used in the electrolysis for the total production would represent only 0.13% of the country's water consumption in 2017.

Figure 1. Levelized cost of hydrogen from hybrid wind-solar PV production for 2050.



An updated state of the art of different storage technologies for power systems and a competitiveness analysis is done considering different applications to show the most suitable technology for each application. Hydrogen energy storage is far from being the most competitive

storage alternative, ranking in 7th place out of 11 evaluated technologies. Further results of this analysis are summarized in Table 1. in a color scale, where green indicates the best performance and red indicates the worst performance for each application.

Table 1. Competitive analysis of energy storage technologies. Ratings shown on a scale of 1 (worst) to 5 (best), and rankings from 1 (most) to (11) least competitive.

	PHS	CAES	FES	MSES	H <sub>2</sub>	LFO	LTO	NMC	VRLA	VRFB	ZBFB
Capacity firming	4.17	3.19	0.79	3.52	3.24	3.17	3.11	3.36	2.59	2.68	1.95
Auxiliary services	1.23	0.97	2.97	1.00	1.47	3.37	3.29	3.55	1.78	0.82	0.61
Renewable shifting	4.28	3.42	0.76	3.76	3.09	3.11	2.91	3.34	2.69	2.80	2.03
Renewable smoothing	1.23	0.97	2.97	1.00	1.47	3.37	3.29	3.55	2.85	0.82	0.61
Average rating	2.72	2.14	1.87	2.32	2.32	3.26	3.15	3.45	2.48	1.78	1.3
Ranking	4	8	9	6	7	2	3	1	5	10	11

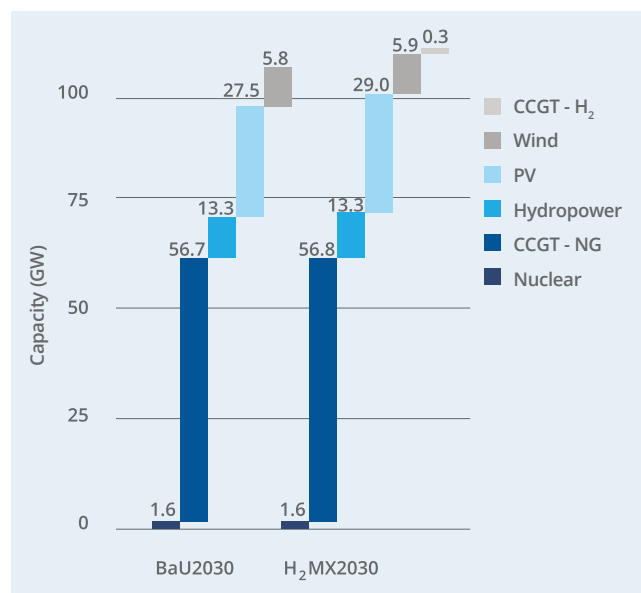
The last step of the study analyses the impact of hydrogen integration in both the national power system and the isolated power grid in Mulege, Baja California. It's important to consider that for this analysis, hydrogen applications are only focused on re-electrification, leaving raw materials and mobility applications aside.

For the national power system a multi-node model is built and analyzed in three time horizons: 2020 (to calibrate), 2030 and 2050 with information obtained mainly from the PRODESEN, international reports, and Hincio know-how. For 2030 and 2050 two scenarios are defined, H<sub>2</sub>MX (with H<sub>2</sub>) and BaU (without H<sub>2</sub>), to compare how hydrogen affects the system.

For 2030 the re-electrification of hydrogen is almost non-existent compared to the more than 100 GW projected installed capacity of the national power system, with only 1 GW of electrolysis capacity needed, producing 60 kton H<sub>2</sub>/year to power a 300 MW hydrogen gas turbine for re-electrification.

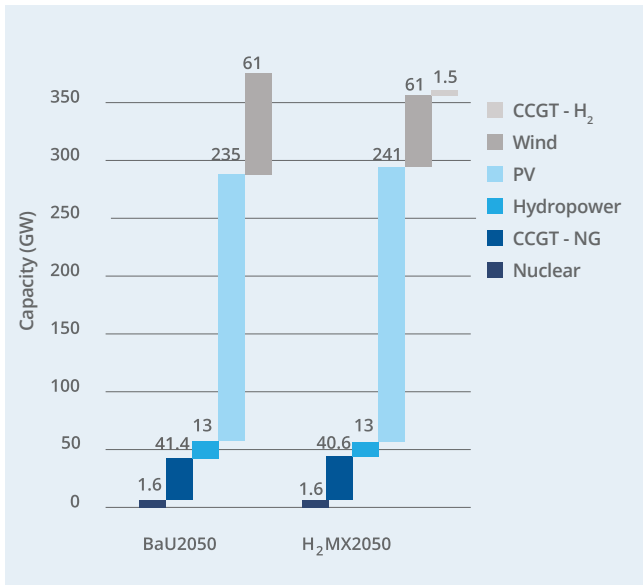
The total emissions of the national power system in the BaU2030 scenario are of 134 MtCO<sub>2</sub>/year, almost the same as the 133 MtCO<sub>2</sub>/year of the H<sub>2</sub>MX2030 scenario. The specific GHG emissions were around 290 gCO<sub>2</sub>/kWh in both cases, a reduction of over 40% compared with the emissions factor of 505 gCO<sub>2</sub>/kWh in 2019 as reported by the Mexican Energy Regulatory Commission (CRE).

Figure 2. Installed capacity for Mexican power system by 2030 for the evaluated scenarios.



It is in 2050 that green H<sub>2</sub> could become more relevant in the National power system, driven mainly by the improvement in prices and performance that can be seen in the current trends. The results of the model show that in 2050 5.5 TWh/year are produced from hydrogen re-electrification, that is about half of the current nuclear electricity generation in the country, for which around 1.5 GW of hydrogen power turbines are needed, as is shown in Figure 2.

Figure 3. Installed capacity in the Mexican power system by 2050 under two scenarios.



Hydrogen integration also allows to increase renewable generation in the system. The results show that in H<sub>2</sub>MX2050 scenario there is an additional 2% generated from renewable sources, or 15 TWh/year growing to a national renewable generation of 815 TWh/year.

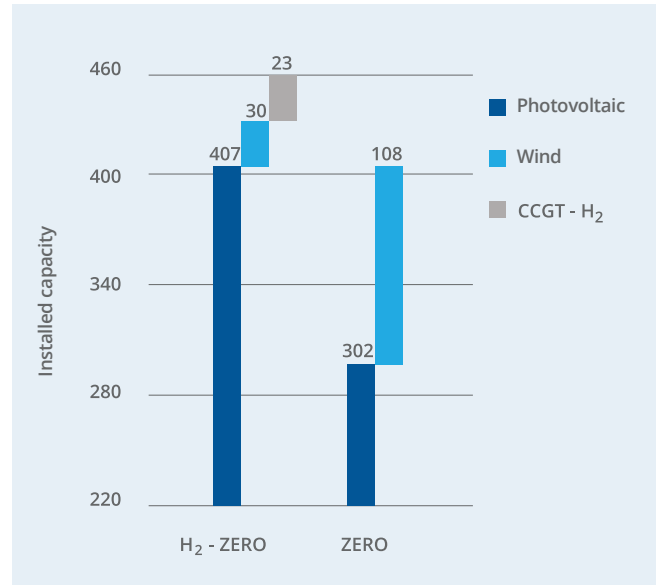
Regarding GHG, the total emissions are similar in both cases, 30 MtCO<sub>2</sub>/year for BaU2050 and 29 MtCO<sub>2</sub>/year for H<sub>2</sub>MX2050, which leads to a specific emission of 39 gCO<sub>2</sub>/kWh and 38 gCO<sub>2</sub>/kWh respectively, 90% less than in 2020. It must be noted, however, that the emissions reduced are mostly due to a higher participation of renewables rather than the use of hydrogen. The water required for this amount of hydrogen accounts for less than the 0.1% of the current consumption in each region of production.

For the power system of Mulegé, Baja California, two scenarios are analyzed in 2050: 100% renewable without hydrogen (scenario ZERO) and 100% renewable with hydrogen (scenario H<sub>2</sub>-ZERO).

As in the 2050 scenarios for the national power system, hydrogen integration enables a competitive storage solution for the low-cost solar energy in Mulegé, which explains why wind capacity is reduced and PV capacity is increased. For wind, capacity is reduced from 108 MW to 30 MW from scenario ZERO to H<sub>2</sub>-ZERO; whereas for solar PV capacity increases from 302 MW to 407 MW as shown in Figure 4.

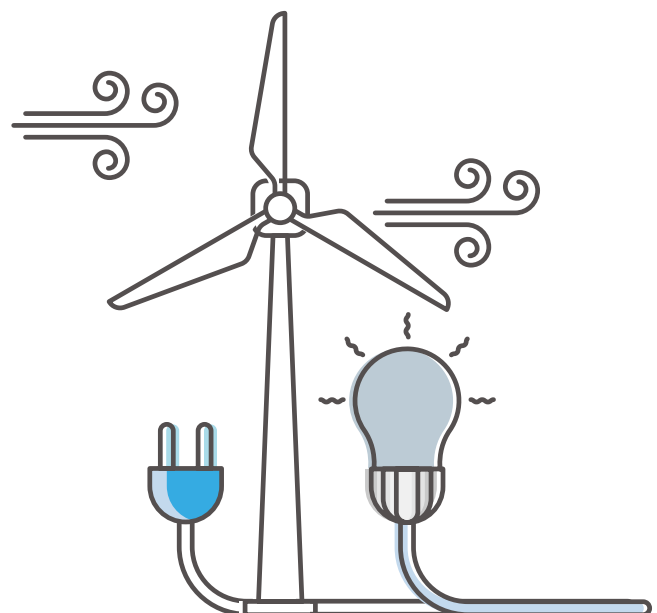
The energy storage capacity increases from 0.9 GWh in the ZERO scenario, to 2.4 GWh (1.7 in form of hydrogen, around 50 ton) in H<sub>2</sub>-ZERO.

Figure 4. Installed capacity in the Mulegé system 100% renewable by 2050.



The analysis done shows an overview of how green hydrogen energy storage and re-electrification could affect the Mexican power system in different times frames.

Further studies would be required to include different sectors of the economy and to analyze how aggregating demands can improve the power system model for the development of hydrogen across all applications.



---

## Introduction

---

This study is framed within the planning of power systems, specifically on the estimation of the potential resource available in the Mexican territory for two variable renewable energy sources (VRES): solar PV and wind. Over the last decade, they have progressively become economically attractive and more efficient globally, and the costs of solar PV have fallen by 82% and of onshore wind by 40%<sup>1</sup>. Nevertheless, some challenges need to be overcome such as their generation intermittency and geographical distribution. To tackle these challenges, assessments of VRES potential are usually carried out in the first place to help identify zones with high generation potential and then look for strategies and new alternatives to achieve a smooth integration of the VRES potential found and existing energy infrastructure without compromising the security of the power supply. In this context, energy carriers such as green hydrogen are being investigated to complement with energy storage and help the integration of VRES in a cost-optimal manner.

The main objectives of the study are to:

- **Estimate the potential of renewable generation (solar PV and onshore wind) in Mexico;**
- **Calculate the potential of green hydrogen production in Mexico;**
- **Provide an updated overview of the state of the art of Energy Storage Systems (ESS) for electric power systems;**
- **Assess the benefits of the integration of renewable generation using green hydrogen in the Mexican Power system;**
- **Explore the integration and the requirements for the region of Mulegé, Baja California, to become 100% renewable.**

While this report follows the detailed methodologic process of the assessments performed, the key results and conclusions for each section can be found in the latest subchapters of each, as well as a synthesis from all the report's in chapter 5. Conclusions and recommendations.



---

<sup>1</sup> IRENA, Renewable Power Generation Costs in 2019.



## 2. Renewable energy and green hydrogen potential

The renewable potential assessment for onshore wind, solar PV, and green hydrogen production in Mexico for a 2050 time horizon is presented in this section. First, the methodology and main assumptions considered are described. Second, the renewable generation potentials and insights from the analysis are presented.

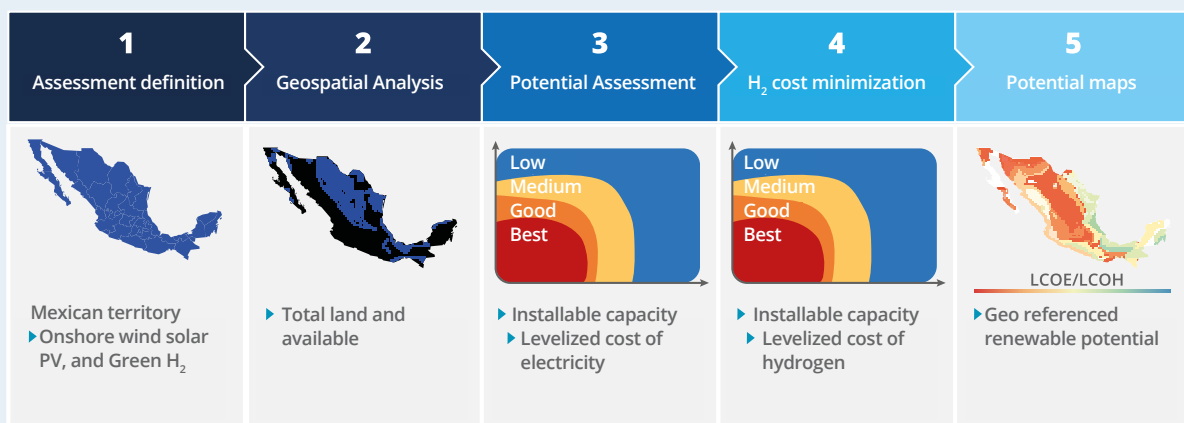
The results and conclusions can be found on subchapters 2.2 and 2.4, respectively.

### 2.1 Methodology

The methodology followed for the renewable potential assessment consists of five steps, as shown in Figure 2-1.

1. **Assessment definition:** define the renewable energy technologies to be considered, techno-economical parameters, regional and temporal context for the assessment.
2. **Geospatial analysis:** computational analysis to determine the amount and distribution of land available for renewable production after applying land restrictions.
3. **Renewable potential assessment:** computational simulation used to determine the renewable energy capacity that could be installed on the land available and its corresponding Levelized Cost of Electricity (LCOE).
4. **H<sub>2</sub> cost minimization:** simulation of hydrogen production via electrolysis based on the LCOE and geospatial analysis from the previous steps.
5. **Potential maps:** the results are shown in maps, plots, and tables, which provides elements for the reader to gain a better understanding of the insights found in the analysis.

Figure 2-1. Methodology block diagram.



### 2.1.1 Assessment definition

The complete Mexican inland territory of around 1.9 million km<sup>2</sup> is analyzed in a 2050 context. The technologies assessed are onshore wind turbines and open-field PV plants with improved efficiency according to the technology development expected by 2050<sup>2</sup>.

Green hydrogen production is evaluated for large-scale stationary Proton exchange Membrane Electrolysers (PEMEL) according to the technology development and costs expected by HINICIO for the same 2050 context.

### 2.1.2 Geospatial Analysis

The geospatial analysis consists of a step-by-step land removal based on certain restrictions that limit the deployment of Variable Renewable Energy Sources (VRES) in areas that do not fulfill the requirements and constraints necessary for power plant development. At the end of the land removal, the total amount of potential land that is available for renewable installations and its geographical distribution is obtained. Figure 2-2. shows a summary of the geospatial analysis procedure.

Two geospatial analyses are carried out, one for solar PV and another for onshore wind turbines. The land restrictions include relevant physical, economical, socio-political, and environmental constraints that are commonly excluded in this type of analysis<sup>3</sup>, as shown in Table 2-1. A buffer area is also excluded when applicable to minimize negative impacts near to land restrictions<sup>4</sup>.



Figure 2-2. Geospatial analysis block diagram.



<sup>2</sup> Ryberg D. S., Generation Lulls from the Future Potential of Wind and Solar Energy in Europe, 2019.

<sup>3</sup> S. D. Heuser, "Techno-economic analysis of a potential energy trading link between Patagonia and Japan based on CO<sub>2</sub>-free hydrogen.," International Journal of Hydrogen Energy, 2019.

<sup>4</sup> Peña Sanchez, E.U., "Techno-economical Analysis of the Production of CO<sub>2</sub>-free Hydrogen from Variable Renewable Energy Sources in Mexico," 2019.

Table 2-1. Land exclusion criteria for PV parks deployment.

Land restrictions	Exclusion rule	Buffer zone	Reference
Agricultural areas	=	0 m	Ryberg, 2017
Archeological areas	<	1000 m	SENER, AZEL 2017
Country borders	<	1000 m	Heuser , 2019
Historical sites	<	1000 m	SENER, AZEL 2017
Jungles	<	1000 m	Peña-Sánchez, 2019
Mining sites	=	0 m	Ryberg, 2017
Protected areas	<	1000 m	Ryberg, 2017
Settlements	<	200 m	Ryberg, 2017
Volcanoes	<	2000 m	Ryberg, 2017
Water bodies	<	1000 m	Ryberg, 2017
Woodlands	=	0 m	Ryberg, 2017
Elevation	<	2 m	Ryberg, 2017
Slope	<	30°	Ryberg, 2017
Northward slope	<	3°	Ryberg, 2017

Table 2-2. Land exclusion criteria for onshore wind turbines deployment.

Land restriction	Exclusion rule	Buffer zone	Reference
Archeological areas	<	1000 m	SENER, AZEL 2017
Country borders	<	1000 m	Heuser , 2019
Historical sites	<	1000 m	SENER, AZEL 2017
Jungles	<	200 m	Peña-Sánchez, 2019
Mining sites	<	200 m	Ryberg, 2017
Protected areas	<	1000 m	Ryberg, 2017
Railways	<	200 m	Ryberg, 2017
Roads	<	300 m	Ryberg, 2017
Settlements	<	1000 m	Ryberg, 2017
Volcanoes	<	2000 m	Ryberg, 2017
Water bodies	<	300 m	Ryberg, 2017
Water lines	<	200 m	Ryberg, 2017
Woodlands	<	200 m	Peña-Sánchez, 2019
Wind speeds	<	5 m/s	Ryberg, 2017
Elevation	>	3 km	Ryberg, 2017
Slope	>	30°	Ryberg, 2017

The land deduction from the complete Mexican territory was carried out using the Geospatial Land Availability for Energy Systems (GLAES) model developed by the Jülich Research Center<sup>5</sup>, and an adapted methodology<sup>6</sup> is followed with adjusted considerations for Mexico. A spatial resolution of 100 m<sup>2</sup> is used which represents a good balance between accuracy and computational complexity.

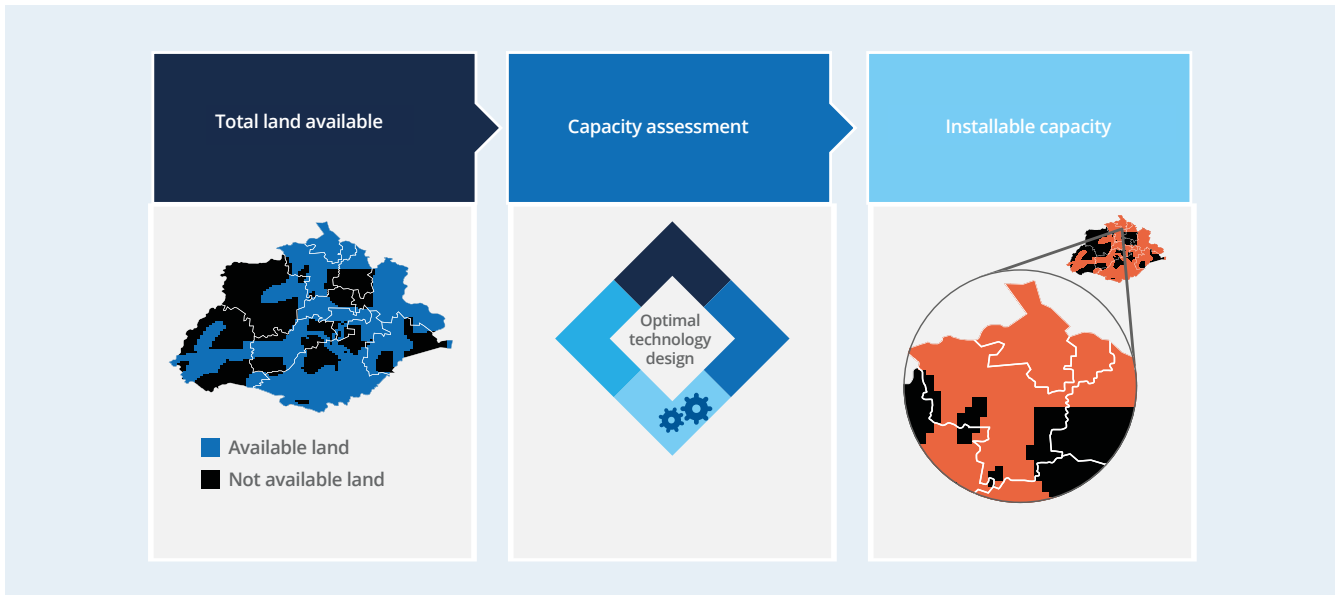
### 2.1.3 Renewable potential assessment

The assessment of renewable potential is aimed at determining the maximum renewable generation capacity that can be installed and its LCOE in the available land estimated in the previous steps for both wind and solar PV. The maximum installable capacity is obtained by placing individual projected turbines and solar PV parks in the remaining land. As an example, the geospatial analysis process for the Mexican state of Aguascalientes for onshore wind turbines is shown in Figure 2-3.

<sup>5</sup> Ryberg, D.S., "Geospatial Land Availability for Energy Systems (GLAES).", 2018.

<sup>6</sup> Ryberg, D. S., Caglayan, D. G., Schmitt, S., Linßen, "The future of European onshore wind energy potential: Detailed distribution and simulation of advanced turbine designs," 2019.

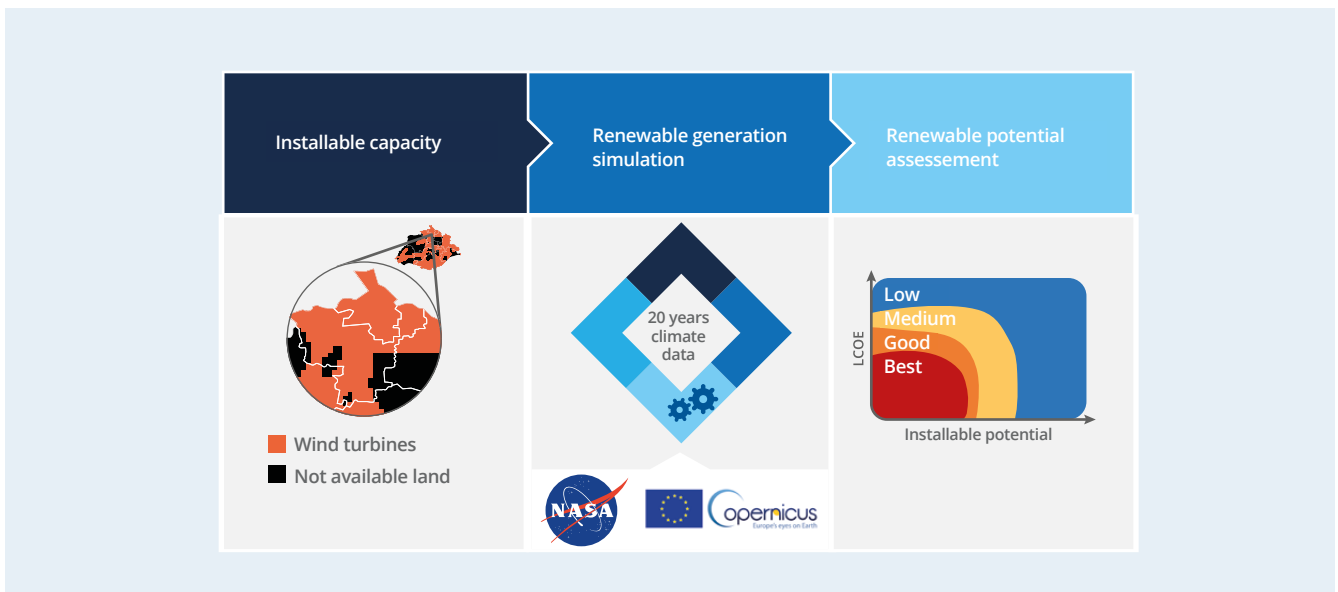
Figure 2-3. Capacity assignment block diagram.



An LCOE is obtained considering a power plant lifetime of 20 years. This is done using the RESKit<sup>7</sup> model developed by the Jülich Research Center and a methodology adapted to Mexico. The simulation model takes as input the installed capacity that was previously estimated, and geo-referenced weather data parameters such as wind speed, temperature, pressure, and irradiance from NASA’s MERRA-2<sup>8</sup> data set.

This weather data is computed to produce time-series generation profiles with a 1-hour resolution for individual wind turbines and solar PV plants. Terrain and location conditions that affect the technology performance are also accounted for. The LCOE calculation procedure is summarized in Figure 2-4.

Figure 2-4. Potential simulation block diagram.



<sup>7</sup> Renewable Energy Simulation toolkit for Python, Jülich Research Center.

<sup>8</sup> Modern-Era Retrospective analysis for Research and Applications, Version 2, NASA.

For this analysis, 20 years of weather data (2000–2019) were considered and averaged to obtain historical time-series generation profiles, the LCOEs, and the renewable techno-economical potential. The main techno-economical parameters used for the calculations are presented in Table 2-3.

Table 2-3. Main techno-economical parameters by 2050 for solar PV and onshore wind turbines according to estimations by HINICIO.

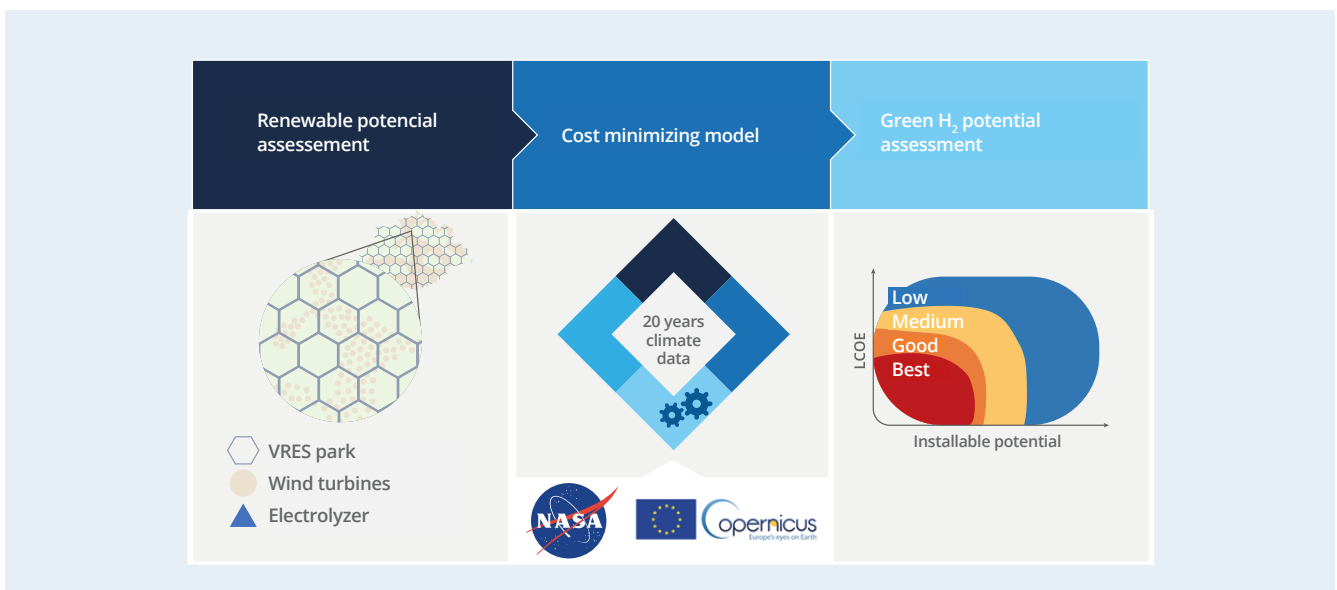
Equipment	Parameter	Value	Unit
Solar PV 	CAPEX	320	USD/kWp
	OPEX	2	% of capex
	Degradation	0.5	%/year
	Land usage	20	m <sup>2</sup> /MWp
	Lifetime	30	years
	Type	Fixed axis	
Onshore wind 	CAPEX	825	USD/kWp
	OPEX	3	% of capex
	Degradation		
	Land usage	0.46	Ha/MWp
	Lifetime	30	years
	Type	Onshore	

#### 2.1.4 Hydrogen production simulation

A simulation algorithm was developed to find the optimal electrolysis capacity while minimizing the green hydrogen production cost. Hybrid solar PV and wind plants were considered to maximize the hours of operation of the electrolyzer, with the hypothesis that they would yield lower costs of hydrogen than with

solar PV or wind alone (however, results showed the lowest LCOHs come from solar PV alone). The simulation computes the theoretical green H<sub>2</sub> production from the PEM electrolyzer according to the 20-years of weather data simulated to determine the corresponding Levelized Cost of Hydrogen (LCOH). A block diagram of the procedure is shown in Figure 2-5.

Figure 2-5. Hydrogen production simulation block diagram.



Around 5,800 renewable generation sites were delineated across the Mexican territory, each spanning on average of 365 km<sup>2</sup> of area containing wind turbines and solar PV modules. Methodologically, each site was defined as a Voronoi polygon<sup>9</sup>.

Then, an optimization is made where the algorithm computes all the possible PEMEL electrolyzer capacities (from 0 MW up to the VRES park capacity) according to the 20-years of weather data and selects the one that yields the lowest LCOH.

The capacity selected represents the on-site optimal electrolyzer capacity for the renewable energy plant. The production cost of green hydrogen (LCOH) includes investment costs, fixed and variable costs, depreciation, and contingencies and is calculated at the outlet of the electrolyzer. Hydrogen storage, conditioning, or transportation are not considered in the reported LCOH. The techno-economic parameters used in the model are shown in Table 2-4.

Table 2-4. Proton exchange membrane electrolyzer (PEMEL) techno-economical parameters used according to technology development expected by HINICIO by 2050.

Equipment	Parameter	Value	Unit
	Type	PEMEL	-
	Scale	Stationary	>10M
	CAPEX	300	USD/kWp
	OPEX	3	% de CAPEX
	Stack replacement	0.5	%/year
	Efficiency	69	%
	Lifetime	30	years
	Demineralized water	1	l/Nm <sup>3</sup> <sub>H<sub>2</sub></sub>
	VRES park size	365	km <sup>2</sup>

## 2.2 Results

This section presents the results of renewable energy and green hydrogen potential. Selected parameters are plotted in heat maps where red colors are associated with the best locations and progressively turn into blue as the potential decrease. White color is assigned to unavailable land according to the geospatial analysis.

Figure 2-6. Potential maps derivation from the potential assessment results.



<sup>9</sup> Voronoi polygons are geometric figures constructed around a set of points (Voronoi centers) such that each polygon contains all points (turbines or PV parks in this case) closer to its Voronoi center than to the center of any other Voronoi polygon, according to Evans, 1987.

## 2.2.1 Onshore wind energy potential

Results show that 430,000 km<sup>2</sup> of land in Mexico (~22% of the total) is eligible to accommodate up to 2.7 TW of onshore wind turbines that can produce up to 6.3 PWh<sup>10</sup> of renewable electricity each year with an LCOE equal to or lower than 60 USD/MWh. The LCOE potential map for onshore wind energy is shown in Figure 2-7. White areas are assigned to un-available land for onshore wind turbine installation.

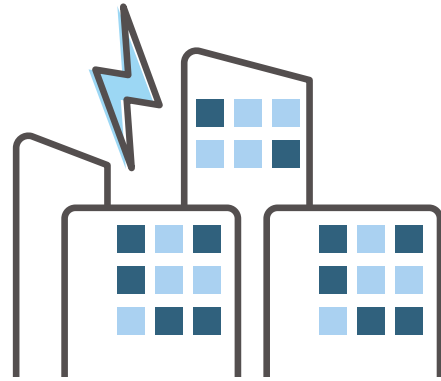
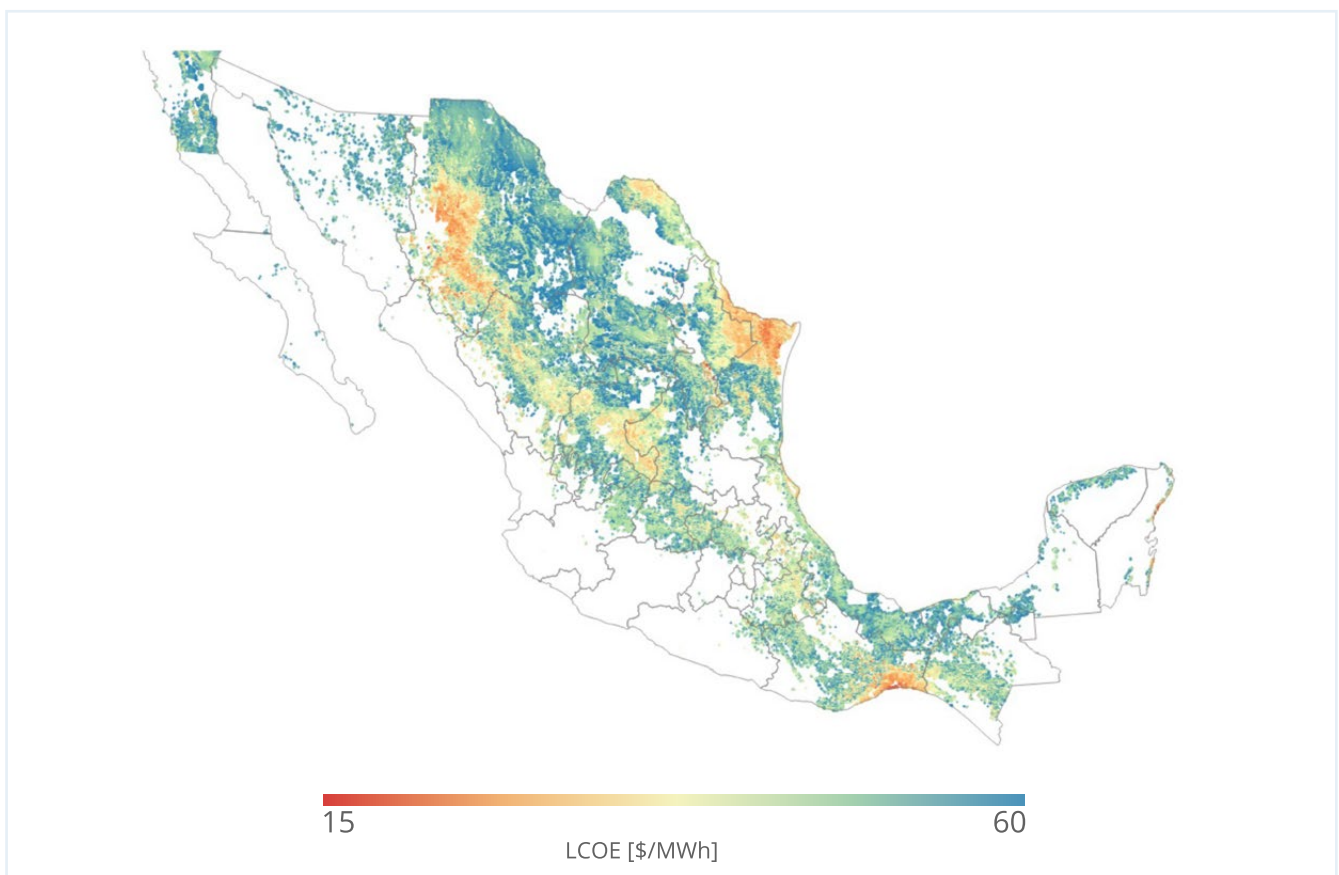


Figure 2-7. Onshore wind LCOE potential map.



Most of the un-available land is found along the Pacific coast, inside the Baja California and Yucatan peninsulas, and around the center of the country. The constraints responsible for this distribution of land are low wind resources and population-related constraints such as proximity to human settlements and roads.

Human settlements-related constraints are especially important for the densely populated center of the country. Constraints related to the conservation, woodlands, jungles, water bodies, and water lines are distributed slightly more towards the south of the country. In opposition, mining sites limiting the onshore wind turbine deployment are found mostly in the north of the country.

Moreover, wind resources are regional and of mountainous origin, as shown in Figure 2-7. There are three notorious wind-rich regions, in which the resulting LCOEs can be yielded at low costs starting from 15 USD/MWh:

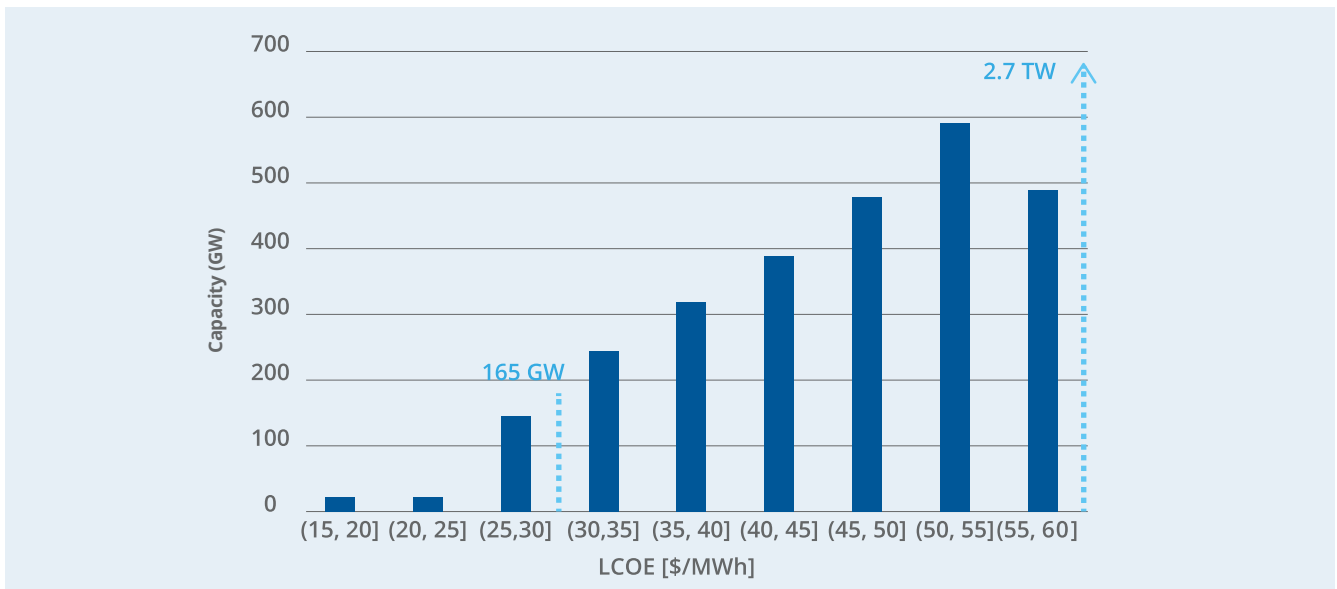
<sup>10</sup> PWh (Petawatt-hour) are equivalent to 1012 kilowatt-hours.

- **In the state of Oaxaca, isthmus of Tehuantepec: this region is currently the location with most of the wind energy installations in the country.**
- **The Western Sierra: the northern-central mountain chain that runs alongside the states of Chihuahua, Durango, and some parts of Zacatecas and San Luis Potosí.**
- **The last area is found in the north-eastern part of the country: in the states of Coahuila, Tamaulipas, and Nuevo León.**

The LCOEs for wind energy represented in the previous map are clustered in bins every 5 USD/MWh increment in Figure 2-8. The corresponding potential that could be

installed is shown in dark blue bars in GW for each bin. The cumulative capacity is marked for reference by the dotted light blue line.

Figure 2-8. Onshore wind capacity potential by LCOE.

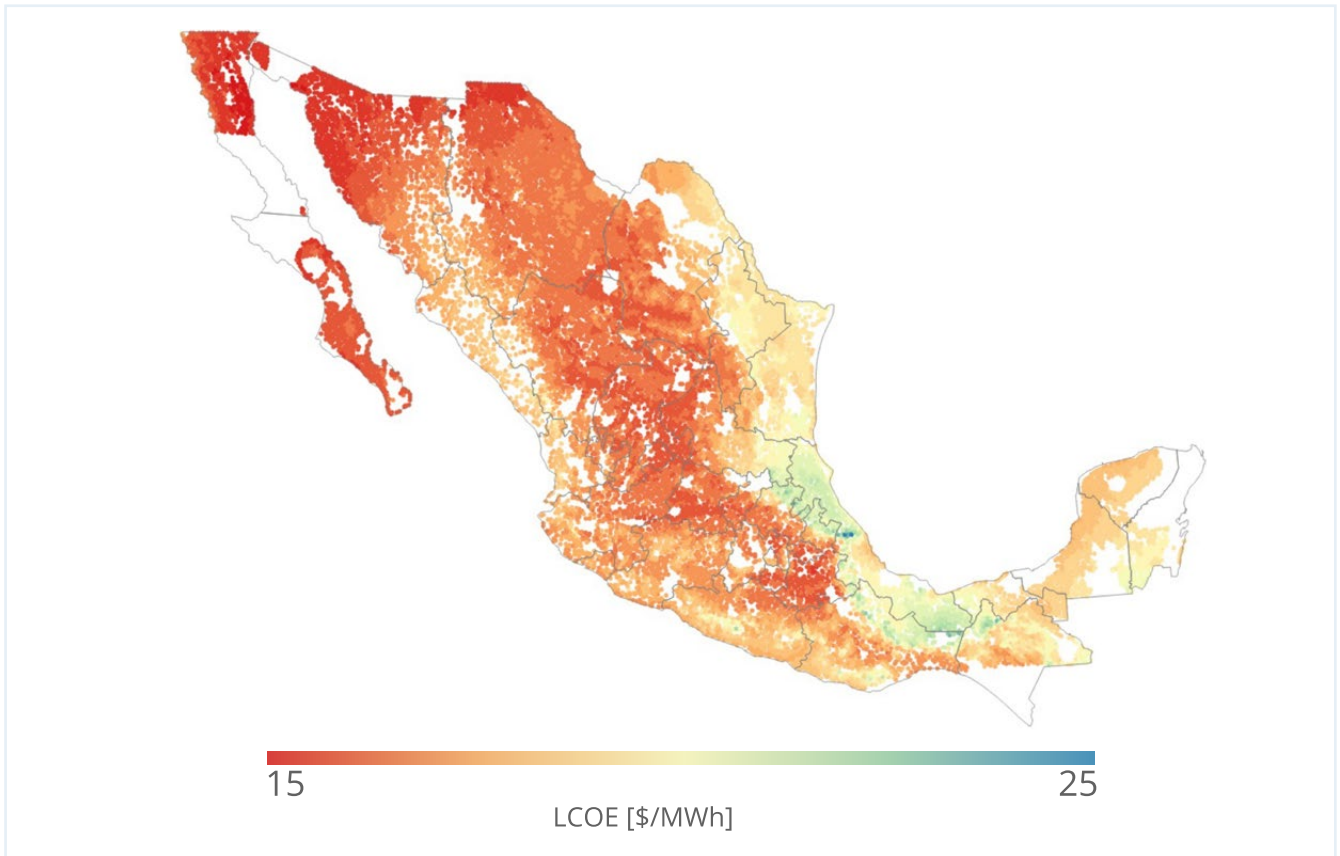


There are up to 165 GW of wind potential with LCOEs lower than 30 USD/MWh capable of producing around 600 TWh/year of electricity. This amount of energy would be enough to power the complete current electricity demand in Mexico. The capacity potential increases as the LCOE threshold increases for this regional resource in Mexico.

## 2.2.2 Solar PV energy potential

Results show that 650,000 km<sup>2</sup> of land in Mexico (~33% of the total) is eligible to accommodate up to 33.5 TW of solar PV parks that can produce up to 69 PWh of renewable electricity each year with an LCOE equal to or lower than 25 USD/MWh. The LCOE potential map for solar PV energy is shown in Figure 2-9. White areas are assigned to un-available land for installations of PV parks.

Figure 2-9. Solar PV LCOE potential map.

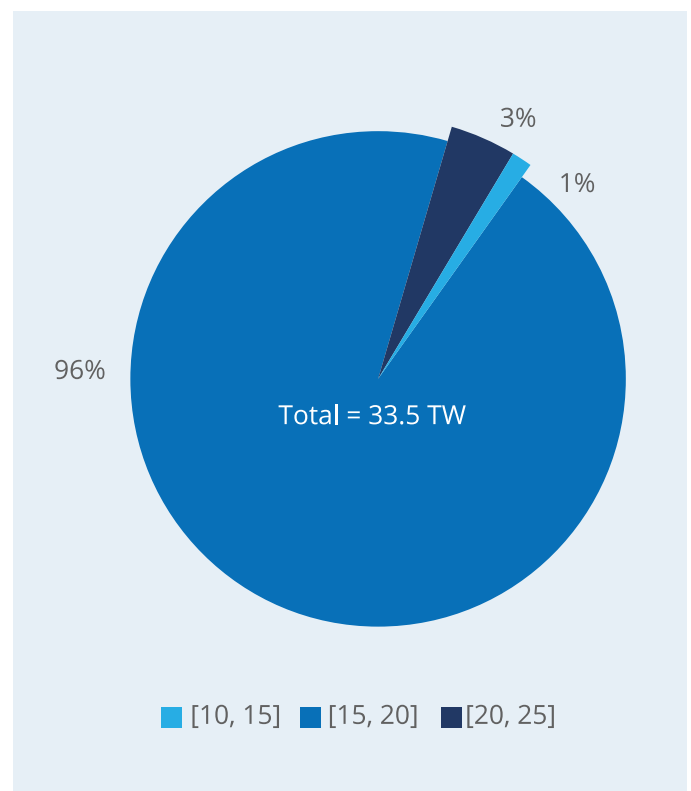


The unavailable land corresponds mostly to slope-related constraints, conservation areas, and settlement-related areas. Slope-related constraints, i.e., terrain too inclined to place PV panels, affect generally all the country. In both the Baja California and Yucatan peninsulas, there are large portions of unavailable land that are due to natural reserves and protected areas. The center of the country and regions with large urban settlements and agriculture show little land availability for PV.

The solar PV potential appears to be affected by regional weather conditions near the coasts. Tropical weather, more clouds, and higher humidity in the air affect the full load hours of the solar PV plants. These effects explain the difference in potential across the country.

Furthermore, the LCOEs coming from PV are much lower and less variable than those from onshore wind, as shown in Figure 2-10. The vast majority of PV potential (96% of the total) falls in the 15 – 20 USD/MWh LCOE range. Only 3% is in regions a bit less favorable with production cost varying from 20-25 USD/MWh and the remaining 1% of the potential can be yielded at LCOES lower than 15 USD/MWh.

Figure 2-10. Solar PV capacity potential by LCOE [USD/MWh].



The energy coming from the 1% best PV locations is enough to satisfy around 1.5 times the current national energy demand, confirming Mexico's expected large PV potential.

### 2.2.3 Hybrid solar PV-wind energy potential

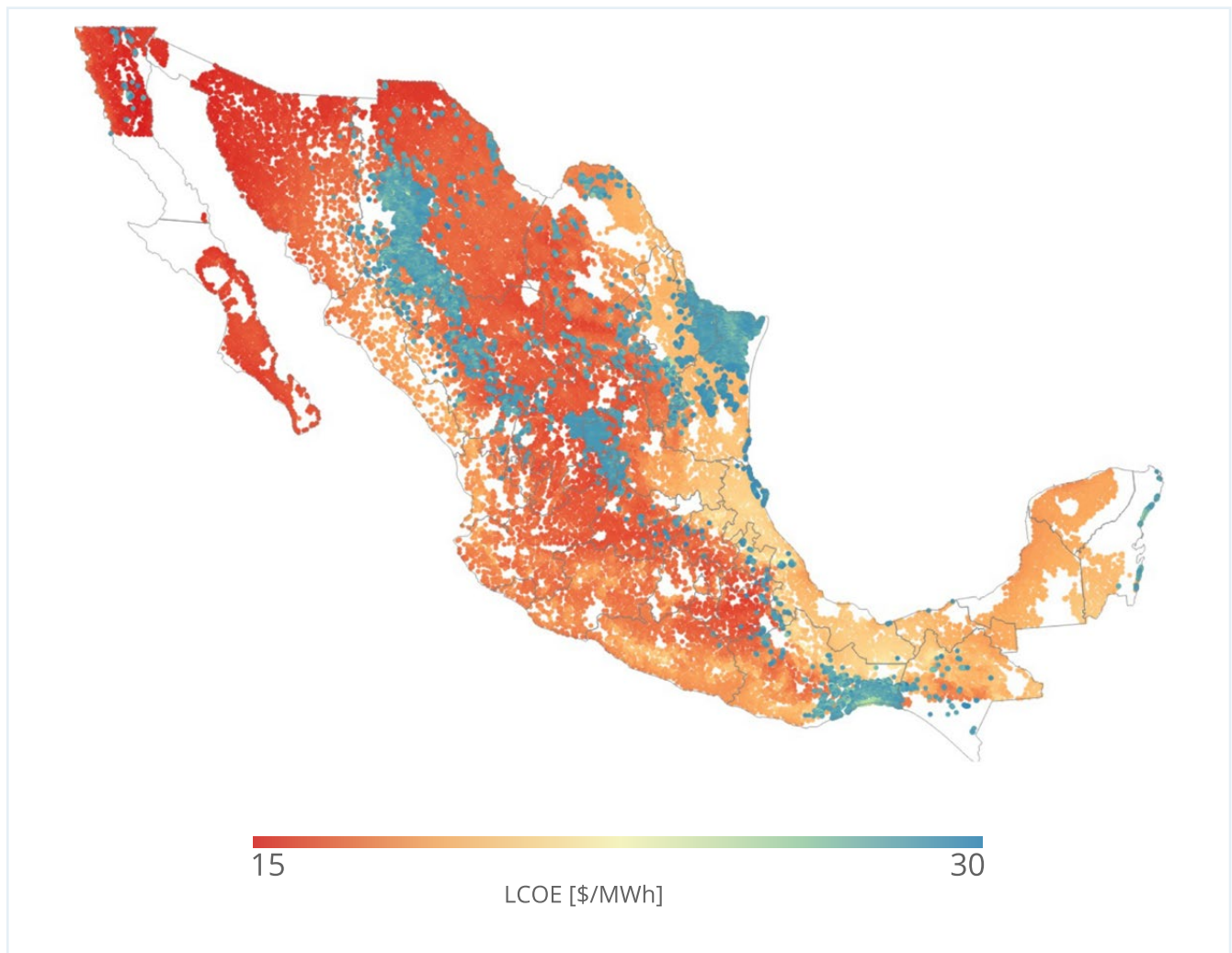
Both the wind and solar PV potentials are merged in a heat map as displayed in Figure 2-11. The LCOEs shown represented are for solar PV and wind energy together. As shown previously by Figure 2-7. and Figure 2-8, only good wind locations can produce LCOEs lower than 30 USD/MWh, which means that virtually all wind locations in Figure 2-11. are shown in blue, which is the highest in the color scale for LCOEs.

When no LCOE is taken into consideration, the solar PV potential is 10 times more abundant than onshore

wind energy. But since there is a lot of wind resource variability, if an LCOE of 30 USD/MWh is considered as a cost ceiling, the proportion is ten folded to 100 times more. This proportion gives clear evidence about the differences in renewable potential between these two VRES technologies and reveals that a strong solar PV dominance for producing green hydrogen is likely to occur.

However, the location of wind resources will determine the possible location of hybrid wind and PV parks. Good wind regions overlap with good solar regions as shown in Figure 2-11, like in the Western Sierra and medium solar regions (such as Oaxaca and Tamaulipas), as well as in regions where no big solar parks can be deployed like the shores of the Yucatán peninsula.

Figure 2-11. Hybrid wind-solar PV levelized cost of electricity potential map.



### 2.2.4 Green hydrogen potential

Up to 22 TW of PEM electrolysis capacity can be installed across Mexico. They can produce up to 1,400 Mth<sub>2</sub>/year with an average of 1.4 USD/kgH<sub>2</sub>. The LCOH potential map locations for green hydrogen production from VRES sources is shown in Figure 2-12.

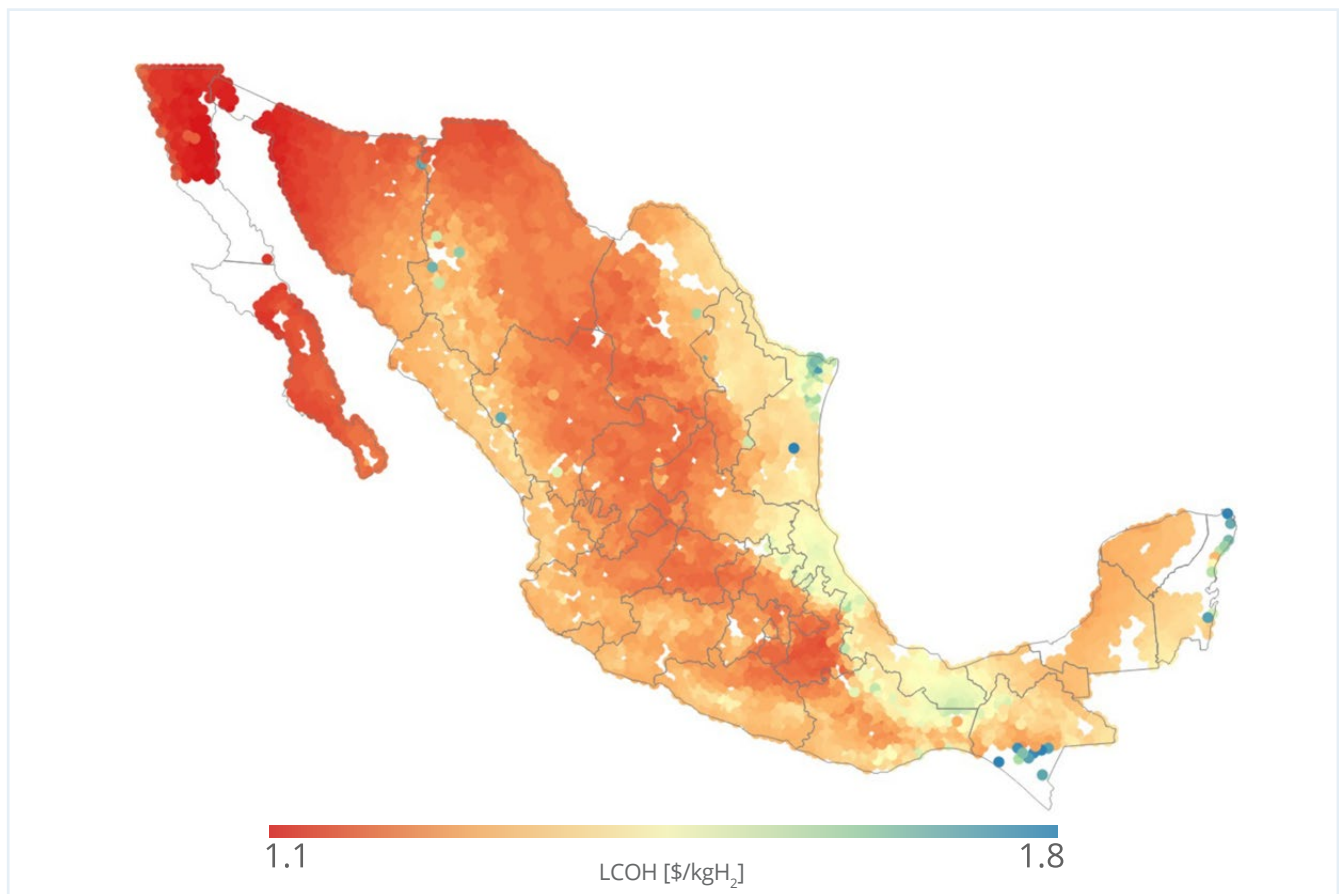
The map reveals that the green hydrogen potential is similar to the solar PV potential, driven by the low-cost solar energy, which enables the most competitive green hydrogen production. Given the large difference between onshore wind and solar potential in Mexico, it is expected that the green hydrogen production at low LCOEs will be powered mainly by solar PV in a 100 to 1 proportion relative to wind. The strong prevalence of solar energy

in green hydrogen production also means that Mexico could follow the same production cycles as solar energy radiation if no energy storage or complementary power from the grid are considered.

Places where there can be hybrid green hydrogen production like in Oaxaca and the Western Sierra appear to have LCOHs of around 1.5 USD/MWh, but not as low as the solar-only green hydrogen production that occurs in the north-western part of the country, for example.

There are also some competitive wind-only green hydrogen production locations like in the western shores of the Yucatán peninsula and the north of Tamaulipas. The LCOHs resulting in these locations are in the upper-cost range of around 1.8 USD/kgH<sub>2</sub>.

Figure 2-12. Levelized cost of hydrogen from hybrid wind-solar PV production.



The water usage for green hydrogen production as compared with the total water use per state according to official CONAGUA records<sup>11</sup>, as shown in Figure 2-13.

If all of the states' shown green hydrogen production potentials were put to use, less than 1% of the water that

is used in each would be compromised. Added together, 116.8 (~0.13%) of water used nationally would be required to produce all the green hydrogen potential.

<sup>11</sup> CONAGUA, Estadísticas del Agua en Mexico 2017.

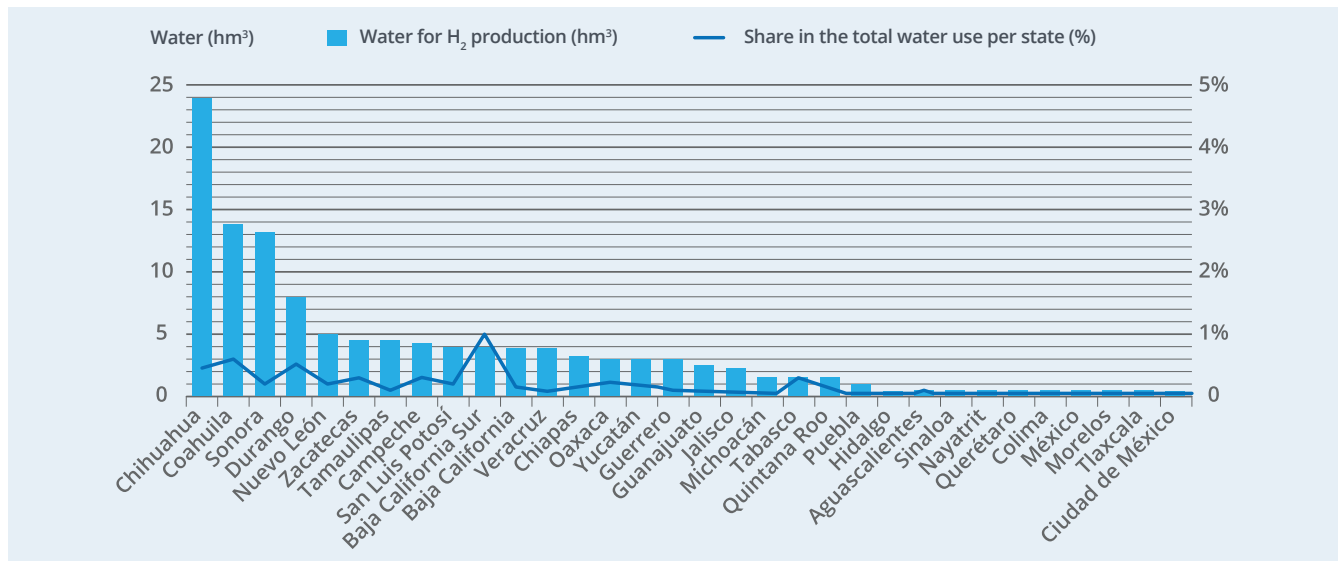
Figure 2-13. Water use of green H<sub>2</sub> production as a share of the total water consumption in 2017.

Table 2-5. Green hydrogen production parameters by state.

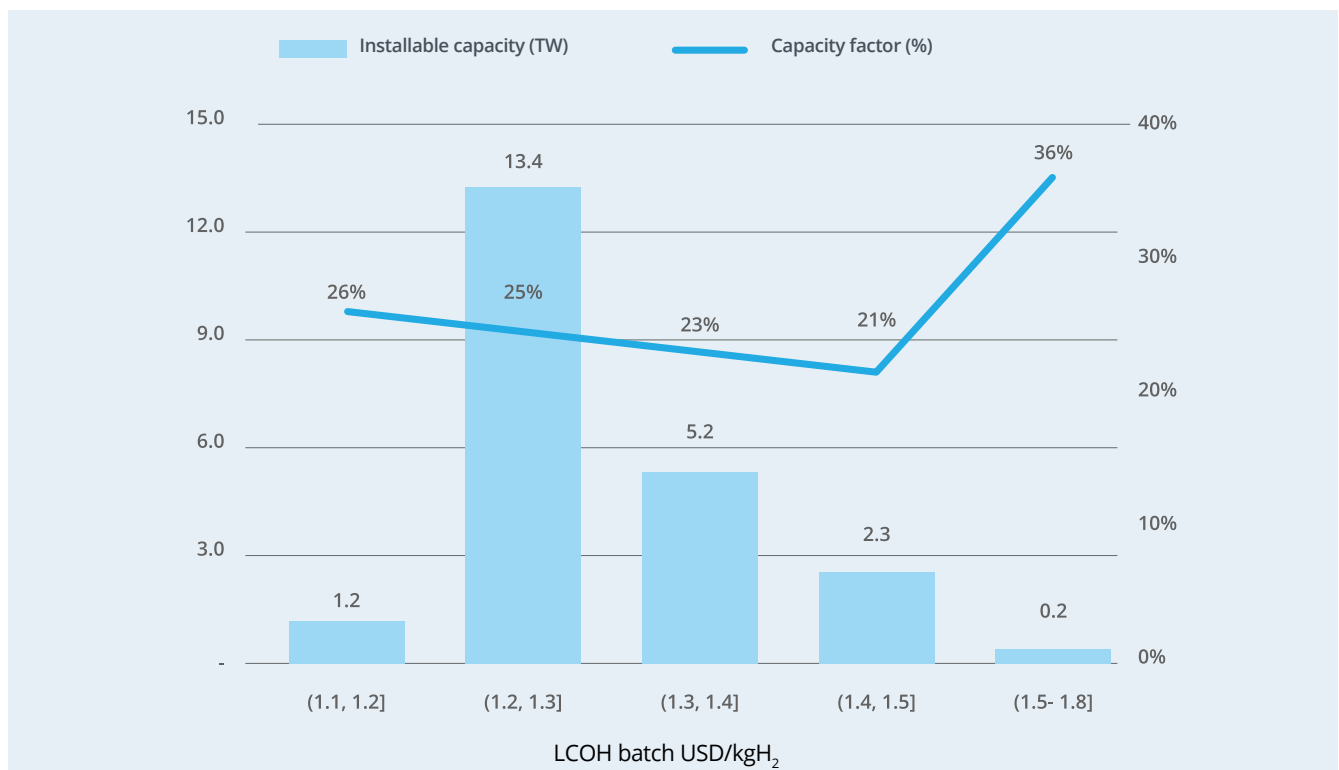
State	Annual green H <sub>2</sub> production [Mt <sub>H<sub>2</sub></sub> /year]	PEMEL capacity [GW]	Average LCOH [USD/kg <sub>H<sub>2</sub></sub> ]	Water consumption [hm <sup>3</sup> /year]
Aguascalientes	4.8	78	1.25	0.4
Baja California	46.8	683	1.18	3.9
Baja California Sur	48.3	747	1.22	4.0
Campeche	50.9	784	1.34	4.2
Coahuila	161.0	2,571	1.30	13.4
Colima	3.5	60	1.33	0.3
Chiapas	38.7	624	1.40	3.2
Chihuahua	291.6	4,619	1.28	24.3
Ciudad de México	0.2	3	1.31	0.02
Durango	99.0	1,589	1.29	8.2
Guanajuato	32.0	512	1.26	2.7
Guerrero	34.4	562	1.33	2.9
Hidalgo	4.8	78	1.35	0.4
Jalisco	26.8	445	1.30	2.2
México	2.8	46	1.29	0.2
Michoacán	16.9	283	1.32	1.4
Morelos	1.1	18	1.25	0.1
Nayarit	4.3	71	1.34	0.4
Nuevo León	59.7	963	1.37	5
Oaxaca	34.6	555	1.38	2.9
Puebla	9.5	149	1.30	0.8
Querétaro	3.6	58	1.27	0.3
Quintana Roo	13.7	217	1.43	1.1
San Luis Potosí	48.4	766	1.32	4.0
Sinaloa	4.8	80	1.36	0.4
Sonora	154.6	2,429	1.24	12.9
Tabasco	14.2	227	1.38	1.2
Tamaulipas	54.1	855	1.42	4.5
Tlaxcala	0.5	9	1.25	0.05
Veracruz	45.9	760	1.46	3.8
Yucatán	34.5	540	1.34	2.9
Zacatecas	55.1	881	1.26	4.6

The installed capacities for electrolyzer and their corresponding capacity factors at several LCOH ranges are shown in Figure 2-14. Most of the hydrogen potential can be produced at around 1.2 - 1.3 USD/kgH<sub>2</sub> with a 25% electrolyzer capacity factor. As expected, the hydrogen production cost increases as the electrolysis capacity factor decreases.

Green hydrogen production sites with 26% capacity factor values can produce hydrogen at 1.1 USD/kg H<sub>2</sub> whereas in sites with 21% capacity factor values the cost of production is up to 27% more expensive at 1.5 USD/kgH<sub>2</sub>.

Nevertheless, hydrogen production sites with LCOHs clustered within the 1.5 - 1.8 USD/kgH<sub>2</sub> range are an exception to the rule. This LCOH bin corresponds to hybrid and wind-only renewable sites.

Figure 2-14. Green hydrogen potential by LCOH.



The capacity factor in these parks is 36% on average but some hybrid parks can have up to 52% capacity factors. The resulting LCOHs at their locations are not lower than solar-only parks because there is a trade-off between higher capacity factors that the wind energy brings to the electrolyzer and the higher electricity cost due to wind energy usage. Moreover, because the wind potential is considerably lower in comparison with solar, only 1% of the electrolysis capacity (200 GW) could be a hybrid or wind-only park. It must be noted, however that this 200 GW of hybrid capacity are several times larger than the total expected installed capacity in Mexico even in 2050.

factors of around 26% coincide perfectly with the best solar energy locations, and higher capacity factors are in wind-rich regions where hybrid and wind-only hydrogen production are possible.

From an electrolyzer capacity factor heat map it can be observed that locations with capacity factors from 20 to 25 % correspond with the less favorable solar locations, as shown in Figure 2-15. Locations with capacity

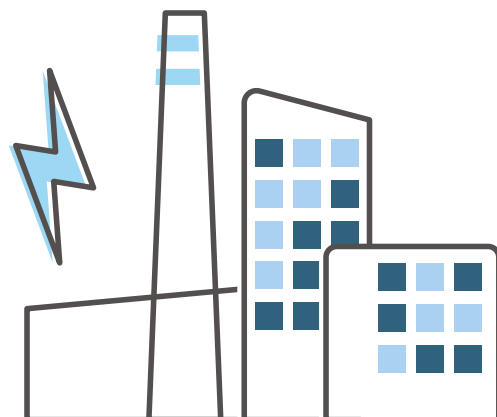
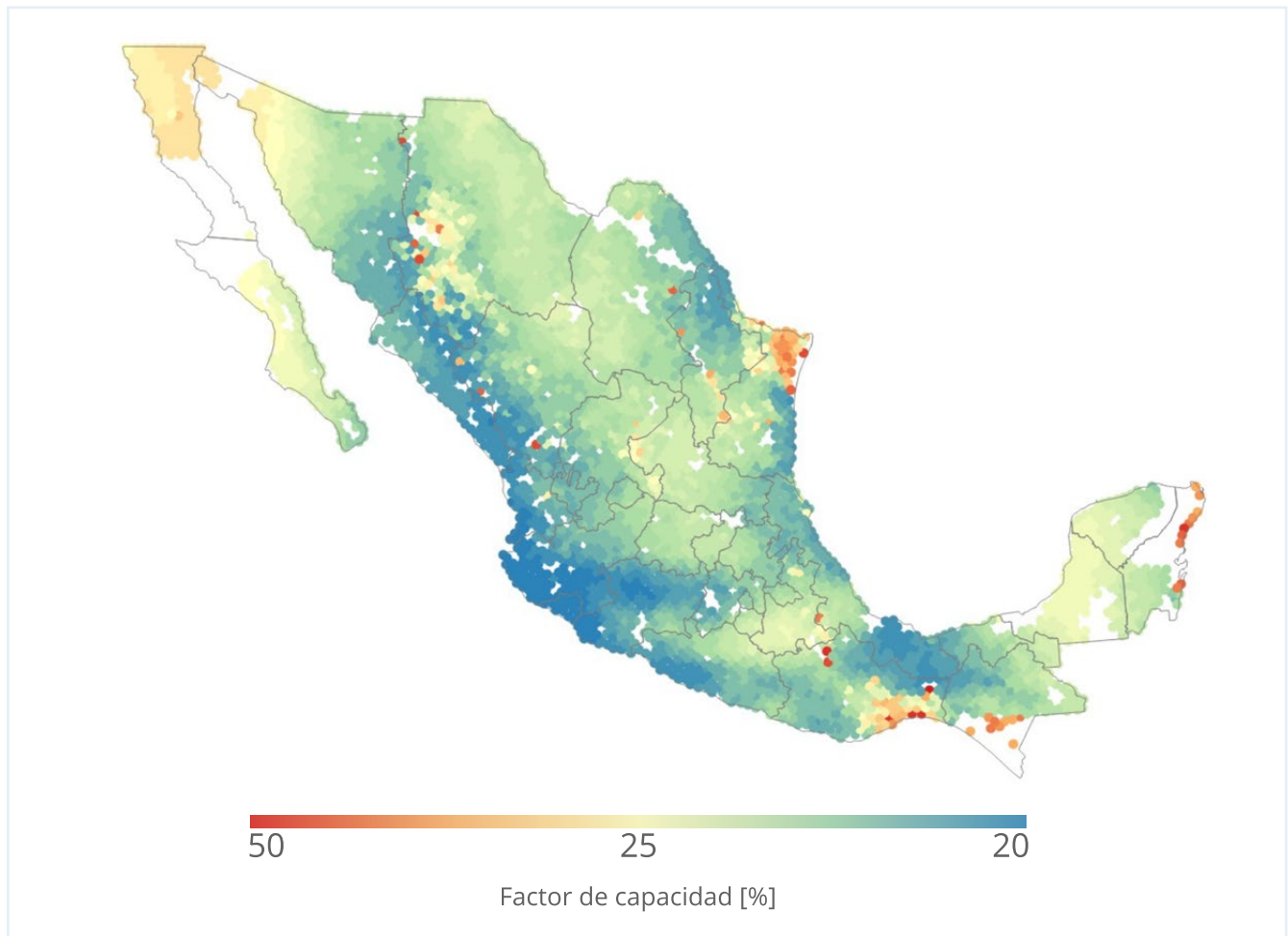


Figure 2-15. PEMEL capacity factor potential map.



It is important to highlight that having electrolyzers with higher capacity factors means that hydrogen production occurs also in non-diurnal times. Since 99% of the hydrogen production could be bounded to solar cycles, investments in hybrid parks could still be attractive under some conditions.

### 2.3 Comparison of results with official estimates

The Mexican Government released in 2017 the National Inventory of Zones with High Potential for Clean Energy or AZEL<sup>12</sup> that assessed the solar and wind potentials in Mexico in four scenarios. HINICIO's wind assessment is comparable with AZEL's wind scenario 3, which only considers sites within 10 km of the national transmission system. HINICIO's solar assessment is comparable with AZEL's solar scenario 1 due to the similar land restrictions considered in the geospatial analysis, which do not consider proximity to transmission lines. In terms of green hydrogen potential, no similar assessment was found by official sources to make a results comparison.

The onshore wind energy generation potential obtained by HINICIO in this assessment is 6.3 PWh/year or ~10% lower than in the 6.9 PWh/year found in the AZEL.

Several differences in the applied methodologies can explain this difference. First, there is a big difference in the land available determined by AZEL's scenario 3. AZEL installable capacity determination does not discriminate between good and bad wind locations which results in around 10% higher generation potentials compared with HINICIO's results despite having similar installable capacities. Another difference is the land available for onshore wind installations. In AZEL's assessment, only land within 10 km from a transmission line is considered. This land consideration largely reduces by 90% the land available for installations compared to HINICIO's assessment, which did not consider it to allow for possible grid expansion that could be directed by the newly found renewable potential. Other land restrictions are similar in both studies. Lastly, the generation estimation by HINICIO was a physics-based simulation

<sup>12</sup> Atlas nacional de Zonas con alto potencial de Energías Limpias, Secretaría de Energía <https://dgel.energia.gob.mx/azel/>

of 20 years of weather data, whereas AZEL used a generation density estimation.

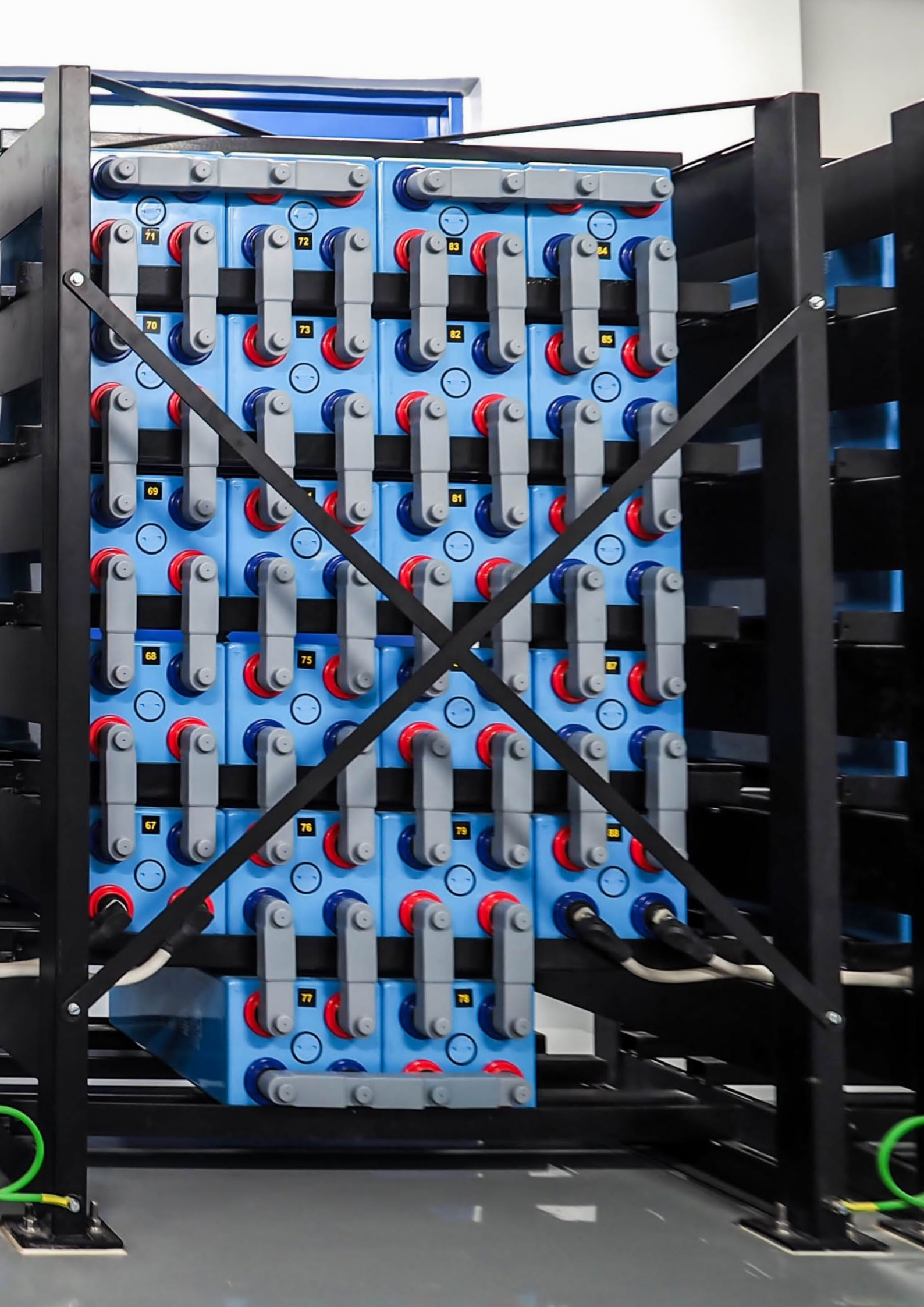
In terms of solar PV potential, AZEL estimates around 511,000 km<sup>2</sup> available for PV installations, whereas HINICIO estimated 650,000 km<sup>2</sup> (~20% more). The difference is due to AZEL does not consider sparse potential (fewer than 150 hectares), whereas HINICIO does. Additionally, AZEL includes restrictions for natural disaster zones, which HINICIO did not consider. The solar generation potential in HINICIO's assessment is 15% larger than AZEL due to improvements in the PV panel efficiency expected by 2050. Nevertheless, the

similar solar potential above 60 PWh/year found in both assessments brings certainty about the large solar PV potential in Mexico.

## 2.4 Conclusions

The results of the assessment presented in this chapter lead to several conclusions which will be used to design an energy system model for the following activities to assess the benefits and integration potential of hydrogen in the Mexican power system.

- **Both wind and solar energy have the potential to cover the entire current electricity demand at a cost lower than 30 USD/MWh by 2050. However, a huge difference between solar and wind energy was found. Solar generation potential is up to 100 times higher than wind at LCOEs equal to or lower than 30 USD/MWh.**
- **The distribution of solar is more homogeneous across the country with a tendency to be higher in the north-west region, whereas wind resources are region-specific.**
- **Up to 33 TW of solar panels can be installed with an LCOE equal to or lower than 26 USD/MWh, whereas the wind potential is up to 2 TW installed capacity with an LCOE equal to or lower than 60 USD/MWh.**
- **Green hydrogen production will be driven strongly by the PV potential due to its large renewable potential and low energy cost, and hydrogen production would be subjected to the same hourly operational characteristics.**
- **Hybrid solar PV-wind hydrogen production can be up to 40% more expensive but from a system perspective it can be useful to match energy consumption by being produced at non-diurnal times. Considering both cases, 1,400 Mton of green hydrogen can be produced yearly.**
- **Since wind energy production has higher LCOEs than solar, renewable hybrid parks for hydrogen generation have a higher LCOH than solar only, despite having a higher capacity factor.**



71

72

83

84

70

73

82

85

69

81

68

75

87

67

76

79

88

77

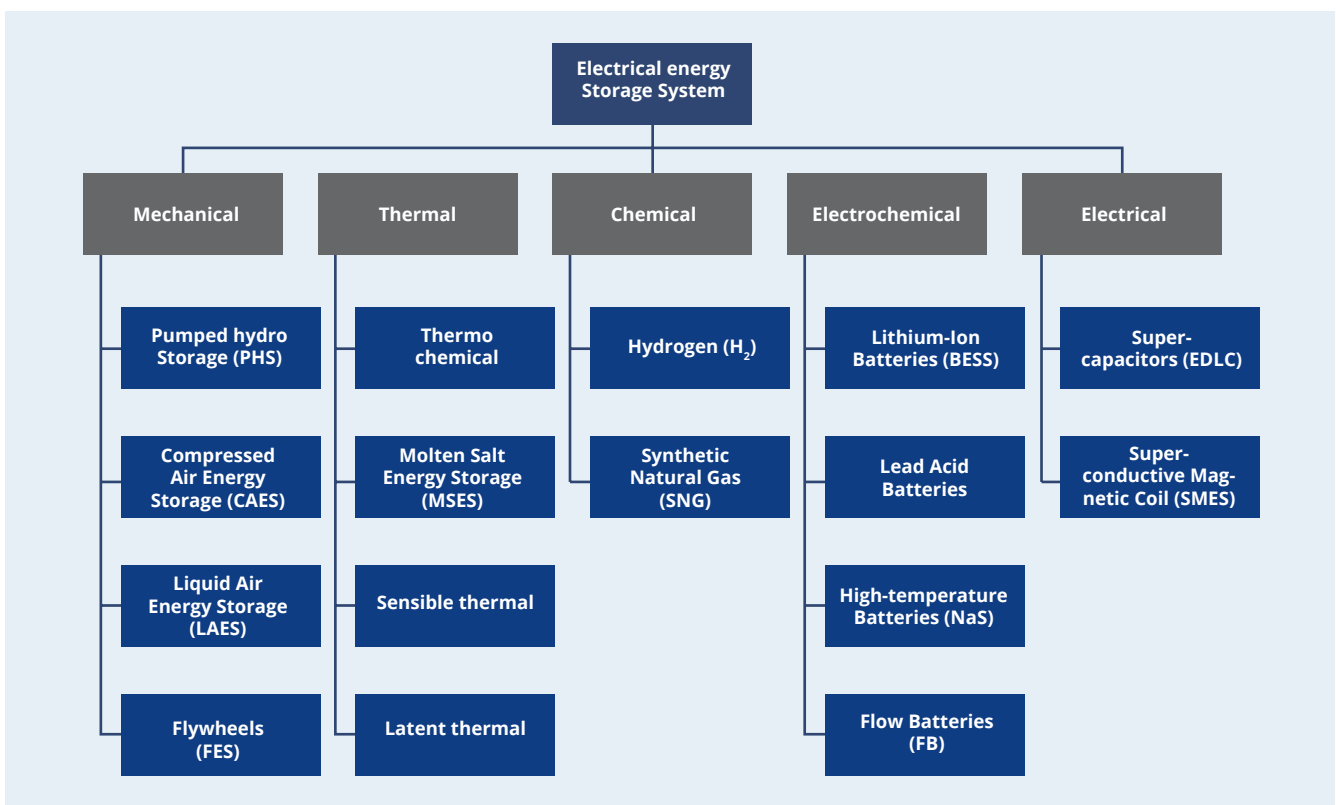
78

## 3. Energy Storage Technologies

### 3.1 Introduction

This chapter provides a detailed review of the basic concepts and an updated state of the art of the main energy storage technologies used in power systems. Additionally, a suitability and performance analysis of each technology on different applications is made. An overall presentation of energy storage systems can be found in this subchapter, 3.1., the methodology followed is illustrated in 3.2, a description of each of the technologies assessed is included in 3.3, a summary of the results in 3.4, and finally the conclusions in 3.5. Energy storage systems (ESS) allow the accumulation of energy in different ways: mechanical, thermal, electromagnetic, chemical, and electrochemical. The most common classification is based on the form of the stored energy as shown in Figure 3-1.

Figure 3-1. Scientific categorization of energy storage technologies<sup>13</sup>.



Energy storage systems (ESS) allow the accumulation of energy in different ways: mechanical, thermal, electromagnetic, chemical, and electrochemical. The most common classification is based on the form of the stored energy as shown in Figure 3.1.

The pumped hydro (PHS), compressed air (CAES), flywheel (FES), molten salt (MSES), and lithium-ion battery (BESS) technologies covered 99.2 % of the total installed capacity worldwide in 2020 with 189 GWh of 191 GWh<sup>14</sup>. Figure 3-2. shows the worldwide installed capacity by technology group and Figure 3-3. shows the global operational energy storage power capacity by technology to date.

<sup>13</sup> World Energy Council, World Energy Resources - E-storage: Shifting from cost to value, 2016.

<sup>14</sup> US Department of Energy, DOE Global Energy Storage Energy Storage Database.

Figure 3-2. Worldwide installed capacity of ESS by technology, Nov-2020.

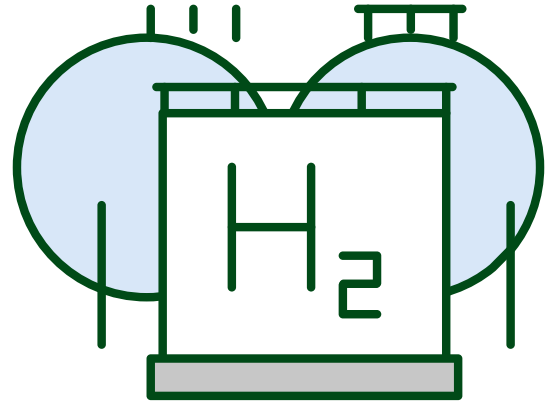
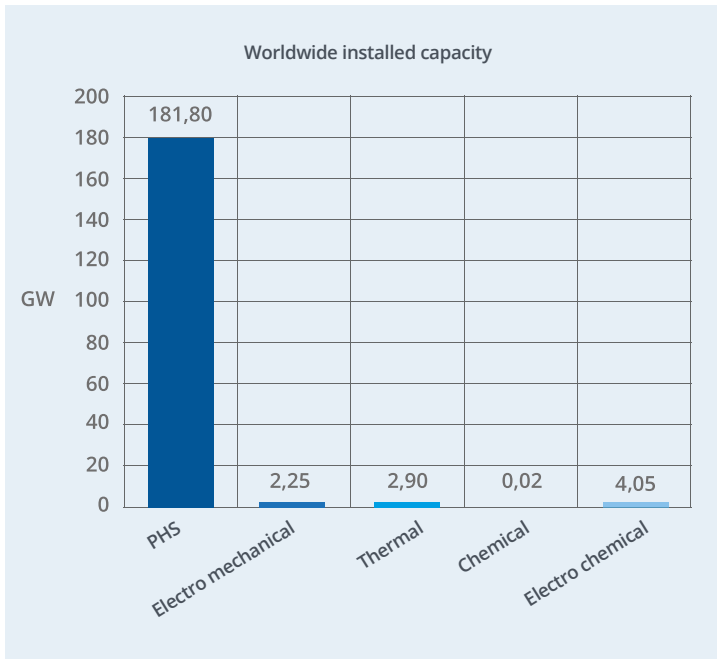


Figure 3-3. Global operational energy storage power capacity by technology excluding PHS, Nov-2020.

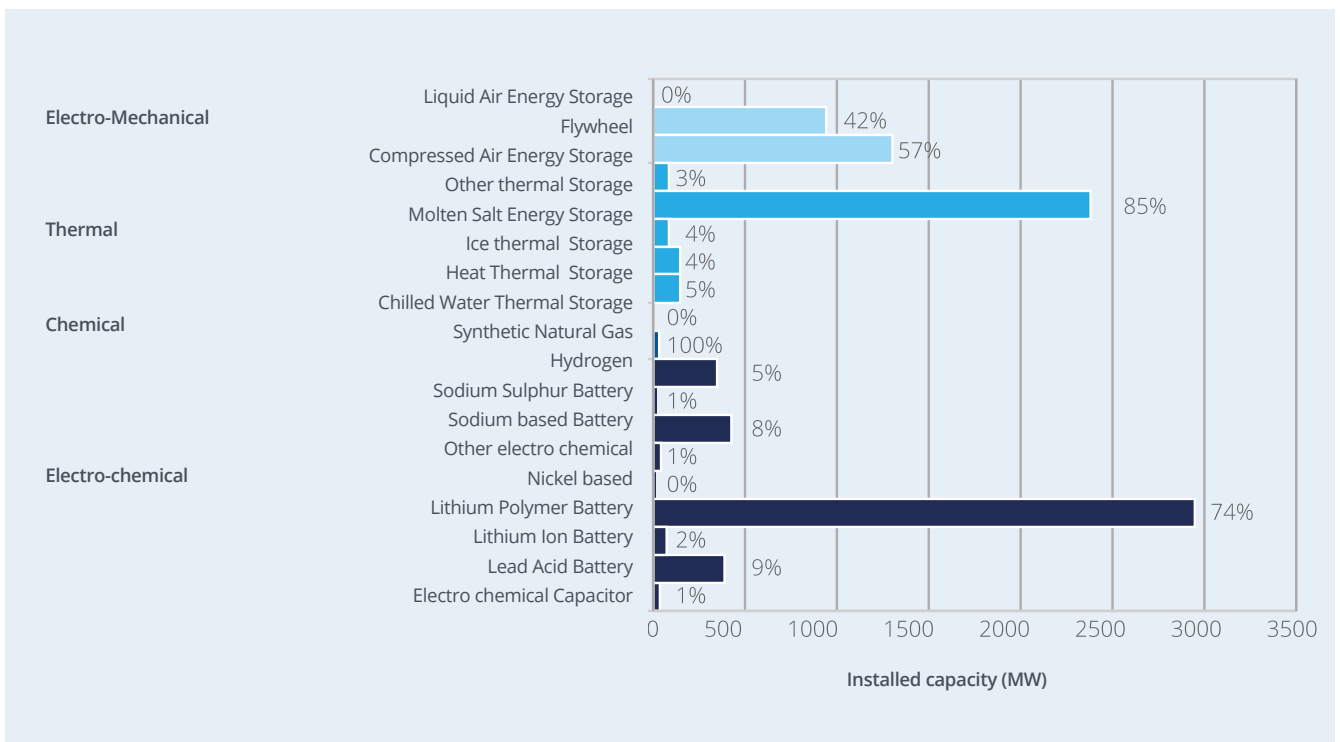
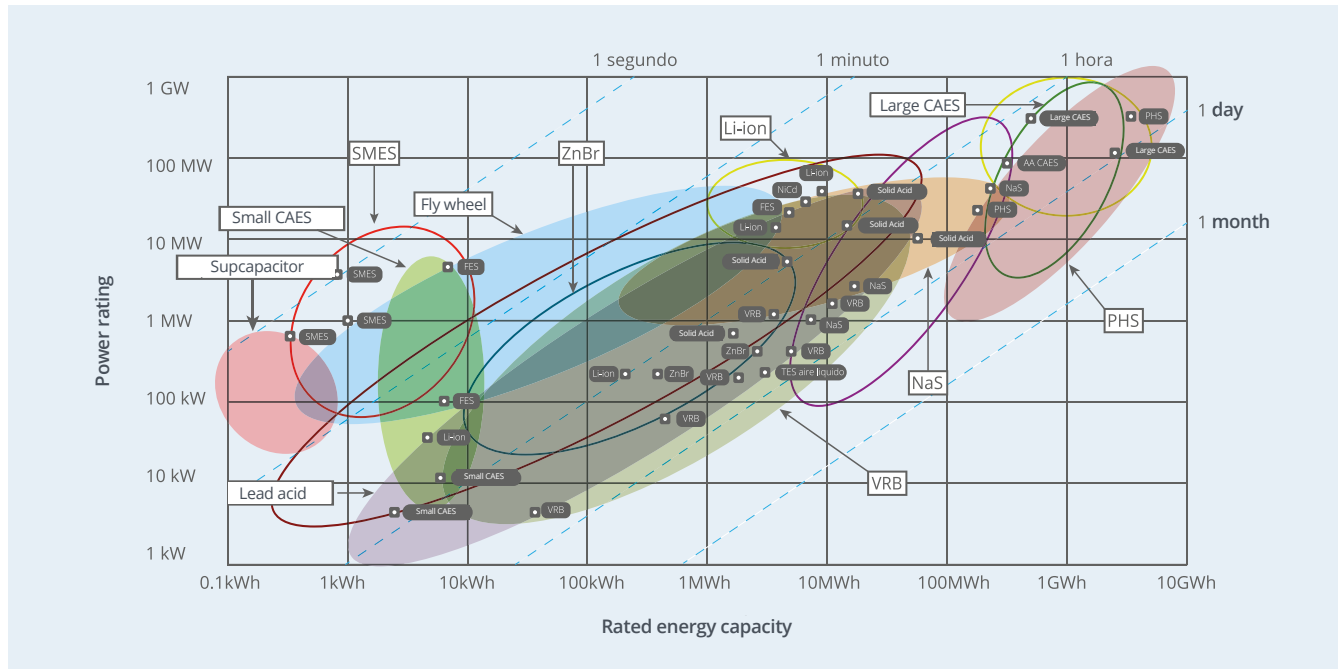


Figure 3-4. below shows the power rating vs the rated energy capacity of each storage technology and the respective time of response.

Figure 3-4. Comparison of nominal power, energy capacity, and time of response<sup>15</sup>.



This provides a general overview of the performance of different technologies. For example, for lithium ion (Li-ion) batteries it is possible to notice that they cover almost the whole center of the graph, between the diagonals of 1 minute and 1 hour response time, which shows that they are a fast technology, with a high power capacity and that they are better suited for short-term non-stationary applications (with rated energy under 30 MWh). On the other hand, pumped hydro and compressed air have a high power rating and a high rated energy capacity, showing that they are more suitable for long-term stationary applications.

### 3.2 Methodology

The first step of methodology consisted in a detailed bibliographic review of the existing storage technologies and their main parameters and characteristics. The review included sources such as the International Renewable Energy Agency (IRENA), Bloomberg NEF, Lazard, the International Energy Agency (IEA), the Institute of Electrical and Electronics Engineers (IEEE), ScienceDirect, World Energy, and the U.S Department of Energy (US DOE).

To make a fair comparison between different energy storage technologies, all the required equipment for storing and delivering energy were included, allowing the inputs and outputs to be the same for all the technologies. After the standardization, all energy storage technologies are comparable within the framework of a power-to-power system. Although the levelized cost of storage (LCOS) can be used to compare the different storage technologies, it will not be used because its calculation requires further research which is beyond the scope of this report.

Once the information was collected and to make a quantitative comparison of the different technologies, a methodology by IRENA was followed which is composed of six phases used to determine which technologies have the best performance per application in electric power systems.

<sup>15</sup> X. Luo, "Overview of current development in electrical energy storage technologies and the application potential in power system operation", 2015.

### Phase 1: Selection of relevant parameters

The selection of the relevant parameters will depend on the application to which the energy storage system is oriented. In this case, the best-adapted technologies are sought for their general application to Electric Power Systems (EPS).

Therefore, it is required a mature technology that can compete with the storage currently installed in power systems, and at the same time, their performance must be good enough to participate in the different markets. For example, the ESS must have a fast time of response to provide ancillary services, store energy for long periods of time to provide capacity firming, or must be able to perform a daily cycle in the case it provides smoothing for renewable energy.

Considering this, the relevant parameters for this study are CAPEX, roundtrip energy efficiency, lifetime, self-discharge, maturity, space required, and response time. Then, depending on the application to be studied in each case, a weighted or “percentage of importance” will be assigned to each relevant parameter, which will be explained in Phase 3 of this methodology.

### Phase 2: Assignment of competitive scores to each parameter of each technology

Based on the values of technical and commercial parameters identified as relevant, competitiveness scores between 1 and 5 were assigned to each parameter, where 5 represents the best score and 1 the worst.

### Phase 3: Parameter weight for applications

Four applications oriented to electric power systems were identified. Depending on the application, a weight was associated with each parameter. In this way, it will be possible to differentiate that for certain applications some parameters are more important than others. The applications to be analyzed are capacity firming, ancillary services, renewable shifting, and renewable smoothing.

### Phase 4: Applying a suitability matrix

The competitiveness score of each technology (Phase 2) and the rated weights (Phase 3) provide an overall picture of how suitable each technology is for each application. However, the combination of scores and weights is often insufficient because they could vary depending on the specific case.

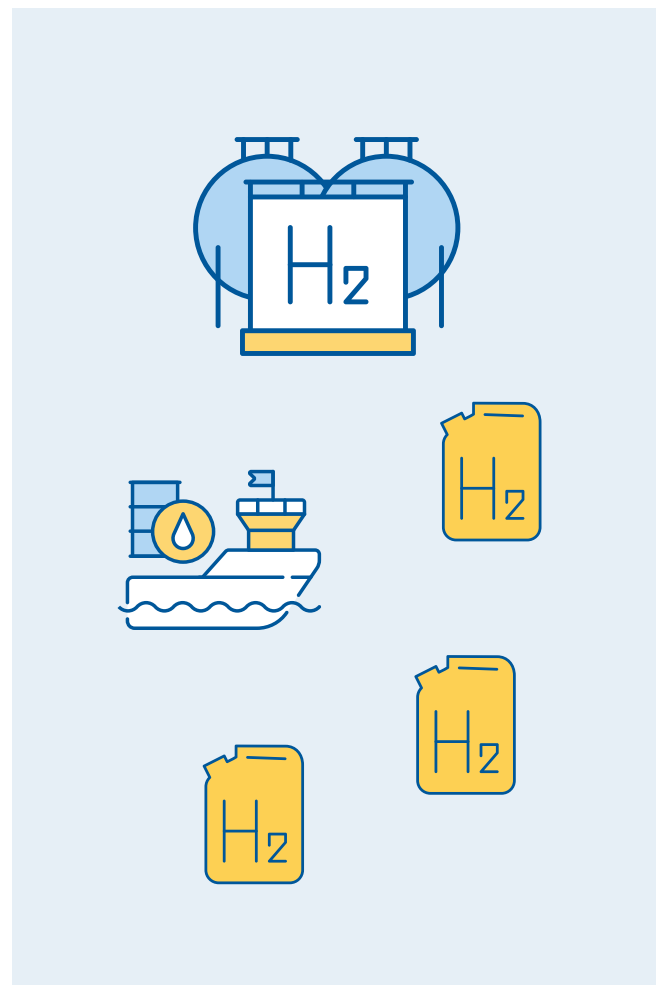
To address this issue, a suitability matrix is created to provide the opportunity of adjusting the weighted score. This is done by associating to each technology a value between 0 and 1, depending on how adapted the technology is to each application.

### Phase 5: Calculation of the final weighted score for each technology

Phase 5 consists of calculating the final weighted score of each technology. First, the factors mentioned in phases 2, 3, and 4 are multiplied, obtaining the weighted score of each parameter. Then all the scores belonging to each technology are added together, obtaining the final weighted score for each application.

### Phase 6: Application ranking

Finally, with the average weighted scores, all the technologies are rated, obtaining a ranking from 1 to 11 of all the analyzed technologies.



### 3.3 Technologies description

#### 3.3.1 Pumped Hydro Storage (PHS)

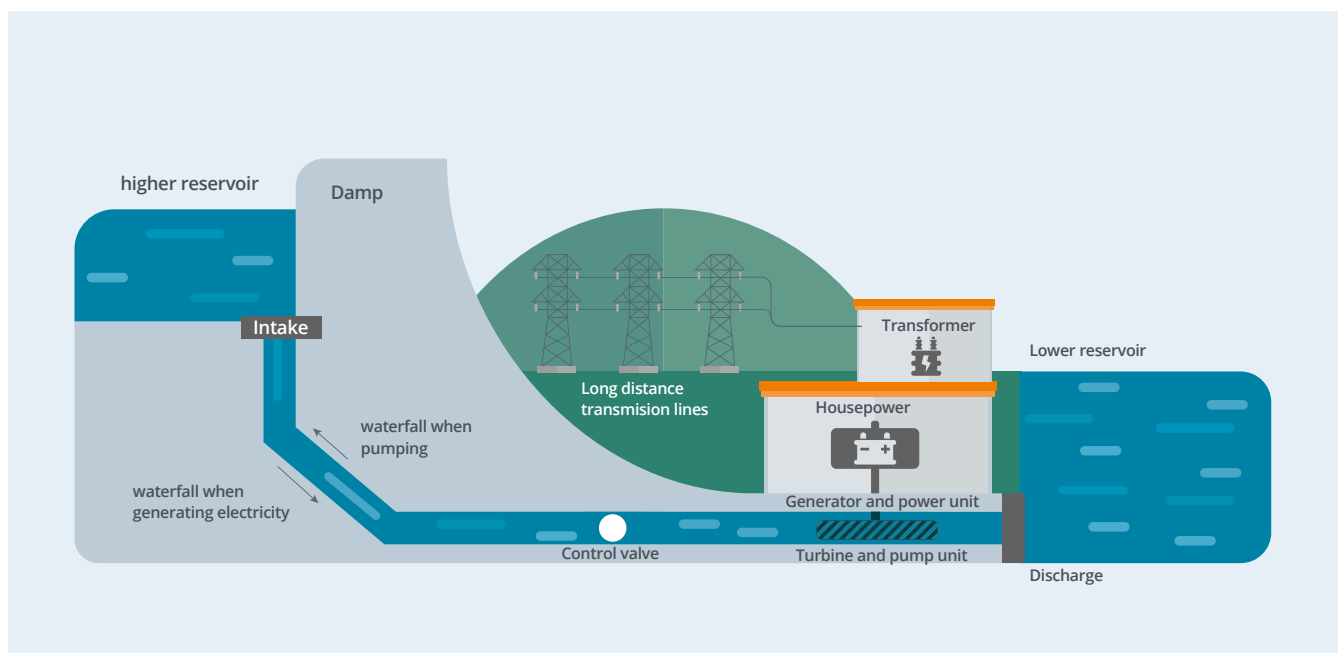
Pumped storage power plants are the most widely developed large-scale energy storage technology available today. In the 1890s it began its commercialization, reaching an installed capacity of 182 GW by the end of 2020. Therefore, PHS is a mature technology that has reached a high level of development in terms of improvements in the efficiency and maintenance of the plants.

PHS consists of a system with two water reservoirs located at different heights, a dam, and an invertible engine/generator. The principle consists of storing

energy in the form of potential gravitational energy in the upper reservoir, then opening the dam and directing the water to the lower reservoir when the electricity demand is high. In the lower part of the channel there is a system of turbines connected to an invertible generator/motor that receives the water at high speed, passes through the turbine, and transforms the mechanical energy of the water into electrical energy.

During the charging process, the inverse process takes place and the water in the lower reservoir is pumped by the generator/motor to the upper dam, using energy from the network. Therefore, charging processes are performed when demand is low and energy costs are low. A general scheme of a pumping station is shown in Figure 3-5.

Figure 3-5. Diagram of the operation of a typical pump hydro station.



The main advantages of PHS are that they correspond to a mature technology with extensive operational experience, they have a good efficiency between 70 and 84%, they can store large volumes of energy and for long periods (low self-discharge), they have low operating costs of 2 USD/kWh and they have an extensive lifetime, up to 40 to 60 years.

On the other hand, the main disadvantages are the geographical restrictions for the installation of the reservoir, low energy density, the slow response time (minutes), long construction periods, and there are environmental barriers due to the need to flood the upper

reservoir area. Currently, pumped storage power plants have become more attractive due to the high potential for development in conjunction with solar power plants.

The main applications are:

- Frequency restoration reserve
- Energy arbitrage
- Load following
- Electric supply capacity
- Renewable capacity firming
- Ancillary services
- Island grid

### 3.3.2 Compressed Air Energy Storage (CAES)

A CAES system stores energy in the form of compressed air (potential elastic energy) in an underground cavern which is used as a reservoir. Old salt deposits or depleted gas fields can be conditioned for use, which lowers costs significantly<sup>16</sup>.

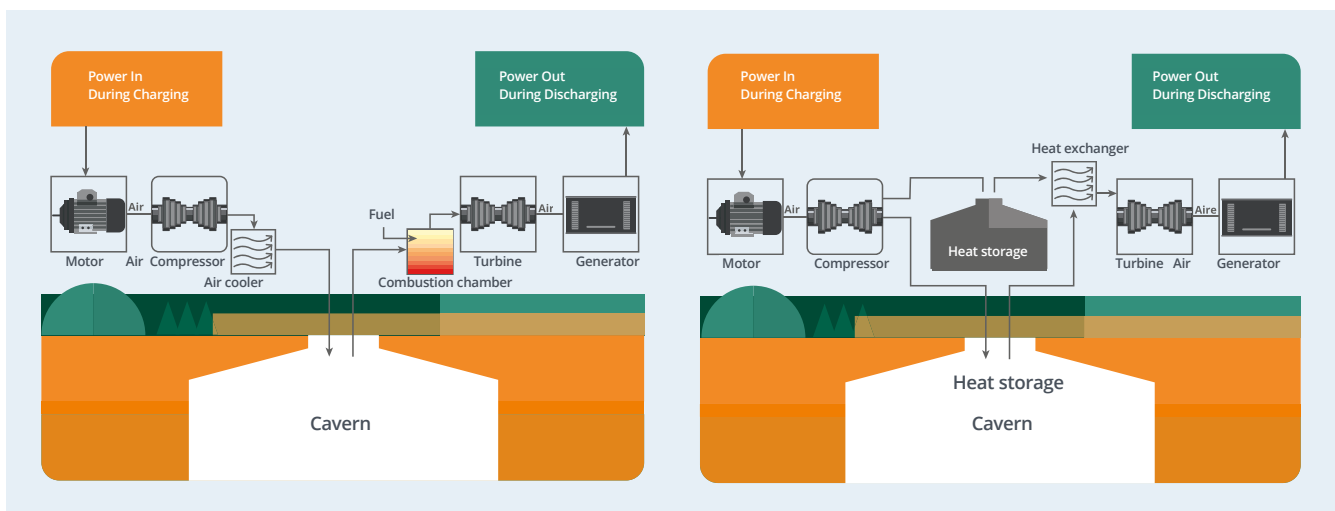
In low-demand periods surplus of electricity is used to power an invertible motor/generator that drives a chain of air compressors and then stores the air in the reservoir. During this process, the air heats up. In a classic (diabatic) CAES system, this heat is removed by an air cooler (radiator) and released into the atmosphere.

When the electricity demand is high, the stored air runs a gas-fired turbine generator. As the compressed air is released from the reservoir (i.e. expanded),

it consequently cools down and needs to be heated to improve efficiency. This is achieved by mixing compressed air with natural gas in a combustion chamber to drive the turbine system as shown in Figure 3-6. The classic CAES design involves fossil fuel combustion in the turbine chambers to provide heat during the expansion phase, with the drawback of emitting CO<sub>2</sub>.

A more recently developed concept is the advanced adiabatic compressed air energy storage (AA-CAES) system that addresses this issue. In this system, the heat that normally would be released to the atmosphere during the compression phase is stored and then added back through heat exchangers. This enables AA-CAES systems to do the charge/discharge process without emitting greenhouse gases.

Figure 3-6. Diagram of a Diabatic (left) and an Adiabatic (right) Compressed Air Energy Storage Systems.



The main advantages are regarding the capability to store energy for a long period with a low self-discharge (0.5% per day), the low capital expenditure costs of 48 USD/kWh (only if a cavern is available), and low OPEX (1 USD/kWh). The main disadvantages are related to the geographical restrictions, low efficiency (64%), CO<sub>2</sub> emissions (diabatic CAES), low energy density (4 Wh/L) and the AA-CAES has not been yet validated on an industrial scale.

The main applications are:

- Frequency restoration reserve
- Electric supply capacity
- Capacity firming
- Flex ramping
- T&D deferral
- Energy arbitrage
- Load following
- Island grid

<sup>16</sup> IRENA, Electricity Storage and Renewables: Costs and markets to 2030, 2017.

Among the large-scale ESS technologies, Liquid Air Energy Storage (LAES) has attracted significant attention in recent years due to the high expansion ratio from the liquid state to the gaseous state and the high power density of liquid air compared to the gaseous one<sup>17</sup>.

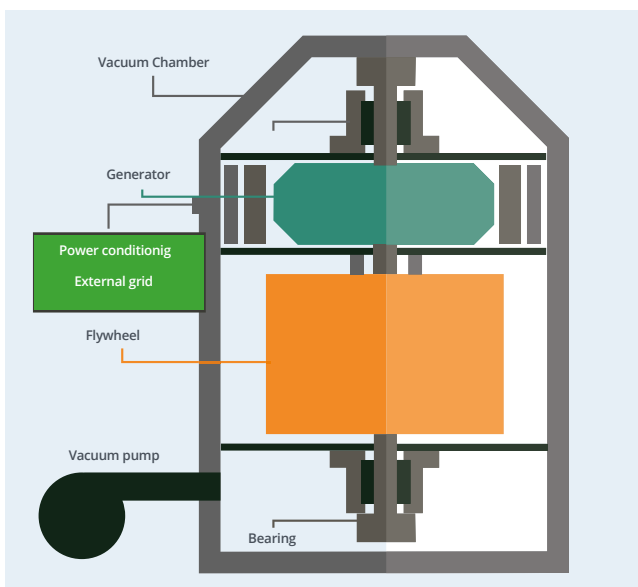
LAES uses electricity to cool the air until it is liquefied, and then it is stored in a tank. For the re-conversion, liquefied air is brought back to a gaseous state by exposure to ambient air or with waste heat from an industrial process. The gas obtained is used to drive a turbine and generate electricity. LAES is sometimes referred to as Cryogenic Energy Storage (CES)<sup>18</sup>.

The main advantages are that the LAES is not subject to geographical constraints such as PHS or CAES and it has a long lifetime (30 years or 20,000 cycles). The main disadvantages are that despite the maturity of machinery used for LAES (compressors, expanders, heat exchangers), the lack of experimental validation of the technology generates a high investment risk reducing the economic viability for investors<sup>19</sup>.

### 3.3.3 Flywheel Energy Storage (FES)

Flywheel Energy Storage (FES) is an electromagnetic system that stores energy as rotational kinetic energy by accelerating and braking a rotating mass around a fixed axis with two magnetic bearings that are coupled to a reversible electric motor/generator. Figure 3-7. shows the components of the FES technology.

Figure 3-7. Diagram of a Flywheel Energy System.



Magnetic bearings have the function of reducing friction at high speed. The whole structure is placed inside a vacuum chamber to reduce the shearing effect of the wind.

The charging process consists in transfer the electrical energy to the flywheel by accelerating it. Kinetic energy is stored by keeping the cylinder rotating at a constant speed. In the discharge process, the cylinder releases kinetic energy (slowing it down) and the system behaves like a generator.

The main advantages of the FES technology are the fast charge capabilities (milliseconds and seconds), the long life cycle (>100,000 cycles), no capacity degradation, high efficiency (85%), low maintenance required, and wide operational experience (due to using in motor and other industrial application). The main disadvantages are the low energy density compared with battery systems (110 Wh/L), the highest self-discharge rate (60% per day), and high CAPEX (2,656 – 3,000 USD/kWh).

The main applications are:

- Fast frequency response
- Frequency restoration reserve
- Capacity firming
- Renewable smoothing
- Ancillary services
- Reactive power management
- Peak shaving
- Island grid

### 3.3.4 Molten Salt Energy Storage (MSES)

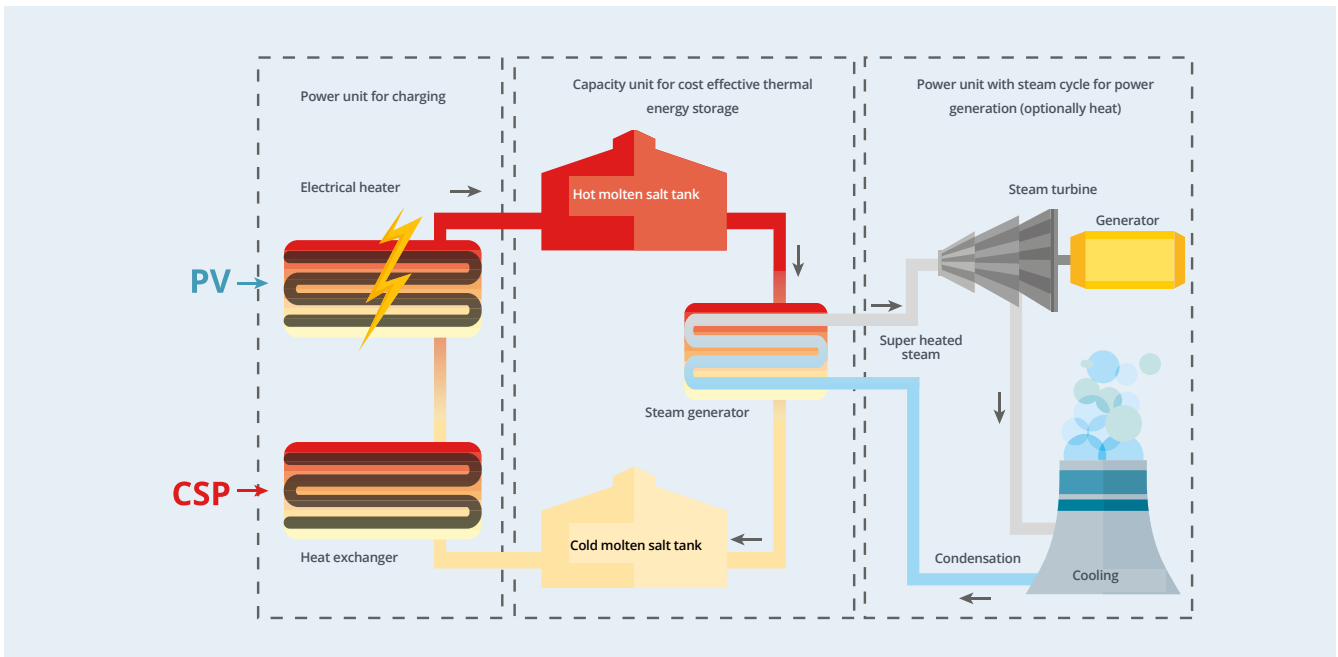
Molten Salt Energy Storage facilities store energy as heat. For this purpose, salts are heated and kept in isolated environments. An MSES system normally consists of a reservoir/tank, a packaged chiller or built-up refrigeration system, piping, pump(s), and controls. When energy needs to be generated, the thermal energy is released by pumping cold water onto the hot salts in order to produce steam which drives the movement of the turbines<sup>20</sup>, as shown in Figure 3-8.

<sup>17</sup> E. Borri, "Recent Trends on Liquid Air Energy Storage: A Bibliometric Analysis," 2020.

<sup>18</sup> Energy Storage Association, "Why Energy Storage – Technologies".

<sup>19</sup> C. Damak, "Liquid Air Energy Storage as a large-scale storage technology for renewable energy integration", 2020.

<sup>20</sup> EESI, "Fact Sheet: Energy Storage", 2019.

Figure 3-8. Diagram of a Molten Salt Energy Storage System<sup>21</sup>.

The main advantages are the good efficiency (80%), low CAPEX and OPEX of 60 USD/kWh and 6 USD/kWh respectively, the large amount of energy can be stored for long periods (low self-discharge = 0.05 % per day). The main disadvantages are the low energy density (200 Wh/l) and the slow time of response (hours).

The Molten Salt Energy Storage is the dominant commercial thermal energy storage solution deployed today and they account for three-quarters of the globally installed capacity of thermal energy storage for electricity applications, mainly in concentrated solar power (CSP) plants. Therefore, the main use case is renewable capacity firming.

The main applications are:

- Renewable smoothing
- Capacity firming
- Ancillary services
- Reactive power management
- Peak shaving
- Island grid

### 3.3.5 Hydrogen (H<sub>2</sub>)

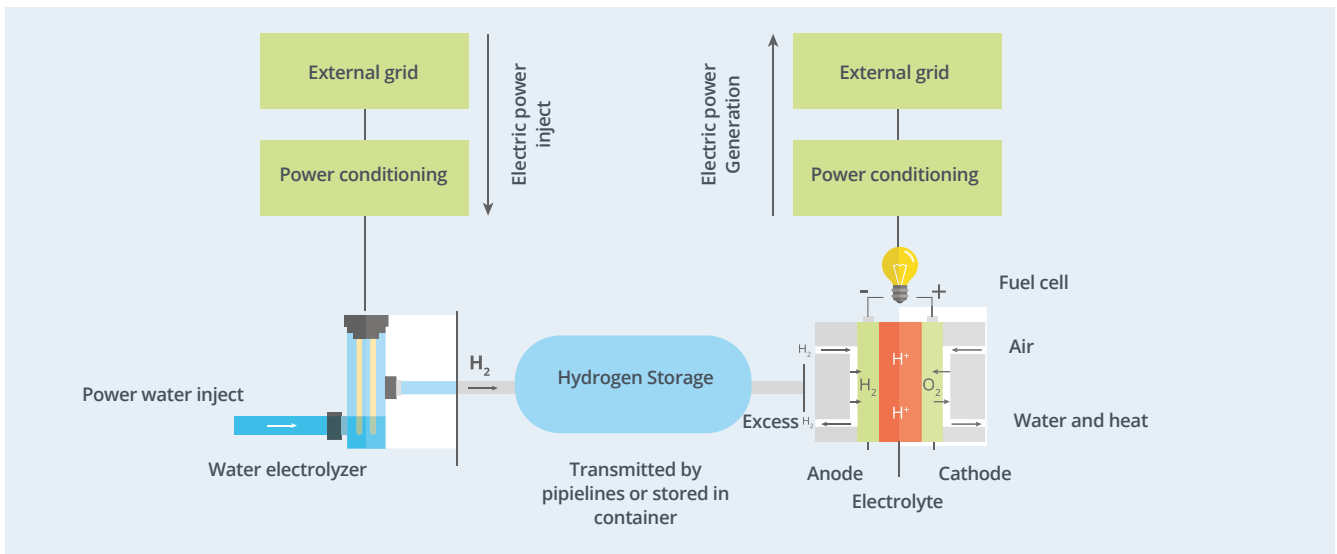
Hydrogen storage systems store energy in the form of chemical energy (hydrogen), which is used to perform a chemical reaction between two reactants (H<sub>2</sub> and O<sub>2</sub>). The three main components are an electrolyzer, that uses electricity and water to generate hydrogen, a hydrogen storage system (tanks, caverns, among others), and a fuel cell, that performs the reverse chemical reaction: combine hydrogen with oxygen obtained from air to generate electricity.

The principle of operation is similar to that of a battery. The main difference is that a battery is usually intended as a portable or self-contained source of electricity and it must carry the reactants to generate electricity within it. Once they are exhausted, the battery can no longer supply any power. A fuel cell, by contrast, does not contain any chemical reactants itself but is supplied with them from an external source. So long as these reactants are made available, the cell will continue to provide power. Figure 3-9. shows the principle of operation of hydrogen energy storage system<sup>22</sup>.

<sup>21</sup> IEA Technology Networks, Solar Power & Chemical Energy Systems, 2020.

<sup>22</sup> P. Breeze, Power Generation Technologies, 2019.

Figure 3-9. Topology of hydrogen storage and fuel cell system.



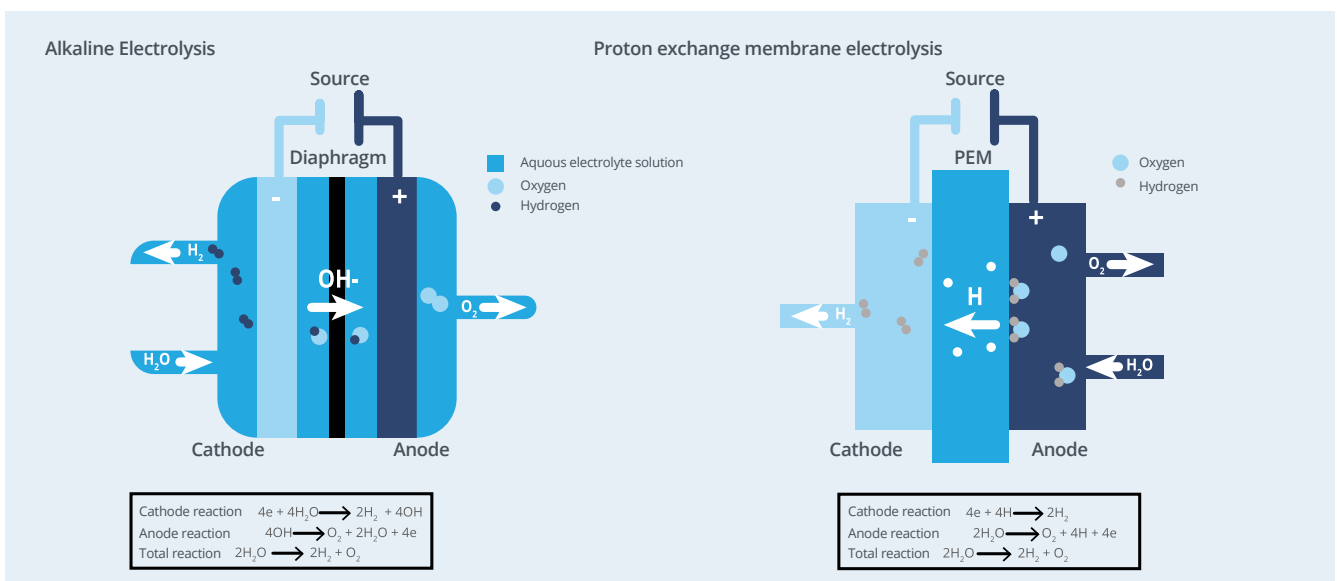
### 3.3.5.1 Electrolyzers

Three main electrolyzer technologies are used or are being developed today: Alkaline EZ (ALK), Proton Exchange Membrane EZ (PEM), and Solid Oxide EZ (SOEC). Of these technologies, the most mature, less expensive, and with a longer lifetime is the ALK<sup>23</sup>. In this one, an aqueous solution (KOH or NaOH) is used as the electrolyte, with an operating pressure between 1 to 15 bar, it can reach efficiencies between 65 – 68% and the capital costs varies between 700 – 1,200 USD/kW (western-made) and 200 USD/kW (Chinese-made)<sup>24</sup>.

On the other hand, PEM is a less mature technology, that is commercially available today and due to R&D efforts,

their capital costs have been dropping significantly. PEM is rapidly gaining market traction because is a flexible technology with a smaller footprint. These factors offer significant advantages in allowing a flexible operation to capture revenues from multiple electricity markets, a wider operating range, and has a shorter response time (1 second to 5 minutes).

Another characteristic is that they have a higher operating pressure than ALK, around 30 bar, making them the best option for applications for mobility. Figure 3-10. shows the topology of both electrolyzers and their techno-economic characteristics.

Figure 3-10. Topology of ALK and PEM electrolyzers<sup>25</sup>.

<sup>23</sup> IRENA, "Hydrogen from renewable power: Technology outlook for the energy transition", 2018.

<sup>24</sup> BloombergNEF, "Hydrogen Economy Outlook", 2020.

<sup>25</sup> BloombergNEF, "Hydrogen: The Economics of Production From Renewables", 2019.

Table 3-1. Techno-economic characteristics of ALK and PEM electrolyzers (2020,2030).

Parameter	Technology Unidad	ALK		PEM	
		2020	2030	2020	2030
Consumption	kWh/kg	53	46	54	49
Efficiency (LHV)	%	65	68	57	64
Lifetime stack	Operating hours	80,000	90,000	40,000	50,000
Total installation costs	USD/kW	1,200	400	1,500	900
OPEX	% of initial CAPEX/year	2	2	2	2
CAPEX – stack replacement	USD/kW	416	253	499	247
Stack degradation	%/year	1	1	1	1
Typical output pressure	bar	1	15	30	60
System lifetime	years	20		20	
Load range	% nominal load	15 – 100		0 – 160	
Start up (warm-cold)	s, min	1 – 10 min		1 s – 5 min	
Ramp-up/ramp-down	%/second	0.2 – 20		100	
Shutdown	s, min	1 – 10 min		seconds	

The values consider a 1 GW green hydrogen electrolyzer plant. The money conversion used is 1.2 USD = 1 EUR (€). Total installation costs consider all costs borne by the owner including procurement engineering construction, commissioning, owner costs, and contingencies of the electrolyzer and BoP.

On the other hand, Solid Oxide EZ holds the potential to improve energy efficiency, but the technology is still being demonstrated at laboratory and small demonstration scale. Its investment costs are currently higher, however, SOEC production mainly requires ceramics and a few rare materials for their catalyst layers, while PEM needs significant amounts of platinum. The need for high-temperature sources of heat close by might also limit the long-term economic viability of SOEC – for which the only renewable sources are likely to be concentrated solar power and high temperature geothermal.

### 3.3.5.2 Hydrogen storage

According to the physical state of the molecule, there are several methods to store hydrogen. The methods of storing hydrogen in a gaseous state are: underground storage (salt caverns, depleted gas fields, and rock caverns), pressurized gas tanks (steel tanks and composite tanks), and pipelines (dedicated and mixed with natural gas). In the liquid state are: liquid hydrogen tanks, liquid ammonia, and liquid organic hydrogen carriers. In solid-state instead, there is only one method of storage which is metal hydrides. Figure 3-11. summarizes all the storage options currently available and their working capacity.



Figure 3-11. Hydrogen storage options available and their working capacity.



### 3.3.5.3 Large-scale storage (more than 100 ton H<sub>2</sub>)

The best option is to store the hydrogen in salt caverns because they have the most competitive cost (LCOS of 0.23 USD/kg H<sub>2</sub>), losses are low, the gas is kept pure, and commercial use is already available. However, salt caverns are limited geographically. In case of the absence of salt caverns, rock caverns with an LCOS of 0.71 USD/kg H<sub>2</sub> and depleted gas fields (LCOS of 1.9 USD/kg H<sub>2</sub>) are the next best solution in terms of cost<sup>26</sup>.

When the geologic options of any of the three storages technologies above are not possible, the fourth-best option for large-scale storage is converting hydrogen to ammonia with a cost of 2.83 USD/kg H<sub>2</sub>, considering the cost of conversion. It is mentioned in "Hydrogen: The Economics of Storage" by BloombergNEF that this cost can fall further to 1.41 USD/kg H<sub>2</sub> by using the ammonia directly, for instance in gas turbines, ships, or solid oxide fuel cells.

In case local transport is required, the cheapest option will depend strongly on the mode, distance, and amount of H<sub>2</sub>, because the additional costs of conversion need

to be weighed against transport savings<sup>27</sup>. Today, the majority of hydrogen is compressed and then distributed by trucks. If larger volumes are needed, then larger pipes reduce the cost of delivery. For example, if 100 ton H<sub>2</sub>/day are required at a location 500 km away from the point of import, then the use of trucks would be cheaper than pipelines. But, if 500 ton H<sub>2</sub>/day are required, then a pipeline would have lower unit cost.

As the transmission distances increases, the cost of transporting hydrogen by pipelines escalates faster than the cost for ammonia since a greater number of compressor stations are required. For inland transmission and distribution, gaseous hydrogen is the cheaper option for distances below 3,500 km. Above this distance, ammonia pipelines would be the cheaper option.

Comparing transport using pipelines and ships, transporting gaseous hydrogen by pipelines is cheaper for distances below 1,500. Above this distance, it is expected that by 2030, LOHC and ammonia transport by ship become the cheaper delivery options.

<sup>26</sup> BloombergNEF, "Hydrogen: The Economics of Storage", 2019.

<sup>27</sup> IEA, "The future of Hydrogen", 2019.

### 3.3.5.4 Small-scale storage (less than 1 ton H<sub>2</sub>)

Regarding the small-scale storage, the most viable option is pressurized hydrogen in steel tanks, with costs starting at 0.19 USD/kgH<sub>2</sub>. Tanks are already widely used and are getting lighter and stronger, storing more hydrogen than before, making them the best option for short distances<sup>28</sup>. It is important to notice that these costs can only be reached if a daily cycle is considered.

For longer distances or if there are space constraints, the best is liquid hydrogen storage, due to its superior density. This characteristic allows to amortize the cost of liquefaction since less investment in tanks is required for each unit delivered, making LH<sub>2</sub> a good candidate for transporting hydrogen by truck (and eventually by ship) across longer distances with an LCOS of 4.57 USD/kgH<sub>2</sub>.

### 3.3.5.5 Fuel Cells

Fuel cells can convert chemical energy into hydrogen and oxygen (from the air) to electricity. The overall reaction is:  $2\text{H}_2 + \text{O}_2 \rightarrow 2\text{H}_2\text{O} + \text{energy}$ . They are composed of two electrodes, the anode with hydrogen molecules, the cathode with oxygen atoms, and an electrolyte that separate the two electrodes.

The electrolyte is the key element in any electrochemical cell because it acts as a filter to both stops the cell reactants from mixing directly with one another and to control how to charged ions created during the partial cell reactions are allowed to reach each other<sup>29</sup>. Depending on the fuel and electrolyte, there are six majors groups of fuel cells, which are: Alkaline Fuel Cell (AFC), Phosphoric Acid Fuel Cell (PAFC), Solid Oxide Fuel Cell (SOFC), Molten Carbonate Fuel Cell (MCFC), Proton Exchange Membrane Fuel Cell (PEMFC) and Direct Methanol Fuel Cell (DMFC)<sup>30</sup>.

The main applications of hydrogen storage are:

- Ancillary services
- Capacity firming
- Renewable smoothing
- Peak shaving
- Island grid

The main advantages of hydrogen storage are its long lifetime (10,000 cycles), it has the highest energy density of all the technologies (2,364 Wh/L liquid hydrogen at 1 bar), it's very suitable for long-term applications due to its low self-discharge (0.01 % per day) and if a PEM electrolyzer is considered, it has a fast time of response (seconds), allowing this technology to provide ancillary services of frequency regulation.

On the other hand, the cons are that it is still a developing technology and therefore its investment costs are still high to compete with other ESS with the same characteristics. Another disadvantage is that its efficiency is the lowest of all storage technologies since it has 2 conversion blocks.

### 3.3.6 Lithium-ion Batteries (BESS)

The rechargeable Battery Energy Storage System is one of the most widely used EES technologies in industry and daily life. The batteries are composed of several electrochemical cells connected in series or parallel, which produce electricity with the desired voltage from an electrochemical reaction. Each cell contains two electrodes (one anode and one cathode) with an electrolyte which can be at the solid, liquid, or viscous states. The electrolyte allows ion exchange between the two electrodes, while the electrons flow through the external circuit<sup>31</sup>.

There are different types of BESS depending on the type of electrolyte. Among them are Li-ion batteries, which are the dominant storage technology today for short-duration applications (i.e., 1-4 hours), representing ~90% of the market<sup>32</sup>. Therefore, this report will only address batteries with Li-Ion electrolytes.

BESS Li-Ion usually has a cathode made of a lithium metal oxide (LiMEO<sub>2</sub>), while the anode is often made of graphite or titanate. The electrolyte, on the other hand, is usually a non-aqueous organic solution containing dissolved lithium salts (LiClO<sub>4</sub>). The charging and discharging cycle of Li-Ion batteries is shown in Figure 3-12. During the charging process, lithium ions (Li<sup>+</sup>) are exchange from the cathode to the anode and during the discharge process, the reverse movement occurs<sup>33</sup>.

<sup>28</sup> BloombergNEF, "Hydrogen: The Economics of Storage", 2019.

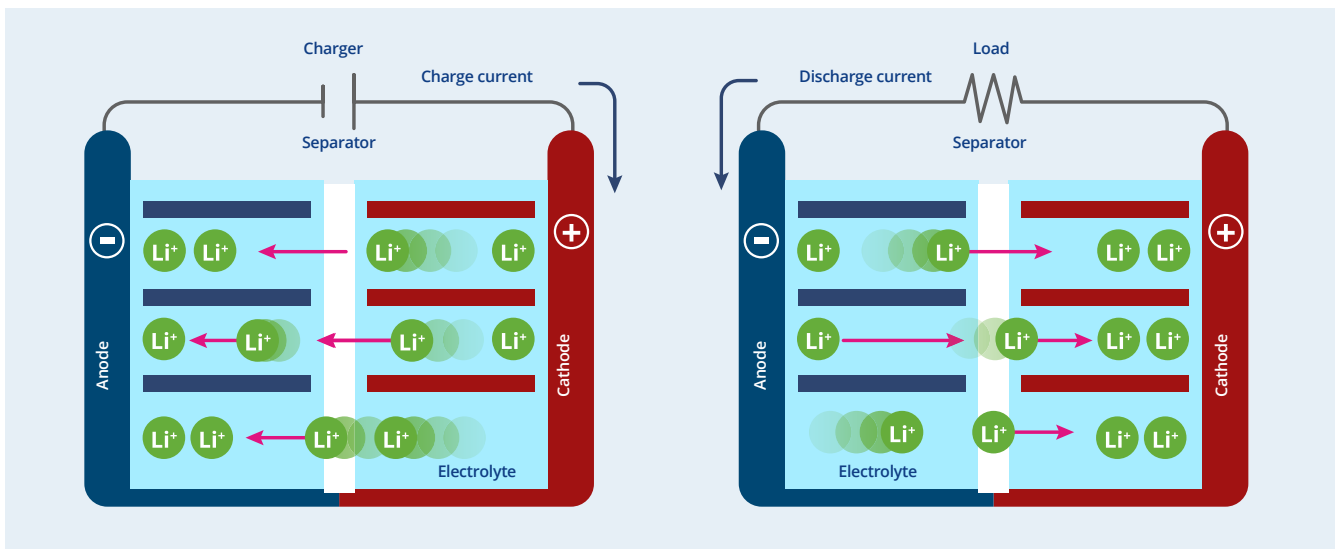
<sup>29</sup> P. Breeze, Power Generation Technologies, 2019.

<sup>30</sup> X. Luo, 2015.

<sup>31</sup> X. Luo, 2015.

<sup>32</sup> Lazard, "Lazard's Levelized Cost of Storage Analysis - Version 6.0", 2020.

<sup>33</sup> Díaz-González F., "A review of energy storage technologies for wind power applications", 2012.

Figure 3-12. Charge and discharge cycle of a lithium-ion battery energy storage system. Toshiba<sup>34</sup>.


Today, due to the advantageous characteristics and the promising avenues to further improve the key parameters of Li-ion batteries, new technologies with different materials for the electrolyte, cathode, and anode have been developed. Among them are lithium titanate batteries, lithium iron phosphate batteries, and

lithium nickel manganese cobalt oxide batteries. Table 3-2. shows the comparison of lithium-ion chemistry properties, advantages, and disadvantages. Although lithium batteries have high investment costs, they are expected to drop by an additional 54-61% by 2030<sup>35</sup>.

Table 3-2. Comparison of lithium-ion chemistry properties, advantages, and disadvantages.

Key active material	Lithium titanate (LTO)	Lithium iron phosphate (LFP)	Lithium nickel manganese cobalt oxide (NMC)
Cathode	Variable	$LiFePO_4$	$LiNi_xMn_{yCo_{1-x-y}}O_2$
Anode	$Li_4Ti_5O_{12}$	C (graphite)	C (graphite)
Safety	● ● ● ●	● ● ● ●	● ● ● ○
Power density	● ● ● ○	● ● ● ○	● ● ● ○
Energy density	● ● ● ●	● ● ● ●	● ● ● ●
Cell costs advantage	● ● ○ ○	● ● ○ ○	● ● ● ●
Lifetime	● ○ ○ ○	● ● ● ○	● ● ● ○
Bess system performance	● ● ● ●	● ● ● ●	● ● ○ ○
Advantages	<ul style="list-style-type: none"> <li>• Very good thermal stability</li> <li>• Long cycle lifetime</li> <li>• High rate discharge capability</li> <li>• No solid electrolyte interphases issues</li> </ul>	<ul style="list-style-type: none"> <li>• Very good thermal stability</li> <li>• Very good cycle life</li> <li>• Very good power capability</li> <li>• Low costs</li> </ul>	<ul style="list-style-type: none"> <li>• Good properties combination</li> <li>• Can be tailored for high power or high energy</li> <li>• Can operate at high voltages</li> </ul>
Disadvantages	<ul style="list-style-type: none"> <li>• The high cost of titanium</li> <li>• Reduced cell voltage</li> <li>• Low energy density</li> </ul>	<ul style="list-style-type: none"> <li>• Lower energy density due to lower cell voltage</li> </ul>	<ul style="list-style-type: none"> <li>• Patent issues in some countries</li> </ul>

<sup>34</sup> TOSHIBA Corporation, "Basics of Lithium-ion Batteries - Battery School", 2020.

<sup>35</sup> IRENA, "Electricity Storage and Renewables: Costs and markets to 2030", 2017.

The structure of lithium titanate (LTO) is gaining attraction due to some advantages over graphite that may be relevant to stationary applications. In particular, LTO cells exhibit benefits in terms of efficiency and lifetime, while the increased ion agility in the LTO structure enables fast charging (i.e. high rate operation).

Although they have the best performance among the lithium-ion batteries, the capital costs are still high to compete with the other Li-Ion batteries.

On the other hand, lithium iron phosphate possesses a relatively high-power capability, the environmental advantage of inexpensive, non-toxic cathode material, and a long lifetime. These characteristics, as well as the relatively low discharge rate, make the LFP BES system a very attractive technology for stationary applications.

Finally, the nickel Manganese Cobalt Oxide (NMC) cells emerged due to the necessity to find lower costs, so the breakthrough was the approach of substituting part of the Ni by Co and Mn. The careful adjustment of the composition succeeded in balancing energy density, stability, safety, and cost concerning the targeted application, which eventually led to the commercial success of NCM. As a result, this material is nowadays dominating the lithium-ion battery market, and a further increase is anticipated<sup>36</sup>.

The main applications of the three technologies are:

- Fast frequency response
- Energy arbitrage
- Ancillary services
- Capacity firming
- Renewable smoothing
- Flex ramping
- Peak shaving
- Island grid
- T&D Deferral
- Reactive power management

### 3.3.7 Lead-acid Batteries

Lead-acid batteries were first developed more than 150 years ago and are the oldest and most widely deployed rechargeable battery. They have the same working principle as the lithium-ion batteries and like them, were specially created to provide fast frequency regulation services. Lead-acid batteries sometimes are combined with other high-power storage technologies, such as Li-ion batteries or flywheels, to create cost-efficient hybrid battery systems that work well<sup>37</sup>.

There are two types of lead-acid batteries: flooded and valve-regulated lead-acid batteries (VRLA). The first one uses liquid sulphuric acid ( $H_2SO_4$ ) as an electrolyte (usually 37% acid weight), a negative electrode made of metallic lead (Pb), a positive electrode made of lead dioxide ( $PbO_2$ ) and a separator used to insulate electrodes from one another as can be seen in Figure 3-13.

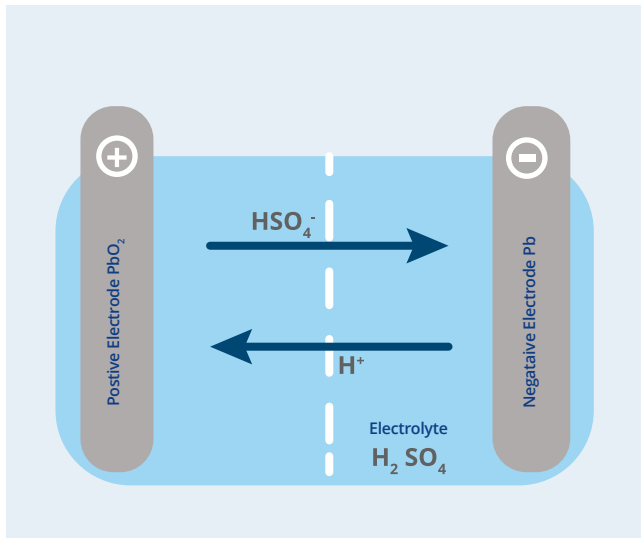
The second one has the same components but has valves that regulate the cell's maximum overpressure, in order to prevent electrolyte loss.



<sup>36</sup> Armand M., "Lithium-ion batteries - Current state of the art and anticipated developments", 2020.

<sup>37</sup> IRENA, "Electricity Storage and Renewables: Costs and markets to 2030", 2017.e

Figure 3-13. Working principle of a lead-acid battery [18]



They typically have a good cost-performance ratio in a wide range of applications. However, they have a relatively low energy density (75 Wh/L), very heavy, typically do not respond well to deep discharging (DoD = 50%), have a short lifetime (500 cycles), and lead may be a restricted material in some applications or locations due to its toxicity. However, lead-acid batteries are relatively easily recycled and there is a large existing market.

The main applications are:

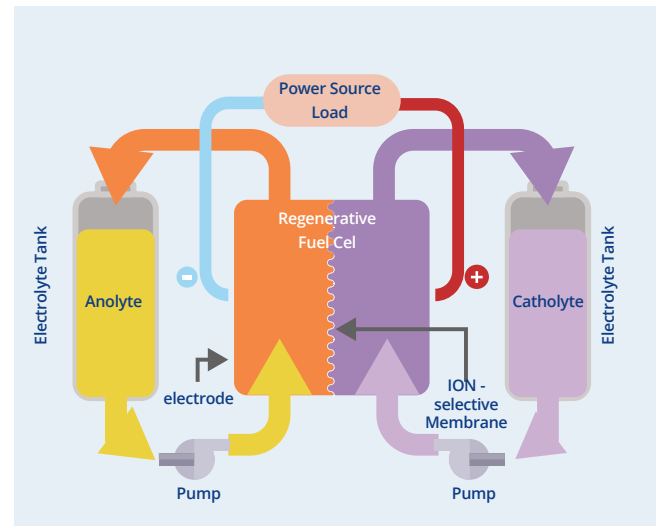
- Fast frequency response
- Renewable shifting
- Flex ramping
- T&D Deferral
- Reactive power management
- Peak shaving
- Island grid

### 3.3.8 Flow Batteries (FB)

Another battery storage technology is the flow batteries also known as regenerative fuel cells. They differ from conventional rechargeable batteries in that the electroactive materials are not all stored within the electrode but, instead, are dissolved in electrolyte solutions that are stored within the electrode. The electrolytes are stored in tanks (one at the anode side and the other one on the cathode side). These two tanks are

separated from the regenerative cell stack (i.e. reaction unit). The electrolytes are pumped from the tanks into the cell stacks where reversible electrochemical reactions occur during charging and discharging of the system as can be seen in Figure 3-14.

Figure 3-14. Working principle of a flow battery.



Depending on the type of electrolyte used, the main technologies on the market are: Vanadium Redox with a total installed cost of 268 USD/kWh and Zinc Bromine with a total installed cost of 696 USD/kWh. By 2030, the cost is expected to come down to 108 USD/kWh and 576 USD/kWh for each of them. Round-trip efficiencies for these flow batteries are expected to improve from 72% in 2020 to 78% by 2030. Although they currently have high upfront investment costs compared to other technologies, these batteries often exceed 10,000 full cycles, enabling them to make up for the high initial cost through very high lifetime energy throughputs.

The main applications are:

- Frequency restoration reserve
- Renewable shifting
- Electric supply capacity
- Capacity firming
- Flex ramping
- T&D deferral
- Energy arbitrage
- Load following
- Peak shaving
- Island grid

### 3.4. Summary and results

The tables below show a summary of the commercial and technical characteristics of the energy storage systems discussed in this chapter, including their Technology Readiness Level (TRL)<sup>38</sup>, and Commercial Readiness Index (CRI)<sup>39</sup>. All the technologies consider a large-

scale project (bigger than 1 MW). Specifically, hydrogen technology considers a 12-hour stationary hydrogen energy storage large-scale project of 2–3 MW, composed of an alkaline electrolyzer, a pressurized hydrogen storage tank (50–80 bar), a compressor, and a Solid Oxide Fuel Cell.

Table 3-3. Commercial characteristics of energy storage systems.

Type	Technology	CAPEX		OPEX	Energy Density	Lifetime	Maturity		
		Power USD/kW	Energy USD/kWh	USD/kWh	Wh/l	N° full cycles	TRL	CRI	
Mechanical	PHS	2,000 - 4,000	21 - 80	2	1	20,000	10	5	
	CAES	400 - 1,000	48 - 53	1	4	20,000	10	3	
	FES	250 - 350	2,656 - 3,000	80	110	100,000	9	2	
Thermal	MSES	200 - 300	30 - 60	6	200	10,000	10	5	
Chemical	Hydrogen	4,000 - 5,000	1,040 - 1,500	< 1	2,364	10,000	9	2	
Electro-chemical Batteries	Li-Ion	1,000 - 1,500	284 - 456	8	410	3,500	10	5	
	Li-Ion LFP	N/D	N/D	8	410	3,500	10	3	
	Li-Ion LTO	N/D	N/D	6	410	10,000	9	2	
	Li-Ion NMC	N/D	N/D	8	470	3,500	10	3	
	Pb-Acid VRLA	300	600	226 - 263	3	75	500	10	5
Electro-chemical Flow Batteries	VRFB	600	1,500	268 - 347	11	42.5	10,000	9	2
	ZBFB	400	1,500	696 - 900	15	45	4,000	9	2

Table 3-4. Technical characteristics of energy storage systems.

Type	Technology	Installed capacity	Round-trip efficiency	Dod	Self-discharge	Time of response
		MW (%)	(%)	(%)	% per day	h, min, s, ms
Mechanical	PHS	181,798 (95.2%)	80 90	2	0.01	min, h
	CAES	1,291 (0.7%)	64 40	1	0.50	min, h
	FES	953 (0.5%)	80 85	80	60.00	ms, s
Thermal	MSES	2,452 (1.3%)	80 100	6	0.05	h
Chemical	Hydrogen	20 (<0.1%)	35 100	< 1	0.01	min, h
Electro-chemical Batteries	Li-Ion General	2,636 (1.4%)	92 90	8	0.20	ms, s
	Li-Ion LFP	191 (0.1%)	86 90	8	0.10	ms, s
	Li-Ion LTO	62 (<0.1%)	96 95	6	0.05	ms, s
	Li-Ion NMC	86 (<0.1%)	92 90	8	0.10	ms, s
	Pb-Acid VRLA	110 (0.1%)	81 50	3	0.25	ms, s
Electro-chemical Flow Batteries	VRFB	327 (0.2%)	72 100	11	0.15	min, h
	ZBFB	85 (<0.1%)	72 100	15	15.00	min, h

Notes: PHS: Pumped hydro Storage; CAES: Compressed Air Energy Storage; FES: Flywheel Energy Storage; MSES: Molten Salt Energy Storage; SNG: Synthetic Natural Gas; LFP: Lithium Iron Phosphate; LTO: Lithium Titanate; NMC: Lithium Nickel Manganese Cobalt Oxide; VRLA: Valve-regulated Lead Acid; VRFB: Vanadium Redox Flow Battery; ZBFB: Zinc Bromine Flow Battery; CZFB: Copper Zinc Flow Battery.

<sup>38</sup> Technology Readiness Levels were developed by NASA and are widely used, ranging from 1 (basic principles observed) to 9 (system proven in operational environment).

<sup>39</sup> Commercial Readiness Index were developed by the Australian Renewable Energy Agency (ARENA) to complement TRLs and go from 1 (hypothetical commercial proposition, TRL 1-8) to 2 (commercial trial, TRL 9+), and up to 6 (Bankable asset class).

Table 3-5. Look-up table for competitive scores.

	5	4	3	2	1
CAPEX	< 100 USD/kWh	100 - 325 USD/kWh	325 - 550 USD/kWh	550 - 800 USD/kWh	> 800 USD/kWh
Lifetime	10,000 - 100,000 cycles	5,000 - 10,000 cycles	3,500 - 5,000 cycles	1,000 - 3,500 cycles	500 - 1,000 cycles
Maturity	TRL=10, CRI=5	TRL=10, CRI=3- 4	TRL=9, CRI=2	TRL < 9, CRI < 2	TRL < 9, CRI < 1
Efficiency	> 90%	80 - 90 %	70 - 80 %	60 - 70 %	< 60 %
Self-discharge	< 0,01	0.01 - 0.02	0.02 - 0.1	0.1 - 0.5	> 0,05
Time of response	Miliseconds (ms)	Seconds(s)	Minutes (min)	Hours (h)	Days (d)
Space required	> 1.000 Wh/l	600 - 1.000 Wh/l	300 - 600 Wh/l	100 - 300 Wh/l	< 100 Wh/l

Table 3-6. Competitive scores for storage.

	PHS	CAES	FES	MSES	H <sub>2</sub>	LFO	LTO	NMC	VRLA	VRFB	ZBFB
CAPEX	4.4	4.3	2.0	4.4	2.0	3.4	2.0	3.8	4.7	3.2	2.3
Lifetime	5.0	5.0	5.0	3.0	3.6	1.4	3.6	1.3	1.1	4.4	3.6
Maturity	5.0	4.0	3.0	5.0	4.0	4.0	3.0	4.0	5.0	2.0	1.0
Efficiency	3.2	1.0	3.7	3.2	1.0	3.9	5.0	4.6	3.4	2.1	2.1
Self-discharge	4.5	2.0	1.0	3.0	5.0	3.0	3.0	3.0	2.0	2.0	1.0
Time of response	2.0	2.0	5.0	1.0	2.0	5.0	5.0	5.0	5.0	2.0	2.0
Space required	1.0	1.0	2.3	2.5	5.0	3.0	3.3	3.3	1.5	1.0	1.2

Table 3-7. Parameter weightings for the selected.

	Capacity firming	Ancillary Services	Renewable shifting	Renewable smoothing
CAPEX	30%	30%	40%	30%
Lifetime	15%	15%	15%	15%
Maturity	10%	10%	10%	10%
Round-trip efficiency	10%	10%	10%	10%
Self-discharge	25%	20%	20%	20%
Time of response	5%	15%	0%	15%
Space required	5%	0%	5%	0%

Table 3-8. Suitability matrix for the selected applications.

	PHS	CAES	FES	MSES	H <sub>2</sub>	LFO	LTO	NMC	VRLA	VRFB	ZBFB
Capacity firming	1.0	1.0	0.3	1.0	1.0	1.0	1.0	1.0	0.8	1.0	1.0
Ancillary Services	0.3	0.3	1.0	0.3	0.5	1.0	1.0	1.0	0.5	0.3	0.3
Renewable shifting	1.0	1.0	0.3	1.0	1.0	1.0	1.0	1.0	0.8	1.0	1.0
Renewable smoothing	0.3	0.3	1.0	0.3	0.5	1.0	1.0	1.0	0.8	0.3	0.3

Table 3-9. Final weighted scores, their average, and ranking.

	PHS	CAES	FES	MSES	H <sub>2</sub>	LFO	LTO	NMC	VRLA	VRFB	ZBFB
Capacity firming	4.17	3.19	0.79	3.52	3.24	3.17	3.11	3.36	2.59	2.68	1.95
Auxiliary Services	1.23	0.97	2.97	1.00	1.47	3.37	3.29	3.55	1.78	0.82	0.61
Renewable shifting	4.28	3.42	0.76	3.76	3.09	3.11	2.91	3.34	2.69	2.80	2.03
Renewable smoothing	1.23	0.97	2.97	1.00	1.47	3.37	3.29	3.55	2.85	0.82	0.61
Average	2.72	2.14	1.87	2.32	2.32	3.26	3.15	3.45	2.48	1.78	1.3
Ranking	4	8	9	6	7	2	3	1	5	10	11

### 3.5 Conclusions

In this chapter, first, the necessary information was collected from reliable sources such as IRENA, IEA, U.S DOE, BNEF, Lazard, Science Direct, among others. Then, the state of the art of energy storage systems was carried out, allowing to construct a general overview of the technologies adapted to electric power systems. Finally, the relevant parameters were chosen, taking into account that the selection will depend on the main application of each energy storage technology.

Based on the previous analysis, only mature technologies can compete with the ESS currently installed in electric power systems, but also their performance must be good enough to participate in the different markets, e.g., time

of response to provide ancillary services, long-term storage to provide capacity firming, or ability to perform daily cycles for renewables smoothing.

In line with this, the relevant parameters considered for this study were: CAPEX, roundtrip efficiency, lifetime, self-discharge, maturity, space required, and response time. Then, depending on the application to be studied in each case, a weighted or “percentage of importance” was assigned to each relevant parameter, and the suitability matrix was defined, to calculate the final weighted scores of each technology. With this, the ranking of the technologies for each application is shown in Table 3-10.

Table 3-10. Ranking of the technologies for each application.

Rank	Capacity firming	Ancillary Services	Renewable Shifting	Renewable smoothing	Average
1	PHS	NMC	PHS	NMC	NMC
2	MSES	LFP	MSES	LFP	LFP
3	NMC	LTO	CAES	LTO	LTO
4	H <sub>2</sub>	FES	NMC	FES	PHS
5	CAES	VRLA	LFP	VRLA	VRLA
6	LFP	H <sub>2</sub>	H <sub>2</sub>	H <sub>2</sub>	MSES
7	LTO	PHS	LTO	PHS	H <sub>2</sub>
8	VRFB	MSES	VRFB	MSES	CAES
9	VRLA	CAES	VRLA	CAES	FES
10	ZBFB	VRFB	ZBFB	VRFB	VRFB
11	FES	ZBFB	FES	ZBFB	ZBFB

Once the results are obtained, they allow the identification of the technologies that are better suited to electric power systems, leading to the following conclusions.

- **For capacity firming the best technologies are pumped hydro (PHS), molten salt (MSES), and lithium nickel manganese cobalt oxide (Li-ion NMC). This is in line with expectations, since PHS provides significant levels of power capacity, making them the best technology to provide this service as a main-use case. MSES is mainly deployed in CSP plants, therefore, today's main-use case is capacity firming. Regarding Li-ion NMC, they are mainly used for fast frequency restoration, due to their fast discharge, but sometimes they are also used for capacity firming if a power-intensive system is installed. PHS, MSES, and Li-ion NMC have in common that they have a low CAPEX, they are a mature technology, and their round-trip efficiency is relatively high.**
- **For Ancillary Services and renewable smoothing, the best technologies are Li-ion batteries (NMC, LFP, and LTO). For these applications, it is mandatory to have a fast response to frequency, load, and renewable generation changes, and therefore, the characteristic that weighs more is the time of response. In line with this, the Li-ion batteries have the fastest discharge time of all technologies. The second feature that weighs more is the capital expenditure, hence the Li-ion NMC battery is the leader of the ranking.**
- **Finally, the general performance required to provide renewable shifting (renewable energy arbitrage) is to be able to perform a daily cycle, in order to charge de ESS in the solar or wind hours, i.e., in off-peak hours (low prices), and then to discharge the ESS in peak hours (high prices). Considering this, the technologies that lead the ranking are PHS, MSES, and CAES. They have in common the characteristic of having a long lifetime, even cycling daily with a low loss of efficiency, making them the best suited for this application.**
- **Hydrogen as an energy storage system does not stand out over other technologies, since its investment costs are still high and it has a very low efficiency as a result of having two energy conversion blocks.**



AGUA DE  
SERVICIOS  
Cap. 1000 mts³

AGUA DE  
SERVICIOS  
Cap. 1000 mts³

## 4. Hydrogen integration potential in the National and Mulegé energy systems

### 4.1. Introduction

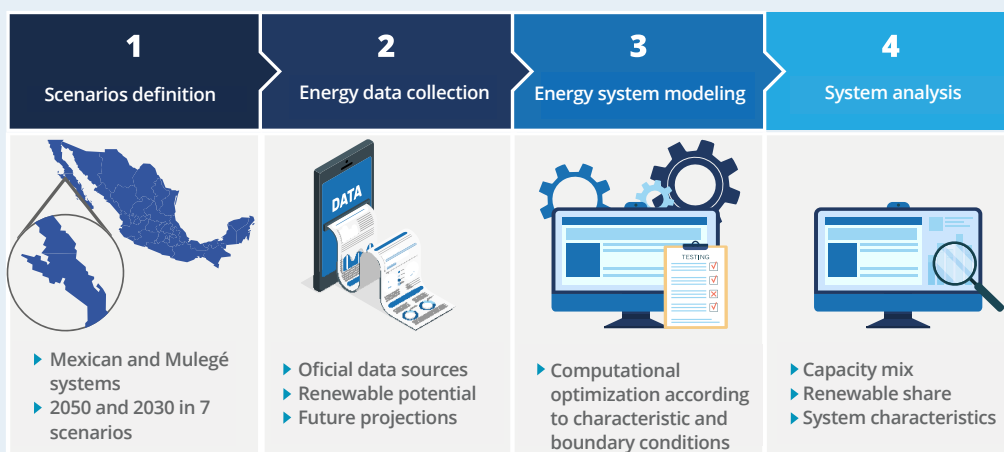
In this chapter, the potential integration of hydrogen into the National power system of Mexico (SEN) and the Mulegé, Baja California, system is investigated, using an energy system model to quantify the benefits of this integration. The chapter follows the next structure: first, the methodology employed for both system models is described jointly due its similarities. Then, the results and important insights from the analysis are presented and discussed for each system separately. Finally, a set of conclusions and recommendations are drawn.

### 4.2. Methodology

The methodology followed for both energy system models can be divided in four steps:

- **Scenario definition:** Selection of the type of energy system model employed, and definition of the parameters for the scenarios to be evaluated.
- **Energy data collection:** Collection of publicly available energy data by official sources and internationally recognized institutions. When needed, it also includes the simulation and/or projection of missing and/or future parameters.
- **Energy system modeling:** Model set up according to the defined scenarios, energy data, and defined boundary conditions.
- **Results analysis:** Evaluation of the system and interpretation of results.

Figure 4-1. Energy system modeling block methodology.



Each step is explained in more detail in the upcoming subchapters.

## 4.2.1 Scenarios definition

This subchapter explains the aspects considered for the design of the scenarios modeled. It begins with a description of five scenarios that were used to model the national power system, and two scenarios that were defined to look at the Mulegé system.

### 4.2.1.1 National power system

Five scenarios were analyzed to investigate the possible development of the Mexican power sector when hydrogen is introduced in it. Furthermore, it is also important to estimate when such hydrogen integration could occur (in the mid-term vs. in the long-term). Consequently, the hydrogen integration potential is investigated for two timeframes (2030 for the mid-term and 2050 for the long-term) in five scenarios. The timeframes were chosen according to the years used by the Mexican government to set Nationally Determined Contributions (NDC). Figure 4-2. Scenarios modeled for the national power system evaluation below shows the scenario timeline with a short description underneath.

Figure 4-2. Scenarios modeled for the national power system evaluation.



- **BaU2020** - “Business-as-Usual by 2020” control scenario used to benchmark, calibrate and normalize the results.
- **BaU2030** - “Business-as-Usual by 2030” Mid-term scenario under foreseeable system characteristics.
- **H<sub>2</sub>MX2030** - “H<sub>2</sub> integrated by 2030” Mid-term scenario under foreseeable system characteristics and hydrogen integration.
- **BaU2050** - “Business-as-Usual by 2050” Long-term scenario at cost-optimal characteristics.
- **H<sub>2</sub>MX2050** - “H<sub>2</sub> integrated by 2050” Long-term scenario at cost-optimal characteristics and hydrogen integration.

In this report, the Mexican power system is thought to be able to develop in one of the two directions represented in Figure 4-2. Scenarios modeled for the national power system evaluation. The “Business-as-Usual” direction represented by the dark blue corresponds to the expected natural development for 2020, 2030, and 2050. Under this direction, the scenario labeled “**BaU2020**” is the first evaluated. It is designed to resemble as close as possible the current power system in Mexico as of 2020 using the publicly available information. The **BaU2020** objective is to normalize the results of the model so the results from other scenarios can be compared against this control scenario. Two scenarios more under this direction, “**BaU2030**” and “**BaU2050**”, are conceived to evaluate an expected development of the Mexican power system by 2030 and 2050.

Alternately, the light-blue line in Figure 4-2. Scenarios modeled for the national power system evaluation represents a system-development direction that is facilitated by hydrogen. Two time frames are

considered for this hydrogen integrated vision; a mid-term integration by 2030 and a long-term integration by 2050. Two scenarios called “**H<sub>2</sub>MX2030**” and “**H<sub>2</sub>MX2050**” model this alternative system development with hydrogen integration. They include the same considerations as the BaU scenarios plus the addition of hydrogen technologies into the system (electrolysis, hydrogen power turbines, hydrogen pipelines, hydrogen vessels).

A multi-nodal energy system modeling approach is chosen to evaluate the multi-regional system, consists of several “nodes” that represent regions. These nodes have energy demands associated with them (in this case, electricity demand) as well as technologies that can provide the energy. The nodes are interconnected, so energy can be transmitted from one node to another to match energy deficits. Nine nodes corresponding to nine transmission regions and their interconnection capacities according to SENER’s National Electricity System Development Program (PRODESEN) 2018 are followed and kept unchanged for all the national energy system scenarios.

#### 4.2.1.2 Mulegé energy system

The Mulegé power system is currently isolated from the rest of the national power system. Due to its geographical location and weather characteristics, Mulegé’s electricity production is more expensive. Nevertheless, its isolation and high electricity cost make it an interesting candidate to develop a zero-emissions power system<sup>40</sup>. Therefore, two scenarios were designed to investigate the extent up to which hydrogen can facilitate turning the Mulegé system into a zero-emissions system by 2050. They are called “**ZERO**” and “**H<sub>2</sub>-ZERO**”. The only difference between them is that the **H<sub>2</sub>-ZERO** scenario includes H<sub>2</sub>-technologies while the **ZERO** scenario does not. Figure 4-3. Scenarios modeled for the Mulegé renewable system shows the two scenarios with a short description underneath.

Figure 4-3. Scenarios modeled for the Mulegé renewable system.



**ZERO** - Cost optimal design for a zero-emissions system with no hydrogen integration.

**H<sub>2</sub>-ZERO** - Cost optimal design for a zero-emissions system with hydrogen integration.

Both scenarios of the Mulegé system are modeled as a single node energy system, which consists of a single demand associated with a region that does not interact with other regions (nodes). There is no transmission modeling in a single-node energy system, so the results will be reported for the generation, conversion, and storage of energy.

#### 4.2.2 Energy data collection

Official data sources by Mexican authorities were preferred when possible, followed by internationally recognized organizations and other similar studies. The main data source is the PRODESEN. The PRODESEN is the main planning instrument for the power sector in Mexico and it is published each year by The Mexican Ministry of Energy (SENER). HINICIO referred to the 2018 and 2019 versions of the PRODESEN to obtain the following data: electricity demands with a hourly resolution, transmission regions and inter-regional transmission capacities, techno-economical parameters of existing hydropower plants, geothermal plants, nuclear plants, conventional generation technologies, and fuel costs. In general, the values for 2020 and 2030 were taken as stated by PRODESEN projections, whereas the values for 2050 were either projected using the expected growth rates of the PRODESEN or assumed the same as the 2030 values.

<sup>40</sup> Zero emissions regarding only the electrical generation of the system.

The 2030 CO<sub>2</sub> emissions reduction targets were taken from Climate Change Mitigation and Adaptation Commitments for 2020–2030 released by the Mexican Government in 2015 in the Nationally Determined Contribution (NDC) to comply with the Paris Agreement. A 2050 emission target is proposed, not being a commitment explicitly stated by the Mexican government. Data regarding the renewable energy

techno-economical parameters, generation time-series, and maximum capacities were obtained from the renewable assessment presented in section 2 of this report. Other techno-economical parameters were taken from the IEA, NREL, and other sources as shown in Table 4-1., which summarizes the input data and references used.

Table 4-1. Energy data inputs.

Data regarding	Description	Reference/ Data source	Notes
Electricity demand	Hourly-electricity demand profile per region of the transmission	PRODESEN, 2018	2020 and 2030 as the planning scenario by the PRODESEN 2018. 2050 values were projected according to the average growth rate reported in the PRODESEN 2018.
Regions	9 transmission regions and inter-regional electric transmission capacity	PRODESEN, 2018	Fixed regions and inter-regional transmission capacity for all scenarios
VRES	Wind and PV generation time-series, maximum installed capacities, and techno-economical parameters	PRODESEN, 2019 and renewable assessment	2020 installed capacities according to PRODESEN 2019 and future potential as per the results of task 2.1
Hydropower	Techno-economical parameters of large hydropower plants	PRODESEN, 2018	Fixed techno-economical parameters for all scenarios
Geothermal	Techno-economical parameters of geothermal power plants' techno-economical parameters	PRODESEN, 2018	Fixed techno-economical parameters for all scenarios
Nuclear	Techno-economical parameters of nuclear power plants	PRODESEN, 2018	Fixed techno-economical parameters for all scenarios
New CCGT-NG	Techno-economical parameters of the new combined-cycle gas turbine – natural gas (CCGT-NG) techno-economical parameters	IEA, 2017	For new installations in 2030 and 2050
Conventional generation technologies	Techno-economical parameters of thermoelectric power plants (fuel-oil), Coal, Internal combustion (diesel), Open-cycle gas turbine – natural gas (OCGT-NG)	PRODESEN, 2018	Fixed techno-economical parameters for all scenarios
Fuel costs	Techno-economical parameters of natural gas, diesel, coal, fuel-oil	PRODESEN, 2018	As PRODESEN projections for 2020 and 2030. Costs for 2050 were taken the same as 2030

Data regarding	Description	Reference/ Data source	Notes
Hydrogen technologies	Techno-economical parameters of combined-cycle gas turbine – H <sub>2</sub> (CCGT-H <sub>2</sub> ), open-cycle gas turbine – H <sub>2</sub> (OCGT-H <sub>2</sub> ), H <sub>2</sub> -vessels, H <sub>2</sub> -pipelines	Peña-Sánchez, HINICIO assumptions	Techno-economical parameters for 2050 as per Pena Sanchez and 2030 as HINICIO's estimates
Li-ion batteries	Techno-economical parameters of Lithium-Ion batteries for stationary energy storage	NREL, 2019	Techno-economical parameters for 203 and 2050 as the standard estimate by NREL
CO <sub>2</sub> reduction target (*)	Reduction in the CO <sub>2</sub> emissions in the power sector according to the nationally determined contributions (NDC)	2030 objectives from the Mexican government commitments and 2050 objectives assumed	2030 NDCs for the national system. The 2050 targets were suggested by the GIZ

\*Referring to the generation stage of the power system only. Not to life-cycle emissions.

### 4.2.3 Energy system model

The tool employed to carry out the energy system optimization model was the Framework for Integrated Energy System Assessment (FINE)<sup>41</sup>. A time-series aggregation algorithm<sup>42</sup> was used to cluster the input time series data into 30 typical days with 1 hour resolution to match the PRODESEN's. The margin of error reported of FINE with this configuration is ~5%<sup>43</sup>.

The generation time-series for wind and solar PV were obtained by simulating the 2019 weather data records according to the renewable assessment methodology presented in section 2.1. Given the hour time resolution of the model, peak capacity technologies like open combined cycle gas turbines (OCCGT) could be underestimated in some scenarios since periods shorter than one hour are not evaluated.

The five scenarios built are:

- **BaU2020:** This scenario control was modeled with the capacity operation “Fixed” which means constant capacity factors for all the input technologies according to PRODESEN 2019, except for the VRES technologies to resemble as much as possible to the current Mexican power system. The

VRES technologies were modeled with the capacity installed as the PROESEN 2018 but the operation was optimized.

- **BaU2030:** In addition to the technologies used in the BaU2020, Li-ion batteries, new natural gas-powered combined cycle gas turbine (CCGT-NG), and more VRES capacity are allowed to enter the system to compete with all other technologies on a cost-optimal basis. Conventional fossil-fuels technologies are modeled as “Fixed+” which means that they start with the same installed capacity as for e with the option to install more capacity if needed. Geothermal energy is modeled with the installed capacity of 2020 but in a cost-optimal dispatch. Nuclear and hydropower plants are input with fixed capacity and operation as the PRODESEN 2018.
- **H<sub>2</sub>MX2030:** It has the same system characteristics as the BaU2030 plus the allowance for hydrogen technologies with a 2030 CAPEX projection to participate in the cost-optimal solution.

<sup>41</sup> Welder L., Spatio-temporal optimization of a future energy system for power-to-hydrogen applications in Germany, 2018.

<sup>42</sup> L., Impact of different time series aggregation methods on optimal energy system design, 2018.

<sup>43</sup> D. G. Caglayan, Robust Design of a Future 100 % Renewable European Energy System with Hydrogen Infrastructure., 2020.

- **BaU2050:** It has the same system characteristics as the **BaU2030** regarding all technologies except for nuclear and hydropower plant set to a cost-optimal capacity expansion and operational dispatched.
- **H<sub>2</sub>MX2030:** It has the same system characteristics as the **BaU2050** plus the allowance for hydrogen technologies with a 2050 CAPEX projection to participate in the cost-optimal solution.

The modeling configuration between scenarios can be compared with Table 4-2. below.

Table 4-2. Comparison of the scenarios modeled.

System Inputs\Scenario	National					Mulegé	
	BaU2020	BaU2030	X2MX2030	BaU2050	X2MX2050	"Zero"	"H <sub>2</sub> Zero"
VRES (PV and Wind)	Fixed	Optimal	Optimal	Optimal	Optimal	Optimal	Optimal
Geothermal	Fixed	Fixed	Fixed	Optimal	Optimal	-	-
Hydropower	Fixed	Fixed	Fixed	Fixed	Fixed	-	-
Conventional technologies	Fixed	Fixed+	Fixed+	Optimal	Optimal	-	-
Nuclear	Fixed	Fixed	Fixed	Fixed	Fixed	-	-
H <sub>2</sub> technologies	-	-	Optimal	-	Optimal	-	Optimal
Li-ion batterie	-	Optimal	Optimal	Optimal	Optimal	Optimal	Optimal
Transmission grid	Fixed	Fixed	Fixed	Fixed	Fixed	-	-
CO <sub>2</sub> reduction target [MtCO <sub>2</sub> /a] (% reduction)	143 (0%)	136 (-30%)	136 (-30%)	174 (-50%)	174 (-50%)	0 (-100%)	0 (-100%)

- **Fixed:** Capacity and operation as given. Not optimized.
- **Fixed+:** Capacity as given and expansion allowed. Operation optimized
- **Optimal:** Capacity and operation allocated at cost-optimal. Fully optimized
- - : Not included in the model

## 4.3 Results

The results for the national power system are presented in the first place. Afterward, the results from the Mulegé zero-emission system are presented.

### 4.3.1 National power system

The five scenarios about the national power system development follow a time-frame order. The first scenario presented is the **BaU2020**, the closest representation of today's Mexican power system, so subsequent results can be compared to these control results. Next, the two scenarios modeling the mid-term time horizon for 2030, **BaU2030** and **H<sub>2</sub>MX2030**, are presented and compared to one another. Finally, the 2050 scenarios for the long-term, **BaU2050** and **H<sub>2</sub>MX2050**, are presented.

#### 4.3.1.1 Control scenario - BaU2020

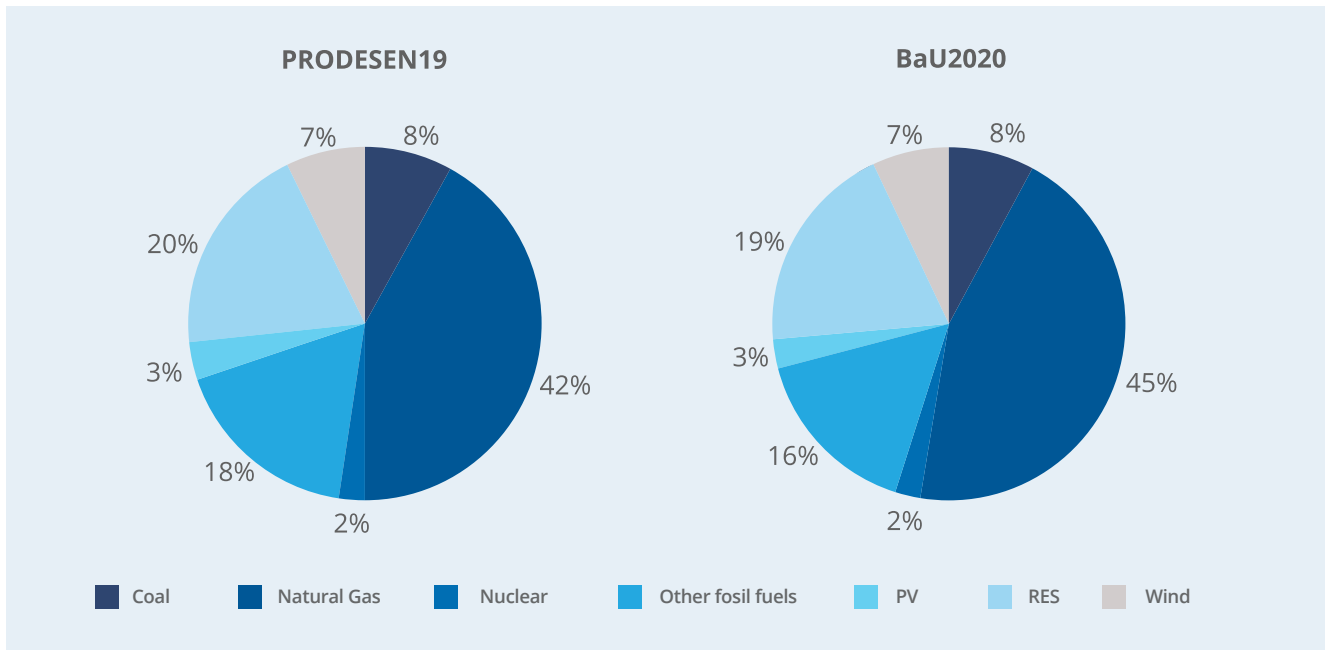
For this control scenario, a total annual cost (TAC)<sup>44</sup> of 35 Billion USD/year was found, which corresponds to an average electricity cost of 100 USD/MWh. The total emissions by the system were estimated at 116 MtCO<sub>2</sub>/year.

Figure 4-4. shows an installed capacity comparison between the PRODESEN 2019 data and the **BaU2020** control scenario. In comparison with the PRODESEN 2019, the **BaU2020** scenario shows a very similar capacity mix.

**BaU2020** TAC does not include charges such as capital cost of the grid, distribution grid costs, taxes, and other charges that could not be included due to lack of information publicly available. Nevertheless, the capacity installed, transmission capacities, and electricity demand were taken from the PRODESEN, making these two systems comparable in the generation and conversion, and transmission stages.

<sup>44</sup> Referring to the annual contribution to the capital costs and operational costs of the generation, conversion, fuel costs, and storage infrastructure of the system. The operation of the transmission lines is also included in this cost.

Figure 4-4. PRODESEN 2019 and BaU2020 capacity mix comparison.



### 4.3.1.2 Hydrogen integration by 2030 - BaU2030 and H<sub>2</sub>MX2030 scenarios

This section compares **BaU2030** against **H<sub>2</sub>MX2030** to assess the hydrogen integration potential by 2030. Firstly, Figure 4-5. compares the installed capacity of the two possible scenarios by 2030. In general terms, both scenarios show a similar capacity mix. Both scenarios rely on 56 GW of fossil-fuels based technologies, 1.6 GW of Nuclear power plants, 13.3 GW of hydropower and geothermal power plants (RES), around 27-29 GW of PV, and nearly 6 GW of wind installations. When looking closer, there are some small changes between the two scenarios such as the addition of 100 MW of wind and 1.5 GW of solar in the **H<sub>2</sub>MX2030** scenario. The **H<sub>2</sub>MX2030** scenario also has 1 GW of PEMEL capacity installed, producing 60 ktH<sub>2</sub>/year. The re-electrification process chosen by the models is carried out by 300 MW of OCGT-H<sub>2</sub>. Despite these differences, the capacity installed in both scenarios remains very similar.

Secondly, Figure 4-6. below shows that the percentage of renewable electricity in both scenarios is also similar. Around 24% of the electricity is expected to come from renewable sources in either scenario. The rest, around 76% of the total, is still of fossil-fuel origin. One difference is that approximately 4 TWh of renewable electricity was facilitated by hydrogen in the **H<sub>2</sub>MX2030** scenario to make up for the power-H<sub>2</sub>-power conversion processes.

Figure 4-5. Capacity installed in the Mexican power system by 2030 under two scenarios.

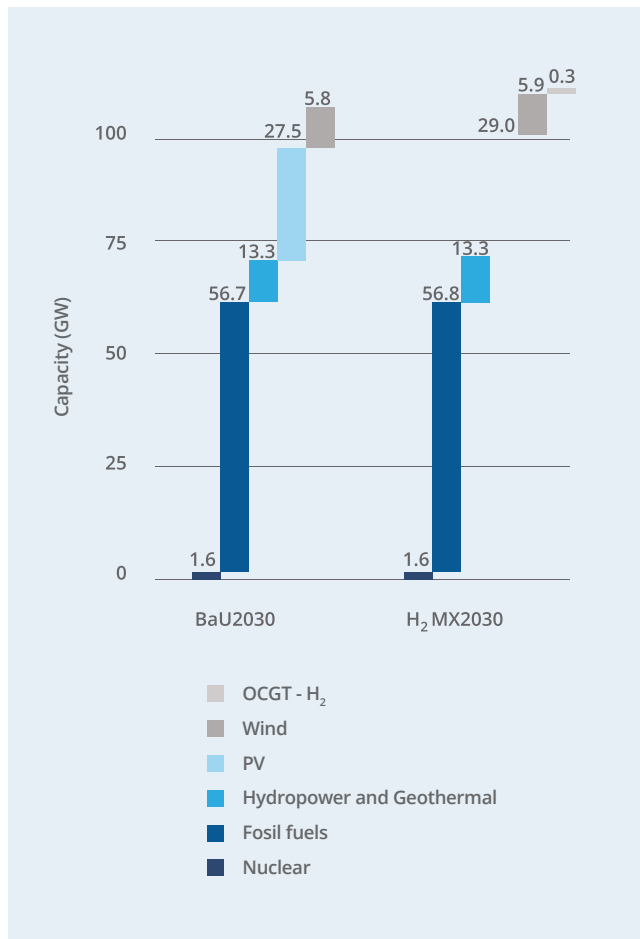
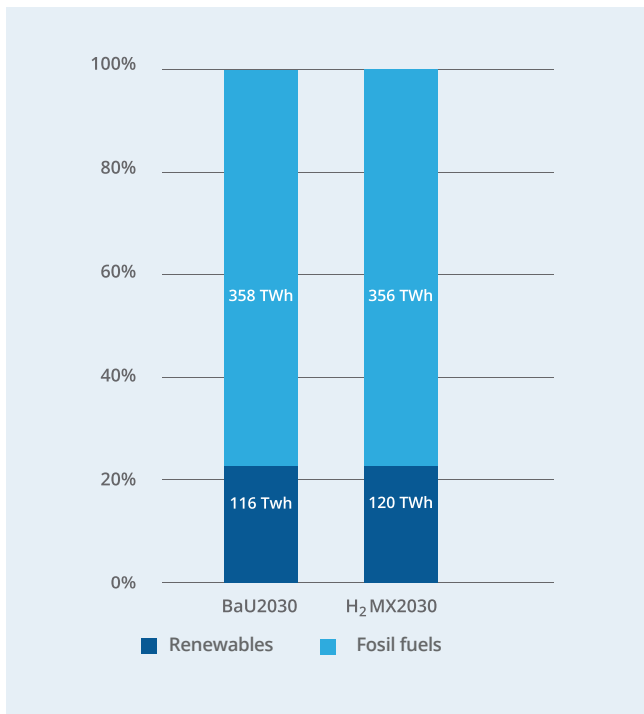
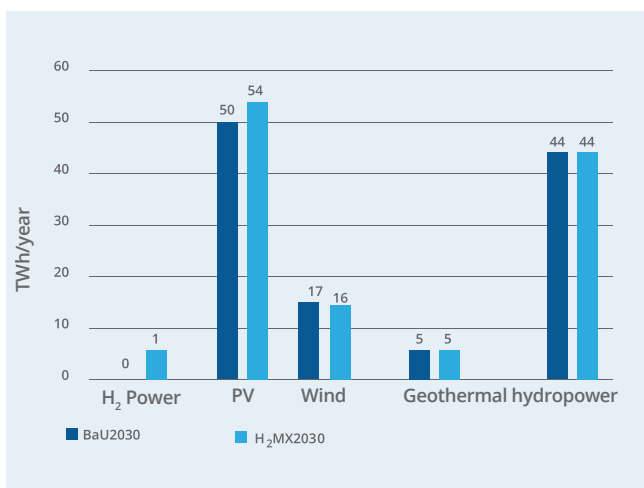


Figure 4-6. Electricity generation by source in the Mexican power system by 2030 under two scenarios.



Complementary, Figure 4-7. shows the electricity production of the different renewable technologies in both 2030 scenarios. PV is the renewable technology with the biggest electricity production in Mexico by 2030. In the **BaU2030** scenario, PV shows an annual generation of 50 TWh, whereas this yearly production increases to 54 TWh in the **H<sub>2</sub>MX2030** scenario. Geothermal and Hydropower technologies show no changes between the 2030 scenarios. The wind electricity output is shown to marginally decrease by 1 TWh/year in the **H<sub>2</sub>MX2030** scenario. Nevertheless, this decrease is offset by 1 TWh/year of electricity produced additionally from hydrogen.

Figure 4-7. Renewable production in the Mexican power system by 2030 under two scenarios.



Thirdly, the storage needs in both systems can be compared in Figure 4-8. In general, hydrogen causes a reduction in the electricity storage needs by allowing physical storage of energy in the form of gaseous hydrogen. In the **BaU2030** scenario, the system storage needs are around 25 GWh of electricity storage.

Figure 4-8. Storage capacity needs in the Mexican power system by 2030 under two scenarios.

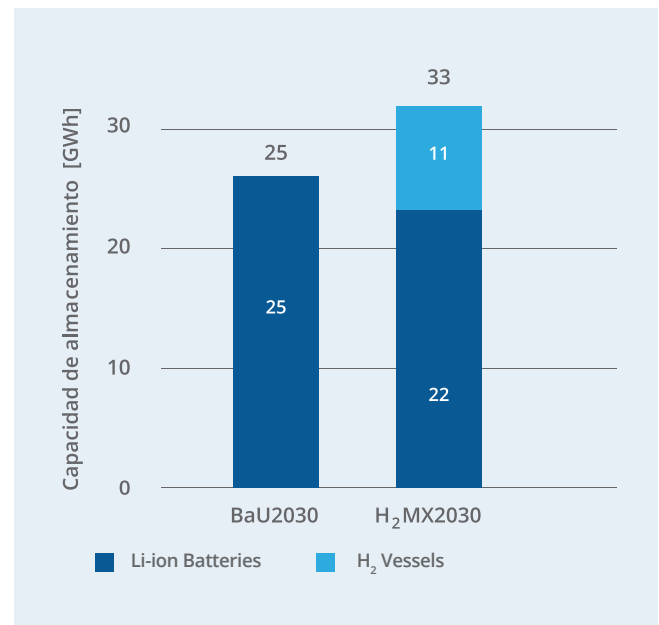


Figure 4-9. Total annual costs of the Mexican power system by 2030 under two scenarios.



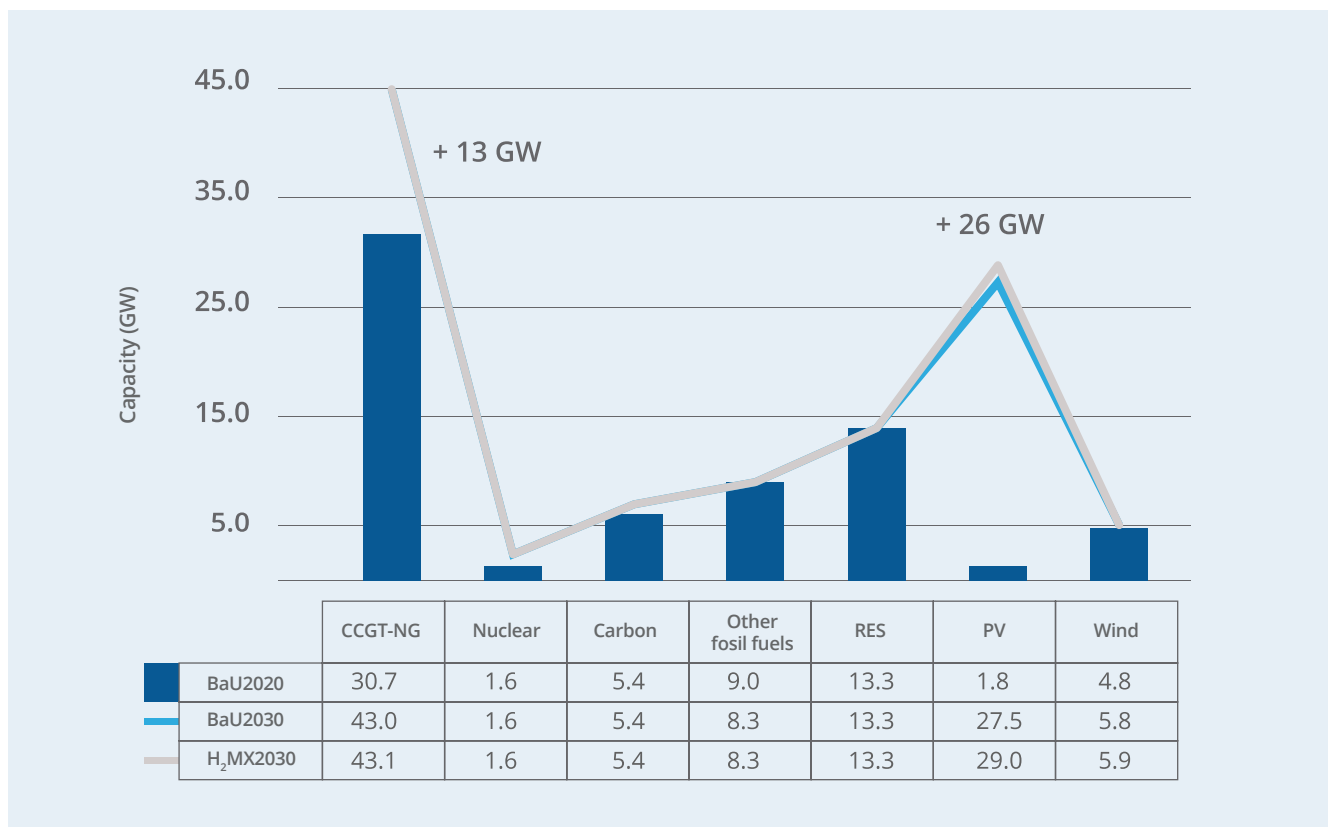
For the **H<sub>2</sub>MX2030** scenario, the electricity storage needs were reduced to 22 GWh, but additional 11 GWh<sub>2</sub> (330 tons of H<sub>2</sub>) were needed in H<sub>2</sub> vessels. Approximately 25% more energy storage was possible in the **H<sub>2</sub>MX2030** scenario compared with the **BaU2030** one at the same cost.

Despite the differences in the two 2030 scenarios, the hydrogen integration caused no sensible changes in the TAC. As shown in Figure 4-9, the TAC of either scenario was found at 43 billion USD/year. The corresponding electricity cost is 91 USD/MWh. There was a ~10% reduction in the electricity cost as compared with the **BaU2020** scenario. The generation and conversion of electricity is the main cost driver. It accounted for approximately 95% of the cost of the system. The total annual emissions by 2030 were estimated at 134 MtCO<sub>2</sub>/year for the BaU2030 scenario and 133 MtCO<sub>2</sub>/year for the **H<sub>2</sub>MX2030** one. This represents an absolute 15% more emissions by 2030 than in 2020. Nevertheless, the increased electricity production by the system increased by around 35% so the specific carbon emissions per kWh of electricity decreased by 18% from 339 to 289 gCO<sub>2</sub>/kWh.

Figure 4-10. presents the installed capacities of **BaU2030** and **H<sub>2</sub>MX2030** compared to the **BaU2020**. From the figure two major changes from 2020 to 2030 can be seen; an additional 13 GW of CCGT-NG installed capacity and 26 GW of PV. Also, around 700 MW of thermo-power plants and diesel generators were shut down. Nuclear, coal, hydropower, geothermal, and wind stayed unchanged.



Figure 4-10. Capacity installed in the Mexican power system by 2030 under two scenarios compared to the 2020 status (CHANGE to PRODESEN 2019).



### 4.3.1.3 Hydrogen integration by 2050 - BaU2050 and H<sub>2</sub>MX2050 scenarios

This section compares BaU2050 against H<sub>2</sub>MX2050 to assess the hydrogen integration potential by 2050. Again, the first comparison is regarding the installed capacities as shown in Figure 4-11.

There is an increase of 6 GW of solar PV and 1.5 GW of hydrogen-powered combined cycle gas turbine (CCGT-H<sub>2</sub>) in the H<sub>2</sub>MX2050 scenario. Also, the installed capacity of the CCGT-NG was reduced by 800MW in the hydrogen integrated scenario.

Similar to the 2030 scenarios, in 2050 PV is the technology that dominates electricity production.

Figure 4-12. shows that PV could be responsible for more than 50% of the total electricity generation by 2050 in either scenario. Wind energy is found to be the second most important electricity source with ~21% of the electricity production share regardless of the scenario, whereas CCGT-NG is third with ~18-19% depending on the scenario.

Figure 4-11. Installed capacity in the Mexican power system by 2050 under two scenarios.

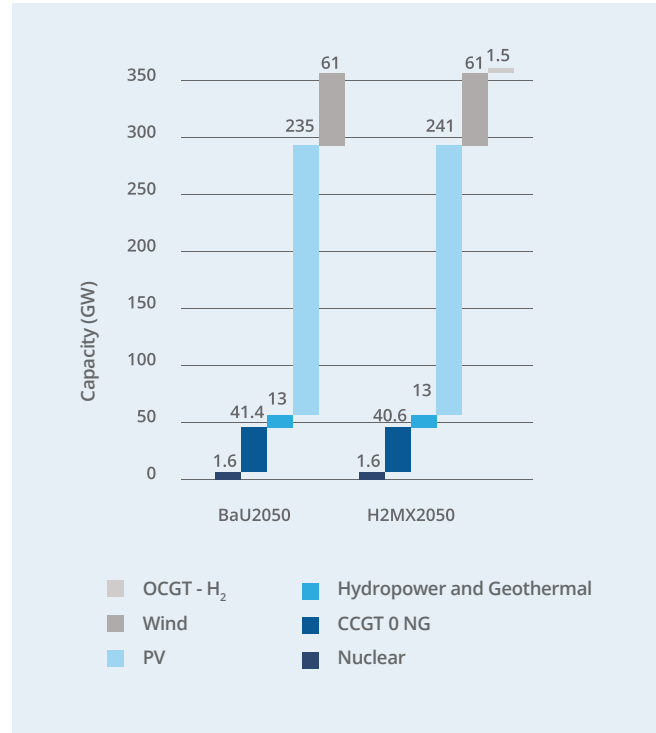
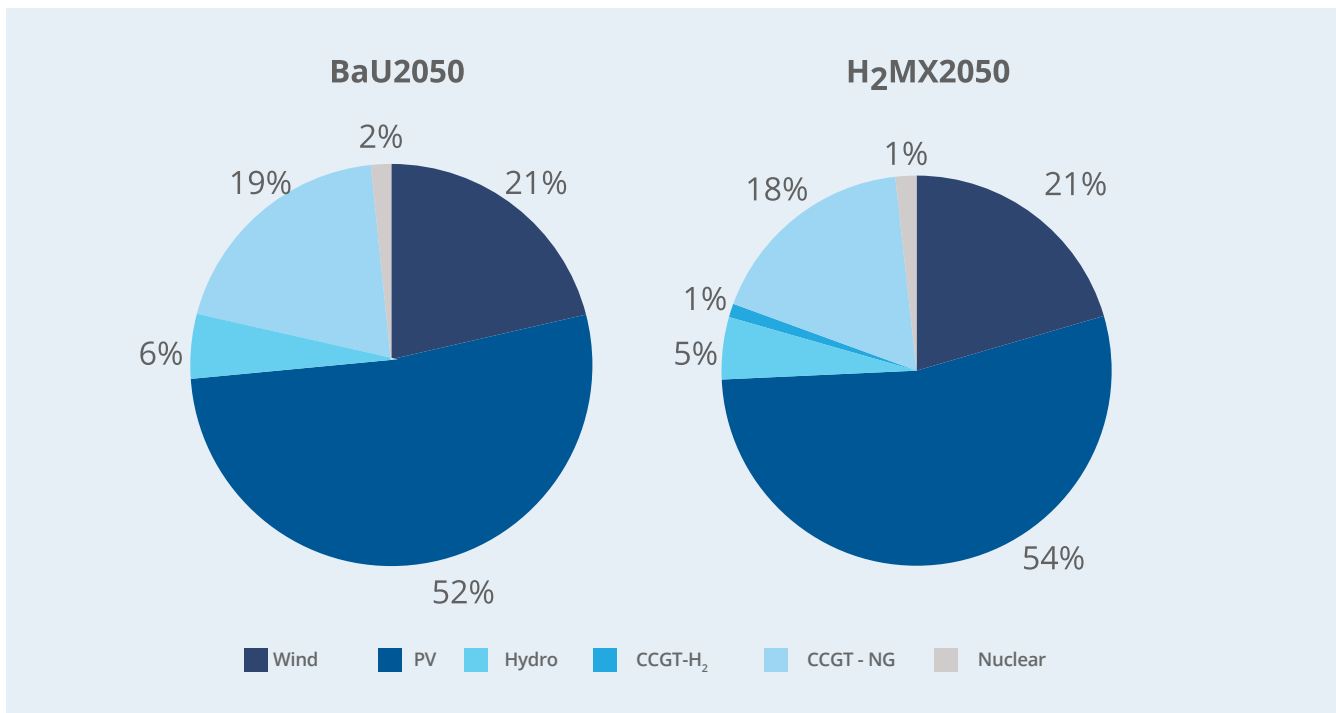


Figure 4-12. Renewable production in the Mexican power system by 2050 under two scenarios.



The model chose not to dispatch any other fossil-fuel-based technology except for CCGT-NG and nuclear power. As explained previously, nuclear energy was modeled fixed, so its share in the energy mix obeys the scenario design decisions rather than to an optimal solution. The lack of other fossil-fuel technologies can be explained by several factors.

Firstly, the costs of fossil fuels cause the marginal cost of production of electricity not to be competitive with VRES technologies. Next, the low efficiencies of present fossil fuel technologies compared to new CCGT-NG or CCGT-H<sub>2</sub>. Another reason is the reduced capacity factors that are a consequence of having a system with such large amounts of renewable energy. Finally, the preference for low-carbon technologies by the optimizer so that the carbon budget is maximized by using less polluting technologies such as CCGT-NG.

In the same line, no dispatch of geothermal power plans was present in either scenario by 2050. This can be explained also by the marginal cost of production of geothermal energy and its reduced load factors. It is important to remark that geothermal technologies were

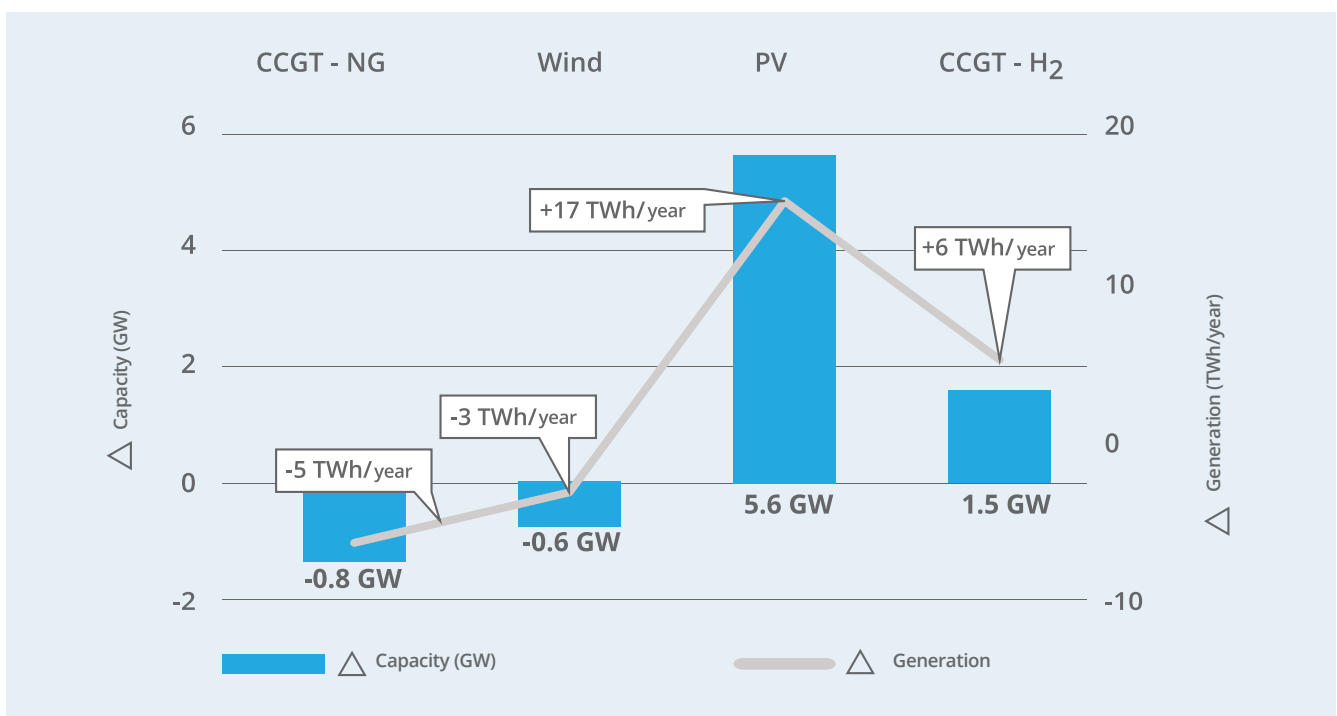
modeled with constant prices for 2020, 2030, 2050 since no major developments in this renewable technology are expected.

Should the investment cost be reduced and the marginal cost of production fall to nearly zero so this technology could compete with VRES and, geothermal energy can have higher importance by 2050.

Another change between the **BaU2050** and the **H<sub>2</sub>MX2050** scenarios is the total amount of energy generated. There are 15 TWh/year of additional electricity generated (~2% of the total) in the **H<sub>2</sub>MX2050** scenario to account for power-H<sub>2</sub>-power conversion processes.

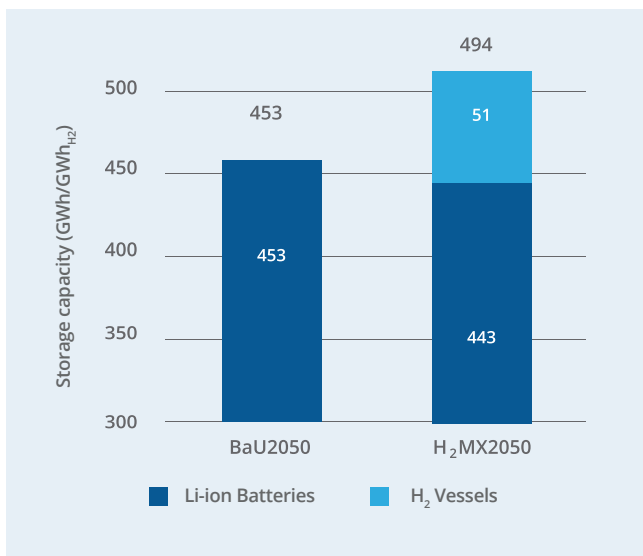
Figure 4-13. shows that the increment is caused by around 20 TWh/year of additional renewable electricity; 17 TWh/year of them coming from an additional 5.6 GW of PV and other 6 TWh/year from 1.5 GW of GGCT-H<sub>2</sub>. There were also 3 TWh/year less wind energy from -600 MW of wind installations. There is also a 5 TWh/year reduction in electricity production by -800 MW of CCGT-NG plants.

Figure 4-13: Changes in electricity production in the Mexican power system by 2050 under the two scenarios.



With nearly 80% VRES penetration, the storage needs by 2050 are approximately 18 times higher than for the 2030 scenarios. There **BaU2050** needs approximately 453 GWh of electric storage, whereas the **H<sub>2</sub>MX2050** needs 443 GWh of electric storage and 52 GWh of H<sub>2</sub> storage (1.5 ktH<sub>2</sub>). The **H<sub>2</sub>MX2050** system needs around 10% more storage to be able to yield more PV energy.

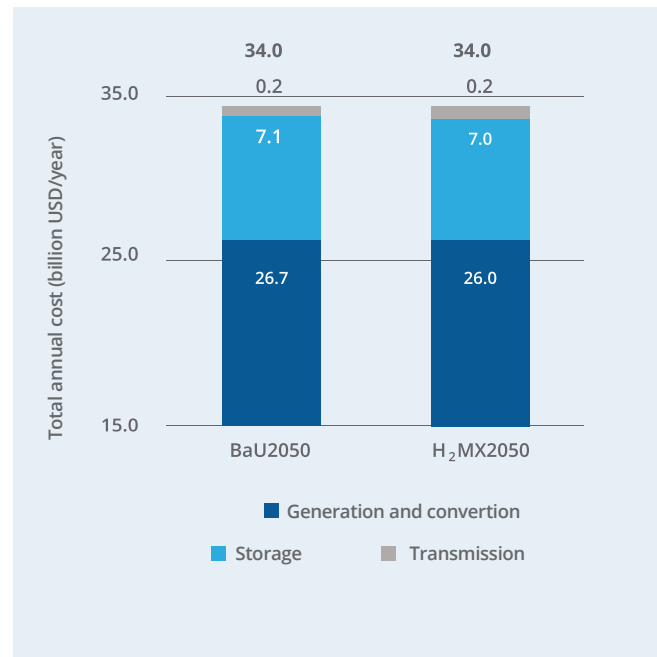
Figure 4-14. Storage needs for a Mexican power system by 2050 under two scenarios.



The TAC of both systems decreased ~20% from the 2030 systems despite producing approximately 60% more electricity. The TAC by either 2050 scenario is found to be 34 billion USD/year. The corresponding electricity cost is 43 USD/MWh. This means that there is a – 57% reduction in the electricity cost compared to the control scenario **BaU2020**. The reduction in the TAC was possible due to the lower capital costs of the PV, wind turbines, and Li-ion-batteries expected by 2050. Given the large amounts of energy that need to be stored, the weight that the energy storage cost has in the TAC is much bigger. By 2050 it will be around 20% of the electricity cost. Generation and conversion of energy is still the higher cost contributor.

The total emissions by 2050 were calculated in 30 MtCO<sub>2</sub>/year and 29 MtCO<sub>2</sub>/year for the **BaU2050** and **H<sub>2</sub>MX2050** respectively, which a decrease of around 75% compared to the **BaU2020**. The specific emissions per kWh of electricity produced decreased by almost 90% from 339 gCO<sub>2</sub>/kWh in the **BaU2030** to 39 gCO<sub>2</sub>/kWh in the **BaU2050** and 38 gCO<sub>2</sub>/kWh in the **H<sub>2</sub>MX2050** scenario.

Figure 4-15. Total annual cost (TAC) of a Mexican power system by 2050 under two scenarios.



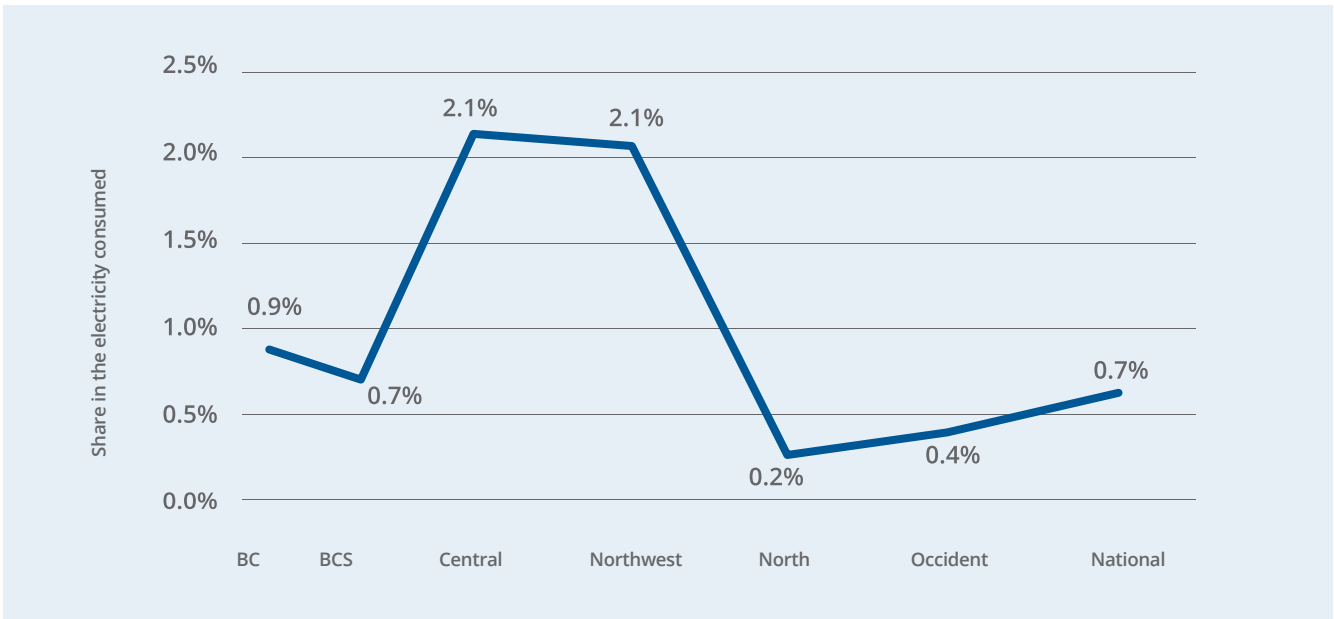
#### 4.3.1.4. Hydrogen in the H<sub>2</sub>MX2050 scenario

The past two sections showed a one-to-one comparison between the scenarios with and without hydrogen integration. This section looks specifically at the hydrogen infrastructure in the **H<sub>2</sub>MX2050** scenario, which was the scenario that showed the largest integration potential.

According to the model results, 5.5 TWh/year of electricity was from hydrogen re-electrification. This amount is approximately 0.7% of the electricity mix at a national level by 2050 and around half of today's Nuclear energy output. The share of re-electrified hydrogen is not the same across the transmission regions of the Mexican power system. Figure 4-16. Share of electricity from hydrogen re-electrification in the total electricity consumed in the **H<sub>2</sub>MX2050** scenario.

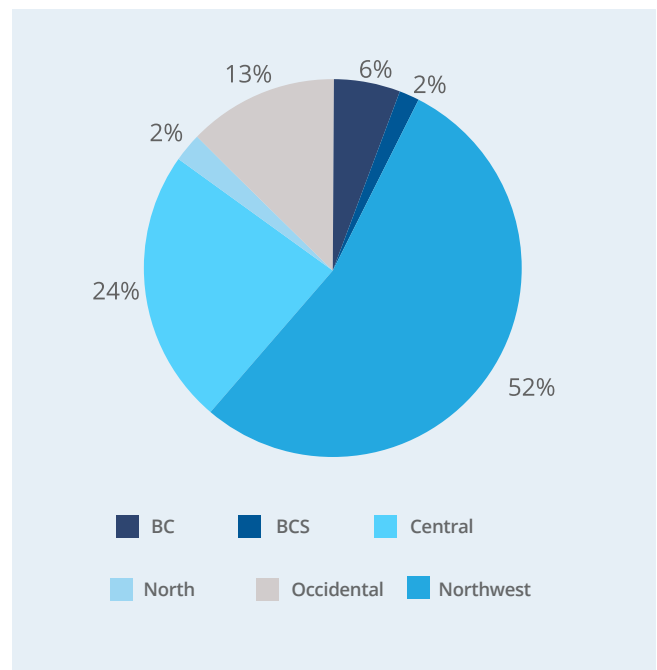
Shows the hydrogen re-electrified share in the electricity by transmission region. In the Central and Noroeste regions, hydrogen has a higher integration potential of up to 2.1% (3 times higher than the national average). In other regions, the integration level is between 0.2% and 0.9% of the total electricity mix. There are two regions, Peninsular and Oriental, where hydrogen showed no integration in the electricity mix.

Figure 4-16. Share of electricity from hydrogen re-electrification in the total electricity consumed in the H<sub>2</sub>MX2050 scenario.



In total 280 ktH<sub>2</sub>/year are produced in 6 regions. Figure 4-17. Hydrogen production by region of transmission in the H<sub>2</sub>MX2050 scenario, shows the hydrogen production share by region. Approximately 148 ktH<sub>2</sub>/year (53% of the total production) occurs in the central region.

Figure 4-17. Hydrogen production by region of transmission in the H<sub>2</sub>MX2050 scenario.



According to the renewable assessment of section 2 this region lacks wind resources and it is the region with the highest electricity demand so hydrogen helps taking advantage of solar energy, the only renewable resource available there. Another 67 ktH<sub>2</sub>/year (24% of the total production) is produced in the Noroeste region where there is the highest solar potential and also a lack of wind resources. The remaining hydrogen is produced among the other regions. No H<sub>2</sub>-pipelines were installed by the model, so all the hydrogen produced in a region is consumed on-site.

The hydrogen was produced by PEMEL with an average capacity factor of 26% which points out that solar energy was the main source of energy to produce hydrogen. Figure 4-18. shows a map of the PEMEL installed capacity per region. In total, 4.2 GW of PEMEL capacity is required and its distribution is proportional to the hydrogen produced with some small differences according to the region's variable resource potential available. Approximately 50% (2.2 GW) of PEMEL capacity will be installed in the central region. Another 25% of PEMEL installed capacity is located in the Noroeste region.

The re-electrification of hydrogen is carried out by CCGT-H<sub>2</sub> with an average capacity factor of 42%. As explained before, the 1-hour time-resolution of the model does not favor OCGT-H<sub>2</sub> installations. It is expected that both technologies would co-exist in a proportion of around 95% CCGT-H<sub>2</sub> and 5% OCGT-H<sub>2</sub>. Other hydrogen re-electrification technologies such as fuel-cells could be considered in a more in-depth analysis at higher spatial and temporal resolution.

Figure 4-18. Proton exchange membrane electrolyzer installed capacity per region in the H<sub>2</sub>MX2050 scenario.



Figure 4-19. shows the distribution of CCGT-H<sub>2</sub> installed capacity by region. In total 1.5 GW of CCGT-H<sub>2</sub> would be needed. The PEMEL and CCGT-H<sub>2</sub> distribution are proportional. There are approximately 3 times more PEMEL installed capacity than CCGT-H<sub>2</sub>.

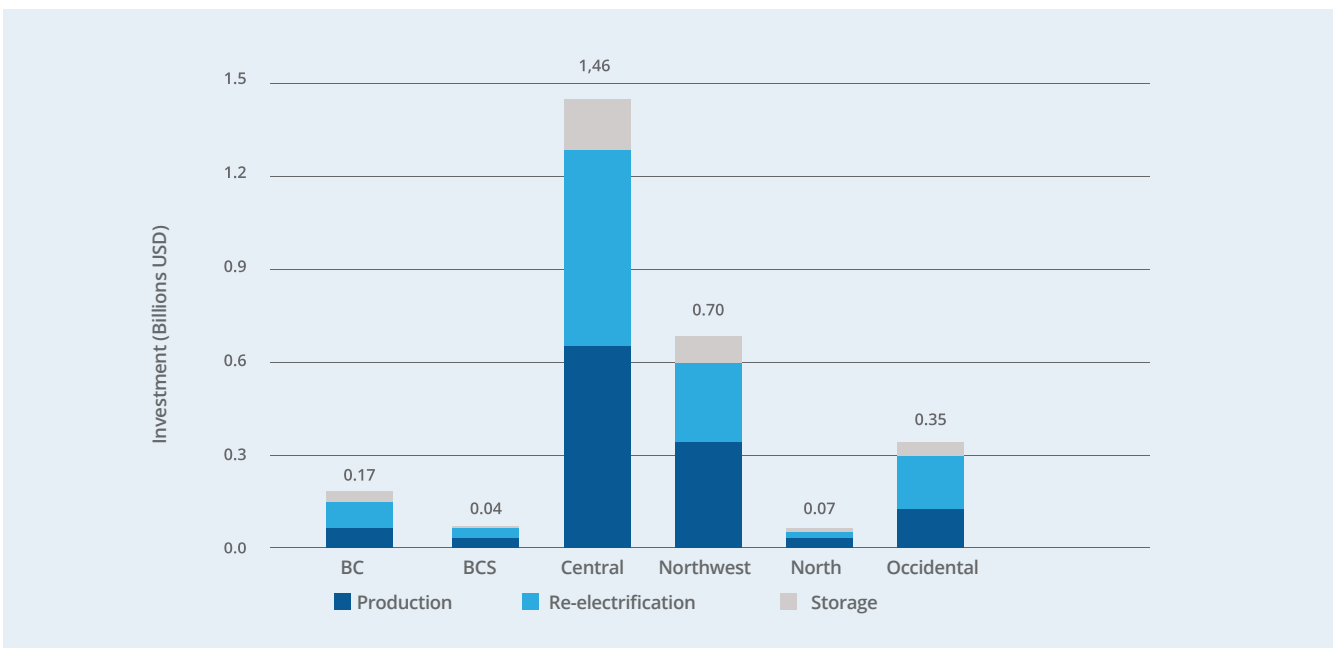


Figure 4-19. Combined-cycle gas turbine (hydrogen) installed capacity per region in the H<sub>2</sub>MX2050 scenario.



According to the model results, 2.8 billion USD are needed for hydrogen infrastructure. The regions with the highest share are again Central and Northwest regions as shown in Figure 4-20. The largest cost contributor is the hydrogen production stage, it represents around 45% of the total investment. The re-electrification stage represents around 40% and the storage of hydrogen around 15%.

Figure 4-20. Investment in hydrogen infrastructure by region under the H<sub>2</sub>MX2050 scenario.

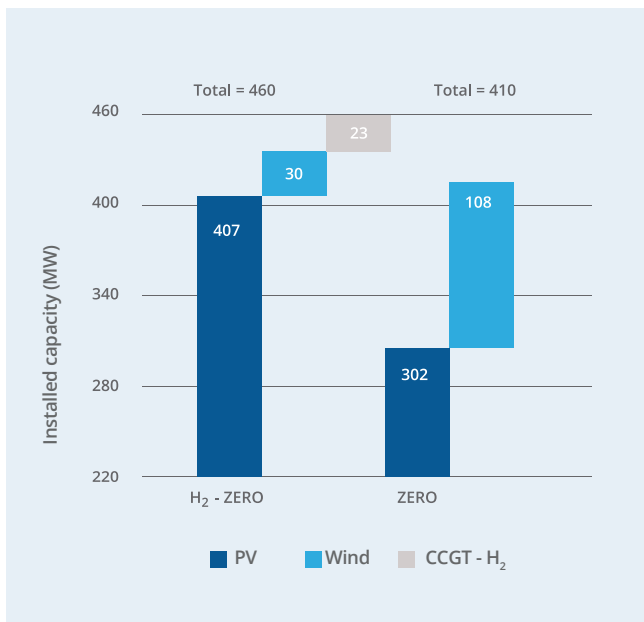


### 4.3.2 Mulegé zero-emission system

There were considerable changes in the Mulegé zero-emissions system with and without hydrogen. The first one is the total installed capacity. For the **H<sub>2</sub>-ZERO** scenario, the total installed capacity is 460 MW whereas for the **ZERO** scenario it is 410 MW. Approximately 11% more capacity installed was chosen in the hydrogen scenario. This change was due to a shift in an energy source that was facilitated by hydrogen. Solar PV is the cheapest energy source, so approximately 105 MW of additional PV was preferred over 78 MW of wind to produce green hydrogen. Besides, 23 MW of CCGT-H<sub>2</sub> was needed to re-electrify the hydrogen produced.

The shift to more solar energy can be seen in the electricity generation mix represented in Figure 4-22. In the **ZERO** scenario, solar energy takes 75% of the total electricity mix and the 25% remaining is electricity coming from the wind. In the hydrogen-integrated scenario, there is up to 86% of solar energy in the system with only 6% of wind and 8% of CCGT-H<sub>2</sub>.

Figure 4-21. Capacity installed in a zero-emissions Mulegé power system by 2050 under two scenarios.



The electricity mix changes are not only in proportions but also in total numbers. The **H<sub>2</sub>-ZERO** scenario needs to produce 19% more energy to make up for the electricity-H<sub>2</sub>-electricity processes.

Figure 4-22. Electricity production by source in a zero-emissions Mulegé power system by 2050.

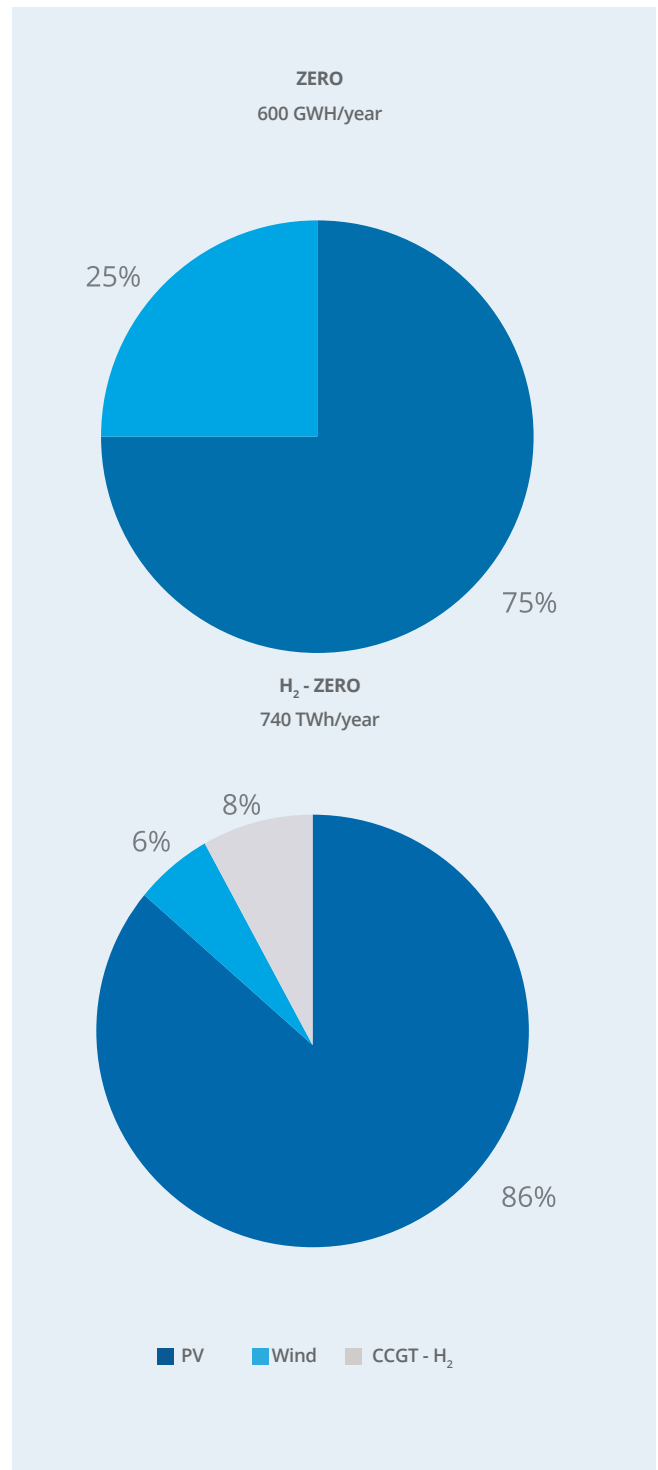
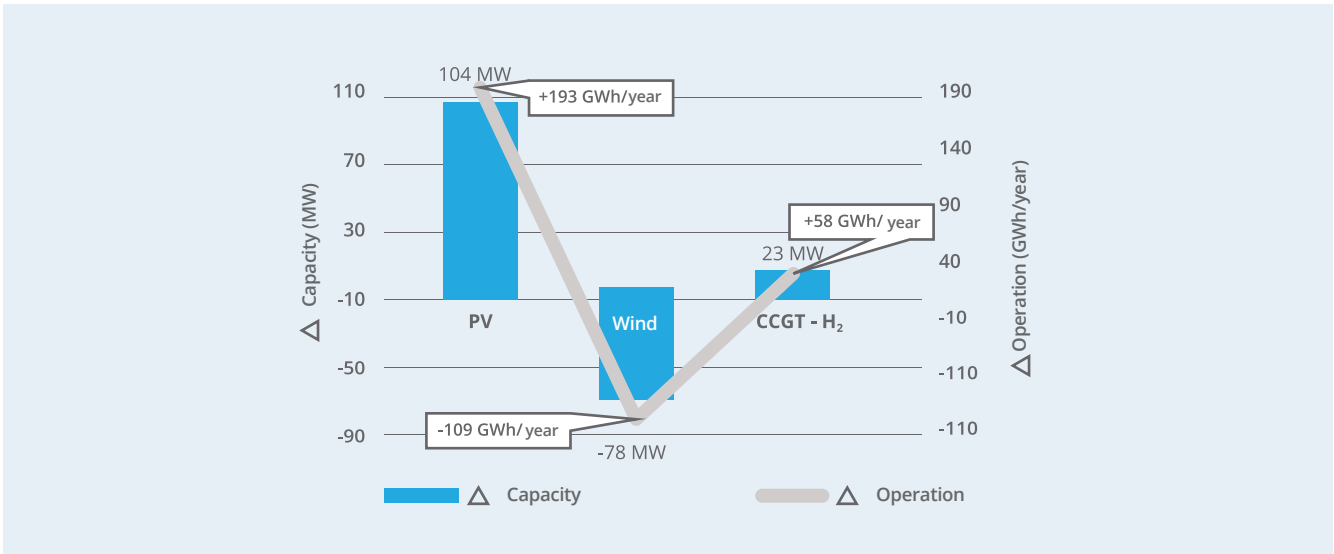


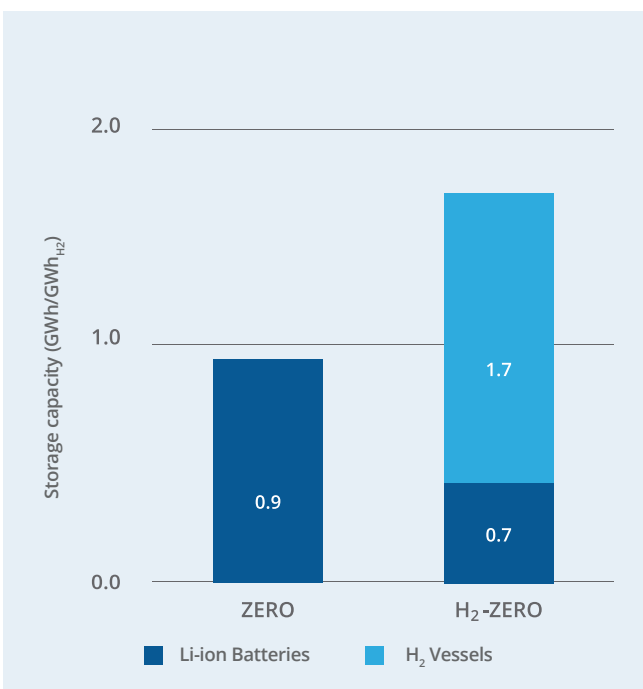
Figure 4-23. shows that the extra energy came from additional 193 GWh/year of electricity by PV plants and 58 GWh/year of electricity by CCGT-H<sub>2</sub>. There was also 109 GWh/year of less wind energy in the system.

Figure 4-23. Changes in electricity generation capacity and operation in a zero-emissions Mulegé power system by 2050 under two scenarios.



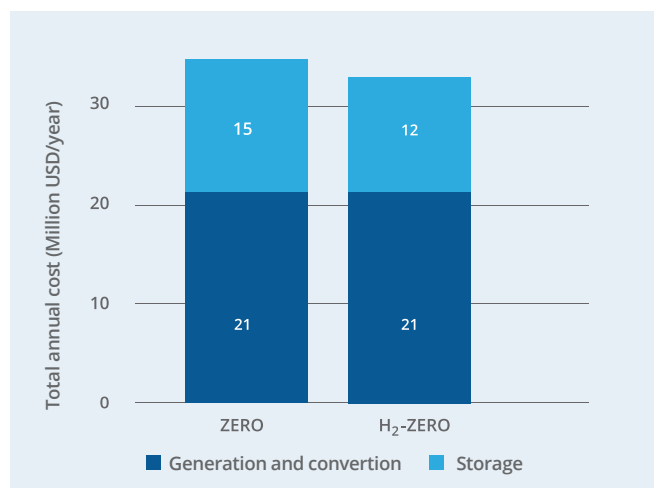
The storage needs of the system also decreased. In the ZERO scenario, 943 MWh of electric storage was needed, whereas in the H<sub>2</sub>-ZERO scenario 718 GWh of electric storage (24% less compared to the ZERO scenario) and 1.6 GWh of H<sub>2</sub> storage (50 tonH<sub>2</sub>) was required. Figure 4-24. shows the storage needs of both systems.

Figure 4-24. Storage needs for a zero-emissions Mulegé power system by 2050 under two scenarios.



The system TAC also shows a reduction when hydrogen was integrated. In the H<sub>2</sub>-ZERO scenario, the TAC was found to be 36 million USD/year and in the H<sub>2</sub>-ZERO the TAC was 33 million USD/year. There was a net 8.3% TAC reduction caused entirely by the reduction in storage needs. Despite having 11% more installed capacity, the H<sub>2</sub>-ZERO scenario did not increase the TAC contribution of the generation and conversion of the electricity stage. The cost of generation and conversion of electricity was maintained at 21 million USD/year in both scenarios. It is important to highlight that no transmission lines were modeled in the single-node energy model used in the Mulegé system, so local distribution lines need to be evaluated and added to the total system cost.

Figure 4-25. Total annual costs (TAC) comparison for a renewable Mulegé system by 2050 under two scenarios.



### 4.3.3. Summary table

Table 4-3. shows a summary of the benefits in percentages of the total that hydrogen brought to the system in the H<sub>2</sub>MX2030, H<sub>2</sub>MX2050, and H<sub>2</sub>-ZERO scenarios compared with the scenarios with no hydrogen integration.

Table 4-3. Summary table of integration potential.

Ranking	SEN 2030	SEN 2050	Mulegé 2050
Share of H <sub>2</sub> re-electrified in the electricity mix	< 0.01%	0.7%	8%
TAC reduction	< 0.01%	< 0.1%	8.3%
CO <sub>2</sub> emissions reduction	< 0.01%	0.03%	-
Solar energy integration	5%	4%	40%
Wind energy integration	-6%	-2%	-72%
Reduction in electric storage	-12%	-2%	-23%
Conclusion	Limited integration potential	Low integration potential	Medium integration potential

Finally, Table 4-4. shows that the water requirements for hydrogen production per region according to the energy system model are negligible in comparison with the total

amount of water consumed. In all cases the water usage for hydrogen production would represent 0.01% or less of the total water consumed in the region.

Table 4-4. Water consumption comparison.

Region	Water consumption for H <sub>2</sub> production estimated by 2050 [hm <sup>3</sup> /year]	Water consumption in the region* [hm <sup>3</sup> /year]	Water consumption for H <sub>2</sub> production as percentage of the water consumption in the region
Baja California	0.2	3,050	<0,01%
Baja California Sur	0.1	424	0.01%
Central	1.8	7,573	0.01%
Noroeste	0.9	16,599	<0,01%
Norte	0.1	6,739	<0,01%
Occidental	0.4	21,065	<0,01%
Mulegé	0.03	141**	0.02%

\* Quantity estimated by adding the water consumption by the states included in the region.

\*\* Quantity estimated by assuming 1/3 of water consumption in the Baja California Sur state according to Mulegé territorial share in the state.

#### 4.4. Conclusions

From the results of the model, several conclusions can be drawn:

##### The national power system and hydrogen integration by 2030

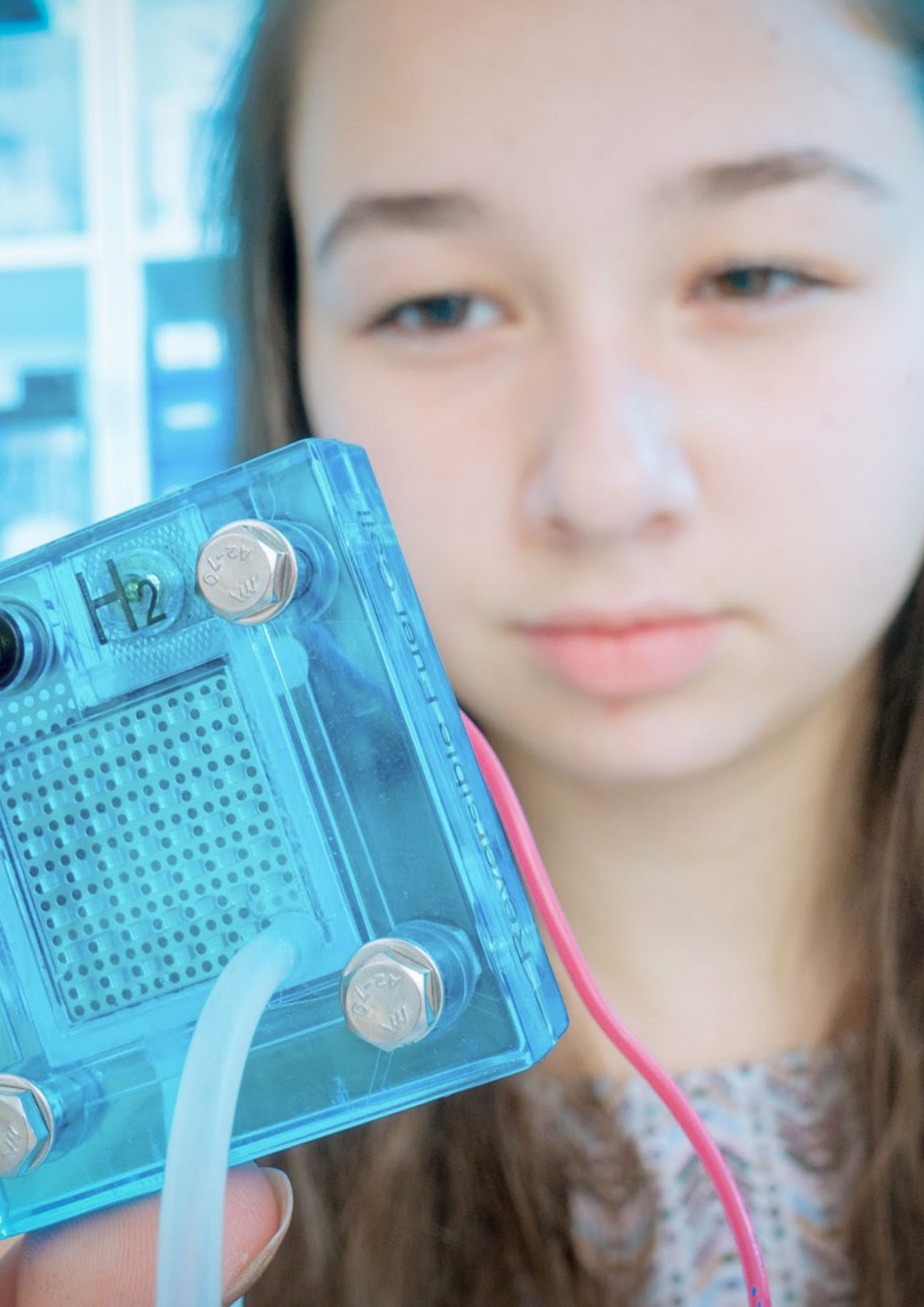
- The electricity production by 2030 will be still dominated by fossil-fuel technologies and the 2030 NDC would not be met unless actions are taken to renovate the existing electricity generation infrastructure, especially the carbon, thermoelectric, and diesel power plants. The optimization model did not consider the installation of more of these technologies, so, unless they dramatically reduce their capital cost and improve their efficiency, the best option is replacing them with renewable energy technologies (mainly solar PV) with utility-scale battery storage systems and new CCGT-NG.
- The similarities between the BaU2030 and H<sub>2</sub>MX2030 scenarios point out that the development of the Mexican power system is going to be more or less the same for the next 10 years. Hydrogen technologies need to take advantage of large amounts of VRES energy at nearly zero marginal cost, but those high levels of renewable energy are not expected in the Mexican power sector by 2030. Therefore, hydrogen integration by 2030 is limited. The hydrogen integration at a large scale is likely to occur after 2030. Still, some hydrogen production clusters could be implemented in the coming decade to pave the way for a larger hydrogen infrastructure deployment in the future. Installing electrolyzers powered by solar energy and hydrogen power turbines as close as possible to electricity (and potentially hydrogen demand centers) is the suggested approach.
- Solar energy could become the largest renewable source of electricity as early as 2030. Combining the projected cost of PV plants of 320 USD/kW by 2030 and the large potential of this resource across the country, the Mexican power system needs to be prepared to handle fluctuations in electricity production according to the solar cycles. Consequently, the Mexican power system needs to invest in the control and dispatchability of its existing and new conventional technologies. Besides, new geological studies to find pumped-hydro possible reservoirs, as well as feasibility location studies for gas storage in salt caverns (hydrogen) are additional options to enable storage of energy and create resilience in the power system. In parallel, the Mexican power system needs to deploy utility-scale battery storage and eventually explore the physical storage of energy in the form of hydrogen.

## The national power system and hydrogen integration by 2050

- The national power system by 2050 will naturally shift from fossil fuel-based to a variable renewable energy-based system according to the VRES technology development and decreasing cost expected by then. According to the model results of either development line, the optimal national power system configuration by 2050 includes approximately 80% of VRES electricity. With this intensity of renewable energy integration, hydrogen integration can occur at a national level.
- The green hydrogen production in Mexico will be mainly of solar origin. Its integration into the system translates into making more use of the low-cost solar energy in non-day times. The level of integration of hydrogen showed in the model is comparatively small (between 0.5% and 1% of participation in the electricity mix). Nevertheless, the hydrogen infrastructure does not require additional investment and could enable strategic sector coupling with other important economic segments.
- The deployment of hydrogen infrastructure will follow demand centers such as the proximity of the Mexico City metropolitan area and regions with the highest solar resources such as the Northeast region.
- According to current technology and cost projections, PEM electrolyzers and CCGT-H<sub>2</sub> are the green hydrogen technologies that will dominate the hydrogen investments for power generation.
- The effect of hydrogen integration in the power systems evaluated is enabling more solar PV into the energy mix and reducing the storage needs. Green hydrogen production will be mostly solar based. Hydrogen integration reduces the needs for onshore wind installations in regions where high proportions of the land are natural reserves and have the best wind locations contained within.
- Energy storage is key for integrating high levels of solar PV and wind into the power system. Batteries and hydrogen storage are responsible for the high VRES integration and cost reductions in the generation of electricity. Around 20% of the cost of the system is going to be spent on energy storage.
- Investigating and keeping up to date on other options of storage such as geological storage of hydrogen in salt caverns and pumped-hydro storage is important. Novel findings and storage potentials can be incorporated into future analyses and reduce the need for Li-ion batteries showed by the model here.

## A zero-emissions Mulegé system by 2050

- Green hydrogen will increase the solar integration level in the system. According to the results of the optimization, the integration of hydrogen would increase the solar share in the energy mix to up to 86%. Having a larger share of solar energy in the system could be beneficial since solar energy is an accessible, predictable, and low-cost energy source available widely in the region. It will also reduce the need for deploying wind energy in protected areas with good wind resources. On the other hand, there must be enough storage capacity in the system to increase the security of supply in order for the system to be able to handle the possibility of not having sunlight in a determined period of time given the large dependency of the system for this energy source.
- Deploying higher quantities of wind energy is not a warranty for a more secure energy supply by the system, despite having higher capacity factors than solar energy. If more wind energy integration was to be encouraged in the system, the energy storage capabilities would also need to be able to handle periods of no wind and no sunlight combined.
- The hydrogen integration would also cause a reduction in storage cost. With large quantities of solar, the system will need to store a large amount of energy. Doing that in Li-ion batteries alone will be 8.3% more expensive than to use hydrogen storage in vessels for a portion of the energy.
- The generation of electricity from re-electrification of hydrogen could have a higher participation in the energy mix than the electricity from wind turbines according to the cost and technology development projections.



## 5. Conclusions and recommendations

Mexico has a large renewable potential for both solar PV and wind plants but due to the resource available, solar PV is more attractive, reaching 15 USD/MWh in a grand part of the territory. The energy that can be produced could be enough to cover all the electricity demand of the country, but this is unlikely to happen in the short term because of the inherent restrictions and challenges of an energy system with high variable renewable energy penetration, despite the cost benefits.

The green hydrogen potential is driven mainly by solar PV plants. Their competitive energy prices could allow to produce green H<sub>2</sub> at a cost around 1.5 USD/kg H<sub>2</sub> in 2050 following the current trend in technology cost decrease. The water that would be required for hydrogen production is almost negligible compared with the current national consumption as seen in Figure 2-13, and water consumption in Mexico will not be threatened with massive-scale green hydrogen production.

Several scenarios were made and evaluated to assess the effects of renewables and green hydrogen integration in both the national energy system and the Mulegé energy system in Baja California. For the national system, it is expected for the midterm that the system will not have significant changes. After several cost reduction and improvements of the technologies leading to 2050, the system will incorporate hydrogen (for power-to-power applications) in significant amounts for economic reasons.

For the Mulegé region, due to its geographical and operational characteristics, a 100% renewable system was analyzed, with and without green hydrogen. To supply the total demand in 2050, more than 4,00 MW of renewable generation will be necessary. The main benefit of integrating hydrogen is that it will allow a higher usage of energy coming from lower-cost solar PV plants, decreasing the total cost of the system.

This study recommends the analysis of the integration of green hydrogen in different sectors, such as heavy-duty transport and chemical and thermal uses in industry in addition to power generation. Coupling different

sectors to the use of green hydrogen could improve its competitiveness and accelerate its deployment, as aggregated demand can create a more suitable scenario for green hydrogen production at a large scale.





# Bibliography

- BloombergNEF, "Hydrogen Economy Outlook," BloombergNEF, London, 2020.
- BloombergNEF, "Hydrogen: The Economics of Production From Renewables," BloombergNEF, London, 2019.
- BloombergNEF, "Hydrogen: The Economics of Storage," BloombergNEF, London, 2019.
- C. Damak, D. Leducq, H. M. Hoang, D. Negro and D. Anthony, "Liquid Air Energy Storage (LAES) as a large-scale storage technology for renewable energy integration – A review of investigation studies and near perspectives of LAES," *International Journal of Refrigeration*, vol. 110, pp. 208-218, 2020.
- CONAGUA, *Estadísticas del Agua en Mexico 2017 - Comisión Nacional del Agua*, 2017.
- D. G. Caglayan, *Robust Design of a Future 100 % Renewable European Energy System with Hydrogen Infrastructure.*, 2020.
- DTU Wind Energy, "Global Wind Atlas," 2019.
- E. Borri, A. Tafone, G. Zsembinski, G. Comodi, A. Romagnoli and L. F. Cabeza, "Recent Trends on Liquid Air Energy Storage: A Bibliometric Analysis," *Applied Sciences*, vol. 10, pp. 2773-2792, 2020.
- EESI, "Fact Sheet: Energy Storage," Environmental and Energy Study Institute, Washington D.C., 2019.
- Energy Storage Association, "Why Energy Storage - Technologies" [Online]. Available: <https://energystorage.org/why-energy-storage/technologies/liquid-air-energy-storage-laes/> [Accessed 3 November 2020].
- ESMAP, SOLARGIS, WB, & IFC, "Global Solar Atlas. In *Global Solar Atlas*," 2019.
- Evans, D.G., Jones, S.M., "Detecting Voronoi (area-of-influence) polygons.," *Mathematical Geology*, 1987.
- F. Díaz-González, A. Sumper, O. Gomis-Bellmunt and R. Villafáfila-Robles, "A review of energy storage technologies for wind power applications," *Renewable and Sustainable Energy Reviews*, vol. 16, pp. 2154-2171, 2012.
- Gobierno de México, *Compromisos de Mitigación y Adaptación ante el Cambio Climático para el periodo 2020-2030*, 2015.
- Heuser, S.D., "Techno-economic analysis of a potential energy trading link between Patagonia and Japan based on CO<sub>2</sub>-free hydrogen.," *International Journal of Hydrogen Energy*, 2019.
- Hydrohub Innovation Program, "Gigawatt green hydrogen plant," Hydrohub Innovation Program, Amersfoort, 2020.
- IEA Technology Networks, "Morocco Pioneers PV with Thermal Storage at 800 MW Midelt CSP Project," *Solar Power & Chemical Energy Systems*, p. 1, 25 April 2020.
- IEA, *Construction costs for most power plant types have fallen in recent years*, 2917.
- International Energy Agency, "The future of Hydrogen," IEA, Paris, 2019.
- International Renewable Energy Agency, "Renewable Power Generation Costs in 2019," IRENA, Abu Dhabi, 2020.
- IRENA, "Electricity Storage and Renewables: Costs and markets to 2030," International Renewable Energy Agency, Abu Dhabi, 2017.
- IRENA, "Electricity Storage Valuation Framework: Assessing System Value and Ensuring Project Viability," International Renewable Energy Agency, Abu Dhabi, 2020.
- IRENA, "Hydrogen from renewable power: Technology outlook for the energy transition," International Renewable Energy Agency, Abu Dhabi, 2018.
- Kotzur, Leander & Markewitz, Peter & Robinius, Martin & Stolten, Detlef. *Impact of different time series aggregation methods on optimal energy system design. Renewable Energy*. 117. Germany, 2017.
- Lazard, "Lazard's Levelized Cost of Storage Analysis - Version 6.0," Lazard, New York, 2020.

- M. Armand, P. Axmann, D. Bresser, M. Copley, K. Edstr, C. Ekberg, D. Guyomard, B. Lestriez, N. Petr, M. Petranikova, W. Porcher, S. Trabesinger, M. Wohlfahrt-Mehrens and H. Zhang, "Lithium-ion batteries – Current state of the art and anticipated developments," *Journal of Power Sources*, vol. 479, pp. 228708-228734, 2020.
- National Aeronautics and Space Administration, "National Aeronautics and Modern-Era Retrospective analysis for Research and Applications, Version 2. NASA Goddard Earth Sciences (GES) Data and Information Services Center (DISC)].," 2019.
- NREL, *Battery storage: Cost Projections for Utility-Scale*, 2019.
- P. Breeze, "Chapter 7 - Fuel Cells," in *Power Generation Technologies (Third Edition)*, Elsevier, 2019, pp. 145-171.
- Peña Sanchez, E.U., "Techno-economical Analysis of the Production of CO<sub>2</sub>-free Hydrogen from Variable Renewable Energy Sources in Mexico - Master Thesis," 2019.
- Ryberg D. S. , "Generation Lulls from the Future Potential of Wind and Solar Energy in Europe," 2019.
- Ryberg, D. S., & Caglayan, D. G., "Renewable Energy Simulation toolkit for Python.," 2019.
- Ryberg, D. S., Caglayan, D. G., Schmitt, S., Linßen, "The future of European onshore wind energy potential: Detailed distribution and simulation of advanced turbine designs," 2019.
- Ryberg, D.S., " Generation Lulls from the Future Potential of Wind and Solar Energy in Europe," 2019.
- Ryberg, D.S., "Geospatial Land Availability for Energy Systems (GLAES).," 2018.
- Ryberg, David & Robinius, Martin & Stolten, Detlef., *Methodological Framework for Determining the Land Eligibility of Renewable Energy Sources*, 2017.
- Secretaría de Energía, *Atlas Nacional de Zonas Con Alto Potencial de Energías Limpias (AZEL)*, 2017.
- Secretaría de Energía, *Programa de Desarrollo del Sistema Eléctrico Nacional - (PRODESEN 2019 - 2033)*, 2019.
- Secretaría de Energía, *Programa de Desarrollo del Sistema Eléctrico Nacional (PRODESEN 2018 - 2032)*, 2018.
- Toshiba Corporation, "Basics of Lithium-ion Batteries - Battery School," SCIB, Tokyo, 2020.
- US Department of Energy, "DOE Global Energy Storage Energy Storage Database: Energy Storage Projects," [Online]. Available: <https://www.sandia.gov/ess-ssl/global-energy-storage-database/>. [Accessed 5 November 2020].
- Welder, Lara & Ryberg, D. Severin & Kotzur, Leander & Grube, Thomas & Robinius, Martin & Stolten, Detlef, 2018. "Spatio-temporal optimization of a future energy system for power-to-hydrogen applications in Germany," *Energy*, Elsevier, vol. 158(C), pages 1130-1149.
- World Energy Council, "World Energy Resources - E-storage: Shifting from cost to value," World Energy Council, London, 2016.
- X. Luo, J. Wang, M. Dooner and J. Clarke, "Overview of current development in electrical energy storage technologies and the application potential in power system operation," *Applied Energy*, vol. 137, pp. 511-536, 2015.

